7-25-2018 10:30 AM

Engineering Graphene Oxide-based Nanostructures for DNA sensors

Aditya Balaji
The University of Western Ontario

Supervisor
Zhang, Jin
The University of Western Ontario

Graduate Program in Biomedical Engineering
A thesis submitted in partial fulfillment of the requirements for the degree in Master of Engineering Science

Abstract

Various nanostructures have been explored in DNA biosensors to convert the hybridization of DNA sequences to easily measurable processes, including optical, mechanical, magnetic, or electrochemical process. In this thesis, graphene oxide, a two-dimensional nanostructure, is applied in quenching the fluorescence of core-shell nanoparticles modified with targeted DNA sequences. The core-shell nanoparticles, iron oxide (Fe_3O_4) core, and fluorescent silica (SiO_2) shell, were produced through a wet chemical process which can directly link to a targeted DNA sequence (DNA-t), and the graphene oxide nanosheets were produced by the oxidation of graphite. In the meantime, a complementary- DNA single strand (DNA-c) is designed to interact with graphene oxide. Two different mechanisms have been investigated in the sensing system; (1) Ionic interaction between the DNA sequences and nanostructures through cationic bridging; and (2) covalent binding between the DNA sequences and nanostructures. In the cationic bridge system, the fluorescence intensity changes with the concentration of DNA-t in the range of 0 to 30 µM with the limitation detection at 0.25 µM without graphene oxide; the other system can detect DNA-t in the range of 0 to 4 µM with limitation detection at 0.41 µM. In addition, the effect of concentration of graphene oxide on the fluorescence intensity of core-shell nanoparticles has been investigated.

We hope that the the validation strategy by engineering the two dimensional nanostructured system can be further applied towards more efficient Cancer diagnosis.

Keywords

Iron Oxide (Fe_3O_4), Silica (SiO_2), DNA-t, Cationic Bridging System, Covalent Interaction System, Selectivity and Selectivity

Co-Authorship Statement

Chapter 1(Introduction), Chapter 2(Background and literature review), Chapter 3(Experiment Procedures) Chapter 4 and Chapter 5 include two different design methods towards DNA sensing from the multifunctional nanomaterials. Chapter 6 concludes with the future perspectives and conclusion. These chapters were written by Aditya Balaji with the assistance of Professor Jin Zhang.

Acknowledgments

I would like to thank several people for their guidance towards my research project and my thesis would not have been accomplished without the gratitude from them. I would like to acknowledge all of them.

Firstly, I would like to give a big gratitude to my supervisor Dr. Jin Zhang for her guidance and support for my research project. The opportunities starting from the NSERC USRA scholarship helped me elevate my interest in the engineering research that Dr. Zhang provided me, which lead to my graduate work in Biomedical Engineering. Dr. Zhang's support, enthusiastic guidance, support, trust and understanding on a daily basis helped me fulfill the fundamentals of how research unfolds which I can utilize in the future for research and development prospects.

Secondly, I would like to thank my advisory committee: Dr. Andy Sun and Dr. Jeff Carson for their guidance and feedback throughout the whole duration of my project.

Thirdly, I would like to thank the members of the Biotron facility, Dr. Richard Gardiner and Mrs. Karen Nygard for their assistance in using the respective equipments associated in the facility.

Next, I would like to thank all the members in the research group: LongYi Chen, Andrew Tse, Songlin Yang, Denghuang Zhang, Yang Che, Yingqi Zhang, and Eugene Hwang for the continuous support, encouragement and the good times we had over the duration of my project.

Lastly, I would like to thank my family for their continuous support, encouragement throughout my life which helped me finish the thesis.

This work has been supported by the Natural Science and Engineering Research Council of Canada (NSERC) through a Discovery Grant and Western Engineering Graduate Scholarship.

Table of Contents

List of Figures

List of Abbreviations

Ab	-	Antibody
AFM	-	Atomic Force Microscopy
Anti CRP	-	Anti C-Reactive Protein
APTES	-	Amino-propyl-tri-ethoxy-silane
BRCA	-	Breast Cancer
C.E.	-	Counter Electrode
CL	-	Chemiluminescence
CRET	-	Chemiluminescence Resonance Energy Transfer
CRP	-	C- Reactive Protein
CT	-	Computed Topography
CTAB	-	Cethyltrimethylammonium Bromide
C.V.	-	Cyclic Voltammetry
CVD	-	Chemical Vapour Deposition
DNA-c	-	Complementary- Deoxyribonucleic Acid
DNA-t	-	Target- Deoxyribonucleic Acid
EDC	-	1-Ethyl-3-dimethylaminopropylcarbodiimide
EIS	-	Electrochemical Impedance Spectroscopy
emu/g	-	Electromagnetic unit/grams
eV	-	ElectronVolt

fcc	-	Face Centered Cubic
FL	-	Fluorescence
fM	-	femtometer
FRET	-	Fluorescence Resonance Energy Transfer
FT-IR	-	Fourier Transform- Infrared Spectroscopy
G	-	Gaussian
Glu	-	Glutaraldehyde
GO	-	Graphene Oxide
GPa	-	GigaPascal
HCl	-	Hydrochloric Acid
kDa	-	kiloDaltons
MDEA	-	N-methyl- diethanolamine
mK	-	MegaKelvin
M_r	-	Remanence Magnetization
MRI	-	Magnetic Resonance Imaging
mRNA	-	Messenger Ribonucleic Acid
M_s	-	Saturation Magnetization
NHS	-	N-Hydroxysuccinimide
NP	-	Nanoparticles
PDT	-	Photo-Dynamic Therapy

PPi	-	Pyrophosphate
PTT	-	Photo-thermal Therapy
PVD	-	Physical Vapour Deposition
QD	-	Quantum Dot
R.E.	-	Reference Electrode
RITC	-	Rhodamine B Isothiocyanate
RNA	-	Ribonucleic Acid
SEM	-	Scanning Electron Microscopy
SPION	-	Superparamagnetic Iron oxide Nanostructures
SPR	-	Surface Plasmon Resonance
T2	-	Transverse 2
TEOS	-	Tetraethylorthosilicate
TPa	-	TeraPascal
VSM	-	Vibrating Sample Magnetometer
UV	-	Ultra-Violet
W.E.	-	Working Electrode
WHO	-	World Health Organization

Chapter 1 : Introduction, Motivation, and Objectives

1.1 Brief Overview of Nanotechnology

Nanotechnology is defined as the manipulation of matter on the atomic or molecular level where the design is used for an application. The structures are worked between 1 nanometer and 100 nanometers in size. It refers to developing structures by top-down or bottom-up processes of individual components. [1,2] From the definition, it acts on the emerging technologies associated with the novel classes of therapeutics. Using the improved technology of nanotechnology, it may be possible to improve upon Targeted Drug Delivery [3], Detection [4], Medical Instrumentation [5] and other specific areas. Many materials will be acted upon where the nanomaterial being used has a large surface area to volume ratio and is size dependable for many applications as stated above.

1.2 Fluorescent Magnetic Core-shell Nanostructures

Nanostructures exhibiting both magnetic and luminescent properties are used towards many biological applications. Nanomaterials with bifunctional properties such as luminescence and magnetism, can be used in a wide range of applications such as high-contrast bio-imaging, early-stage diagnostics, and more efficient therapeutics. The growing potential of the bifunctional nanomaterials have enhanced the likelihood of nano bio-interaction, protecting the core from aggregation, and improving the stability of the nanostructures. Silica, which is shown as the inorganic core is a good non-cytotoxic and biocompatible material which has been shown to provide some prime advantages for nanoparticles. The silica shell can decrease the polydispersity of the particles to prevent flocculation of particles, thus producing a greater stability in biological buffers. Second, it minimizes the oxidation from the magnetic core helping to maintain the physical and chemical properties. Third, silica can be used to surface modify with other functional groups to enhance the application in the field of study. Having silica surrounding the core structure is through the silanization process as one of the ways. [6-9]

1.2.1 Fluorescent Shell Structures

Magneto-fluorescent particles have been recognized as the cutting edge materials for biological applications. Size and morphology has become a challenge in synthesizing magneto-fluorescent nanomaterials that exhibit uniform and tunable sizes, high magnetic moment, and maximized fluorophore coverage. To fully cover the potential of fluorescent shell structures for their optimal performance, the design criteria has to be fulfilled: uniform and tunable sizes, high magnetic content loading for magnetic properties, maximum loading of the fluorophore at the surface for an optimal fluorescence signal, long-term colloidal stability and a versatile surface functionality for the varied requirements of different applications in the biomedical sector. [10,11]

1.2.2 Magnetite Core Structures

Magnetite Core Structures possesses the chemical composition Fe_3O_4 where its unique properties and applications are studied upon in the area of nanotechnology. Different syntheses processes are involved to control the sizes for scientific and technological interest. [12,13] Fe_3O_4 has a cubic inverse structure with oxygen forming a fcc closed packing where Fe cations adhere two oxidation states of Fe^{+2} and Fe^{+3}. [14] When the Fe cation is in a +2 state, the cation state can achieve an octahedral and a tetrahedral state. As opposed to the state of +3, it only has one state which it adheres, which is the octahedral state. The electrons move around the two oxidation states in the octahedral state. From the different applications ranging from MRI Imaging to Bio-sensing, it has its advantages and disadvantages which can be improved upon. The advantages of using magnetic nanostructures in various applications are that they are chemically stable under physiological conditions [15], low in toxicity [16], and have a good magnetic moment which corresponds to the good magnetic properties it consists. [17] The disadvantages of using these magnetic nanostructures in these applications are that the particles aggregate [18], have a poor water solubility [19], and a low cellular uptake efficiency. [20] Due to the intrinsic instability over periods of time, efforts of surface modifying the core structure is being done to minimize the instability through gravitational force, avoid strong interaction and aggregation of the nanostructures. [21]

Many factors are instigated to make the composition of the iron oxide structures more efficient in many different applications. There are many different techniques to obtain these nanostructures,

but one of the conventional methods for the simplest and cheapest process is to imply the precipitation technique. The size is dependable on the various properties as a small size in shape implies a high surface-area-to-volume ratio which interacts with various types of chemical species, both aqueous and gaseous. The controlled factors associated with the shape, nucleation, growth, durability, reproducibility, scalability, dispersibility play a key role for building complex nanostructures. Magnetic enhancement can be achieved by tailoring the diameter of the coated iron oxide NP with the adjustment of the reduction and repeated time. Surface chemistry/modification can be specific to certain biomedical applications making it more cell internalized, biocompatible, lipophilic, etc. [22-25]

1.2.3 Role of Magnetic Structures in DNA Sensing

The use of magnetic structures demonstrates bifunctional properties that can be used to improve their biocompatibility, and stability. The functionalization of silica surrounding the core structure is one prime example that allows the attachment towards the target DNA as a better sensing technique.

Magnetic nanoparticles owe their popularity to their numerous attributes such as their magnetic properties that enable them to be directed by an external magnetic field, the possibility to separate them from a reaction mixture, in addition to their low toxicity and biocompatibility. The magnetic properties of magnetite can help separate the multifunctional particles from the target DNA to study the quantification aspect of the target DNA. The role of magnetite also helps in the kinetics of hybridization of oligonucleotides. [24,25]

1.3 Applications of Fluorescent Magnetic Core-shell Nanostructures

1.3.1 Imaging

One of the major applications (SPIONS) take place in Imaging [24-27]. In MRI imaging, these magnetic structures act on T 2 acquisitions where it can be used for better contrast imaging. [27-29]. For better contrast imaging, nanoparticle surfaces can be conjugated with targeting species such as antibodies, aptamers, peptides, etc. This enables nanoparticle-based imaging probes to be substantially more specific than the conventional contrast agents. Other benefits include:

Reduction in material needed to achieve a set contrast, long blood-pool residence times, ability to undertake single cell tracking, reduced toxicity making it biocompatible. The precision control over size, shape and architecture has an impact in the physical attribute to determine their ability to provide contrast, i.e. ability to interact with the external magnetic field. [30]

One other area this technology can be used is in fluorescence imaging. The surface modification on the multifunctional nanostructures play a vital role on the ability to determine their ability to fluoresce. By having the ability to image fluorescent nanostructures, the species can be detected that are not amenable to direct fluorometric imaging (such as pH, concentration, etc.) [31]

1.3.2 Biosensor

Starting with the definition of a biosensor, it is a small device which targets a specific analyte. It contains three components to be a functional device. First, there has to be a biological component that attaches to the analyte ,which couples to a form of transducer where the signal processor outputs the information. One of the most utilized methods is the fluorescence-based detection due to its high sensitivity, simplicity, and diversity. The advancements of nanotechnology using bifunctional nanomaterials have opened up to new horizons for fluorescence detection. The absorption as well as the luminescence peaks can be controlled to the particle size and size distribution based on the type of method. The advantages associated in bio-sensing: (1) silicon is abundant and non-toxic; (2) high surface-to-volume ratio of the nanoparticles facilitates their binding to biomolecules; (3) the inclusion of the fluorescent dye inside each nanoparticle results in excellent photo-stability due to the shielding effect of silica from molecular oxygen, leading to high signal amplification factors during detection; (4) silica allows for further functionalization for a wider range to see the control in the fluorescence on the selectivity and sensitivity. [32-34]

1.4 Challenges Faced with Nanostructured Biosensor

Nanostructured materials provide an effective surface of biomolecule immobilization for the transducer to recognize the signal. The properties from the bi-functional materials provide an interesting platform for interfacing bio recognition elements with transducers for signal amplification. To optimize the signal, the properties related to morphology, particle size,

effective surface area, functionality, adsorption capability have to be taken into consideration. Current challenges associated with the magnetic- based nanotechnology in nanostructured biosensors are how to control precisely the morphology and monodispersed size of the nanoparticles to obtain high quality signals. The conformational changes of the biological agent and analyte could lead to discrepancies in understanding the signal. Larger targets that adhere to the analyte could be replaced due to a larger surface area and more functional groups in pursuing the interest from the transducer. The selectivity and specificity is another area that is in need of improvement where the suitable interface could be optimized. Another challenge that needs to be faced is the reproducibility which depends on the stability of the bio-receptor and the fabrication of the biosensor itself. Novel improvements can advance the technology, but the uncertainty is unavoidable, and always a great challenge. The calibration in some biosensors have to be done for every measurement and could be avoided if the samples are conducted in similar biological environments. To minimize the measurement uncertainty, it is crucial to use similar medium conditions for both standard calibrations as well as for the sample. Regeneration is another challenge where some sensors have a difficulty in being re-used. The complex immobilization can deteriorate the biosensor from being used multiple times and improvements are still sought out in the future. Signal enhancement is another proposed area where challenges are sought out. Reaction conditions such as pH and temperature can hinder the signal amplification causing a discrepancy. [35-37]

1.5 Surface Modification of Nanostructures

Surface Modification refers to modifying the surface of the material where properties associated with physical, chemical and/or biological characteristics differ from the original surface material. [38] Some of the prime characteristics that change upon modification include: roughness, cell internalization, lipophilicity, aggregation, surface charge, biocompatibility and reactivity. [39] Surface Modification can be sub categorized into two processes: Top-down Process and Bottom-Up Process. Both of these processes are used in nanofabrication. [40]

The top-down approach is characterized by the synthesis of the etching out of crystal plane (removing crystal plane) which are present on the substrate. The structure is cut out from a

bigger piece in a self structuring process and fabricated to the particular design. The advantages associated with the top down approach would be the cost, better control and scalability.

Two processes that are characterized under the top-down approach: Physical Vapour Deposition (PVD) and Chemical Vapour Deposition (CVD). [41] In physical vapour deposition (PVD), the particles will be transformed from a solid to a gaseous state, either through the thermal evaporation process or through resistive etching. The ejected molecules will travel from the target to the substrate and form the thin film. The bombardment of ions takes place where the kinetic energy is about 1-10 eV. [42-49] In Chemical Vapor Deposition (CVD), the material will be in a gaseous state which later condenses on the substrate through chemical precursors. There are advantages associated with the CVD process where it can enhance the hydrophilicity by increasing the functionality of the molecule. This process depends on the surface chemistry as the precursors involved can be toxic.

The limitations associated with the top-down approach is from the UV light where the small wavelengths become deleterious to the material. [50-60]

A bottom up method is the process of stacking atoms onto the substrate. [58] The small buildup of atoms happens to be crafted through covalent or supramolecular interactions. [58-59] The self assembly process undergoes an ordered process through various supramolecular interactions (i.e. hydrogen bonding, van der waals, electrostatic, pi-pi interactions, hydrophilic-hydrophilic, and hydrophobic-hydrophobic interactions). The bottom-up approach technique is one of the processes involved in biological applications. [59-62]

1.6 Graphene and Graphene Oxide Derivatives

Graphene is an allotrope of carbon which forms a 2D, atomic scale hexagonal lattice and it is able to effectively conduct heat and electricity. The shape is made up of a hexagonal lattice of carbon atoms in a honeycomb structure. It is made out of carbon atoms where each atom consists of four bonds, three sigma bonds and one pi bond out of the plane. The stability of the material is dependent on how tightly packed carbon atoms are from the sp^2 hybridization. [63] Fascinating properties of graphene arise from its high surface area combined with electronic and thermal conductivity and its mechanical strength. Due to the material's high surface area-to-

volume ratio and high conductivity, it leads to significant improvements in many applications. [63]

Due to its unique microstructures, graphene demonstrates special and always enhanced physiochemical properties. For instance, the Young's modulus and the intrinsic strength of graphene are around 1 TPa and 130 GPa respectively. The electron mobility and thermal conductivity of graphene are 2.5×10^5 cm^2 V^{-1} s^{-1} and 3000 W mK^{-1} respectively. [64] Graphene has been used to fabricate flexible electronics [65], high-frequency and logic transistors. [66] Recent studies show that graphene can be applied in electrochemical and optical biosensors to detect small levels of cancer biomarkers. [67]

Hummer's approach is the most common one for the synthesis of graphene sheets from graphene oxide. [68-71] The reduced form of graphene oxide is graphene through an oxidizing agent, like hydrazine or ascorbic acid. Overall, using Hummer's approach is one of the best methods in producing both of these compounds.

The oxygen functional groups on the surface of graphene oxide (GO) provide good sites for a myriad of interactions for linking molecules such as polymers, nanoparticles (NPs), etc. In GO, the associated functional groups are epoxy bridges, hydroxyl and carboxyl groups. Due to the disruption of sp^2 bonding, it acts as an electrical insulator. The advantages of using GO for enzyme immobilization induces many explorations of its properties and applications where techniques, such as Atomic Force Microscopy (AFM) and Scanning Electron Microscopy (SEM) could be used to view the immobilized structure. [72-77]

1.7 Motivation

DNA sequencing is the process of determining the precise order of the nucleotides. It determines the order of the bases in a strand of DNA. The knowledge of DNA sequences has become indispensable in basic biological research, and applied in applications in medical diagnosis, biotechnology, forensic biology, and biological systematics. DNA sequencing is the standard method utilized for initial identification of mutations. People study the DNA sequences for human beings who have genetic disorders of the immune system. Specific DNA sequences can

serve as a reliable biomarker for the detection of Cancer as well and many methods are in place. [78-79]

The main methods researchers are working on in DNA detection are using the polymerase chain reaction (PCR), radioisotopes, intercalating dyes exposed with UV light, and silver staining process.

The first method involving PCR is a powerful tool to analyze samples of DNA sequences apart from amplifying minute amounts of nucleic acids. The drawback associated with PCR is that it is not only a very sensitive technique, but also specific. The primers have to be directly complementary to the target DNA for DNA sequencing detection and amplification. As the technique is too specific, it can cause false negative results. [80,81] Using radioisotopes by incorporating P32 into one of the dNTP can be dangerous, expensive and a long time for the detection to occur. [82,83] The third method of intercalating dyes exposed to UV light will label DNA but not differentiate between different amplicons. [84] The fourth method involves the silver staining process can result in poor images from the high background noise and the expense of the reagents. [85]

From these shortcomes from these primary methods, the use of the fluorescent detection is a good approach for its low cost, high sensitivity, and low background noise. In particular, DNA offers a number of potential advantages for use in this setting. One is water solubility where it is highly soluble in biological settings, while achieving the water solubility is a challenge for small molecules. Second is the ease of synthesis where it could be bounded to fluorescent tags and quenchers. With all the advantages associated, the fluorescence detection is one of the ways that leads to the objective of my thesis.

Materials like gold and quantum dots have been utilized for the application of DNA biosensors. This project revolves around the use of nanomaterials in two different mechanisms and see the sensitivity of the target DNA.These magnetic nanoparticles are technologically challenging to control the size, shape, stability, and dispersibility in desired solvents. The magnetic iron oxide NPs have a large surface-to-volume ratio where the major drawbacks of using only the core structure will lead to aggregation, oxidation, loss of magnetism and dispersibility. The main objective of this thesis outlines having two different systems: Cationic Bridge System and

Covalent Interaction System. The cationic bridge system involves using a cationic molecule to bridge the interaction between the DNA with silica particles as well DNA-c on GO. The DNA gets hybridized in solution to study how selective and sensitive it is towards DNA using an optical sensor and study the effect of GO. Second, the covalent interaction involves modifying 5' DNA-t and interacting it with the silica particles. DNA-c will also be modified where it interacts with the COOH on GO. The DNA will be hybridized in solution and the DNA-t on silica particles at different concentrations will be studied upon.

The objectives of this thesis:

- The synthesis of Iron Oxide nanostructures (Formation of the Core): (1) First process delves into the chemical synthesis; (2) Second process delves into the coating process of the inorganic core on iron oxide; (3) Third process involves for further functionalization onto the inorganic core.
- The synthesis of the Graphene Derivatives and further functionalization onto the material
- To compare the characterization of Iron oxide and the core-shell using Vibration Sample Magnetometer(VSM), Transmission Electron Microscopy(TEM)
- To compare the DNA adsorption on the two different systems by looking at various characterizations as well on the effect of graphene oxide

1.8 Thesis Overview

Chapter 2 Literature review

This chapter outlines the applications revolving around iron oxide and the functionalized uses of this material in the biomedical industry. The advantages of iron oxide when functionalized produces better properties associated with better sensitivity and selectivity due to the magnetic properties associated with the core material. The advantages associated with the material are introduced to show how early it can detect the biomarker activity and act as a better biosensor. The idea of what a typical biosensor is introduced to apply how early cancer tumor cells can be detected. Also, the problems associated with just iron oxide is encountered to see the difference. Different functionalized materials are discussed in the chapter and various surface modification techniques are included using two different transducers.

Chapter 3 Experimental procedure

This chapter outlines the experimental procedure for the different synthetic procedures of the core and the shell. Also, in addition, the process to synthesize the derivatives of graphene is also shown. In addition to this, various characterization techniques are observed in this research to later observe the DNA adsorption onto the functionalized material for application use. The two different mechanisms of the Cationic Bridge System and Covalent Interaction System adhere to different synthetic processes which are explained. Different synthetic procedures are put in place to explain the two different mechanisms which later view the difference in the two different systems of how selective and sensitive DNA could adhere to the sensing system that the signal processor outputs.

Chapter 4 Cationic Bridge System with Core-Shell and Graphene Oxide System as a Biosensor for DNA Sensing

The core and its shell have been synthesized by thermal decomposition and silanization processes, respectively. In this chapter, various characterization techniques like TEM and UV-Vis spectroscopy were used to confirm the nanomaterial coating. Other techniques like FTIR was used to differentiate the peaks of the various graphene derivatives and the results of the DNA adsorption as well. This chapter will derive its use on using a cationic bridge interaction system to view the selectivity and sensitivity of DNA-t on the silica particles without graphene oxide. In addition, the effect of concentration of graphene oxide on the fluorescence intensity of core-shell nanoparticles has been investigated.

Chapter 5 Covalent Interaction with Core-Shell and Graphene Oxide System as a Biosensor for DNA Sensing

The core and its shell have been synthesized in the same procedure. The shell has been coated with amino groups that surround the silica structure and later attached to glutaraldehyde that attaches to the 5’ Modification of DNA-t that contains an amino group. The DNA-t hybridizes with DNA-c that is covalently bonded to GO. This chapter focuses on a different type of interaction to see how selective and sensitive the system adheres to the DNA before graphene

oxide. In addition, the effect of concentration of graphene oxide on the fluorescence intensity of core-shell nanoparticles has been investigated.

Chapter 6 Summary and future work

This chapter gives a detailed summary and conclusions of this research. Future work on the development of the DNA- biosensor model is discussed with other plausible design modifications.

1.9 References

[1] Ehdaie B, " Application of Nanotechnology in Cancer Research: Review of Progress in the National Cancer Institute's Alliance for Nanotechnology. *Int J Biol Sci*, 2007; 3(2): 108-110

[2] Saxena A, Tripathi R, Singh R, Biological Synthesis of Silver Nanoparticles By Using Onion (Allium Cepa) Extract And Their Antibacterial Activity. Digest Journal of Nanomaterials and Biostructures, 2010; 5(2): 427-432

[3] Singh R, Lillard J, "Nanoparticle-based Targeted Drug Delivery." *Experimental and Molecular Pathology*. 2009; 86(3): 215-223

[4] Choi Y, Kwak J, Park J. Nanotechnology for Early Cancer Detection. *Sensors* 2010, 10(1), 428-455.

[5] Yun Y, Eteshola E, Bhattacharya A, Dong Z, Shim J, Conforti L, Kim D, Schulz M, Ahn C, Watts N. Tiny Medicine: Nanomaterial-Based Biosensors. *Sensors*, 2009; 9(11), 9275-9299.

[6] Tiwari D, Behari J, Sen P. Application of Nanoparticles in Waste Water Treatment 1. *World Applied Sciences Journal*. 2008; 3(3): 417-433.

[7] Vallabani N, et al. Recent Advances and Future Prospects of Iron Oxide Nanoparticles in Biomedicine and Diagnostics. 3 Biotech. 2018; 8(6): 279

[8] Gupta B, et al. Bifunctional Luminomagnetic Rare- Earth Nanorods for High-Contrast Bioimaging Nanoprobes. Scientific Reports. 2016; 6: 1-12

[9] Burns A, et al. Fluorescent Core-Shell Silica Nanoparticles: Towards “Lab on a Particle” Architectures for Nanobiotechnology. Chem. Soc. Rev. 2006; 35: 1028-1042

[10] Nagao D, et al. Synthesis of Highly Monodisperse Particles Composed of a Magnetic Core and Fluorescent Shell. Langmuir. 2008; 24(17): 9804-9808

[11] Ow H, et al. Bright and Stable Core-Shell Fluorescent Silica Nanoparticles. Nano Lett. 5;1: 113-117

[12] Sun S, Zeng H. Size-Controlled Synthesis of Magnetite Nanoparticles. J. Am. Chem. Soc. 2002; 124(28): 8204-8205.

[13] Itoh H, Sugimoto T. Systematic Control of Size, shape, structure, and magnetic properties of uniform magnetite and maghemite particles. Journal of Colloid and Interface Science. 2003; 265(2): 283-295.

[14] Karim W, Kleibert A, Hartfelder U, Balan A, Gobrecht J, Bokhoven J, Ekinci Y. Size-dependent redox behaviour of iron observed by in-situ single nanoparticle spectro-microscopy on well-defined model systems. Scientific Reports. 2016;6:1-8.

[15] Parkinson G. Iron Oxide Surfaces. Surface Science Reports. 2016; 71(1); 272-365.

[16] Acharya G, Mitra A, Cholkar K. Emerging Nanotechnologies for Diagnostics, Drug Delivery and Medical Devices. A volume in Micro and Nano Technologies. 2017, 217-248

[17] Wahajuddin S, Arora S. Superparamagnetic iron oxide nanoparticles: magnetic nanoplatforms as drug carriers. Int J Nanomedicine. 2012; 7:3445-3471.

[18] Wu W, He Q, Jiang C. Magnetic Iron Oxide nanoparticles: Synthesis and Surface Functionalization Strategies. Nanoscale Res Lett. 2008; 3(11): 397-415.

[19] Qiang Y, Antony J, Sharma A, Nutting J, Sikes D, Meyer D. Iron/ iron oxide core-shell nanoclusters for biomedical applications. Journal of Nanoparticle Research. 2006; 8(3); 489-496.

[20] Ramaswamy S, Greco J, Uluer M, Zhang Z, Zhang Z, Fishbein K, Spencer R. Magnetic Resonance Imaging of Chondrocytes Labelled with Superparamagnetic Iron Oxide Nanoparticles in Tissue-Engineered Cartilage. Tissue Eng Part A. 2009; 15(12): 3899-3910.

[21] Sun P, Zhang H, Liu C, Fang J, Wang M, Chen J, Zhang J, Mao C, Xu S. Preparation and Characterization of Fe3O4/CdTe Magnetic/ Fluorescent Nanocomposites and Their Applications in Immuno-labeling and Fluorescent Imaging of Cancer Cells. Langmuir. 2010; 26(2): 1278-1284.

[22] Gupta A, Gupta M. Synthesis and Surface Engineering of Iron oxide Nanoparticles for Biomedical Applications. Biomaterials. 2005; 26(18); 3995-4021

[23] Laurent S, Forge D, Port M, Roch A, Robic C, Elst L, Muller R. Magnetic Iron Oxide Nanoparticles: Synthesis, Stabilization, Vectorization, Physicochemical Characterizations, and Biological Applications. Chem. Rev. 2008; 108(6); 2064-2110

[24] Lu A, Salabas E, Schuth F. Magnetic Nanoparticles: Synthesis, Protection, Functionalization, and Application. Angew. Chem. Int. Ed. 2007; 46: 1222-1244

[25] Martin J, Nogues J, Liu K, Vicent J, Schuller I. Ordered Magnetic Nanostructures: Fabrication and Properties. Journal of Magnetism and Magnetic Materials. 2003; 256: 449-501

[26] Hasan A, Nurunnabi Md, Morshed M, Paul A, Polini A, Kuila T, Hariri M, Lee Y, Jaffa A. Recent Advances in Application of Biosensors in Tissue Engineering. Biomed Res Int. 2014;2014:1-18.

[27] Lapshin R, Alekhin A, Kirilenko A, Odintsov S, Krotkov V. Vacuum ultraviolet smoothing of nanometer-scale asperities of Poly(methyl methacrylate) surface. *Journal of Surface Investigation. X-ray, Synchotron and Neutron Techniques*. 2010; 4:1-11.

[28] Alekhin A, Boleiko G, Gudkova S, Markeev A, Sigarev A, Toknova V, et al.

Synthesis of Biocompatible Surfaces by Nanotechnology Methods. *Nanotechnologies in Russia*. 2010;5: 696-708.

[29] Bertazzo S, Rezwan K. Control of α-Alumina Surface Charge with Carboxylic Acids. Langmuir. 2010; 26:3364-3371.

[30] Xie J, et al. Nanoparticle-based Theranostic Agents. Adv Drug Deliv Rev. 2010; 62(11): 1064-1079

[31] Wolfbeis O. An Overview of Nanoparticles Commonly Used in Fluorescent Bioimaging. Chem. SOc. Rev. 2015; 44: 4743-4768

[32] Zhong W. Nanomaterials in Fluorescence-based Biosensing. Anal Bioanal Chem. 2009; 394: 47-59

[33] Chinen A, et al. Nanoparticle Probes for the Detection of Cancer Biomarkers, Cells, and Tissues by Fluorescence. Chem Rev. 2015; 115(19): 10530-10574

[34] Chen G, et al. Fluorescent Nanosensors Based on Fluorescence Resonance Energy Transfer (FRET). Ind. Eng. Chem. Res. 2013; 52(33): 11228-11245

[35] Soleymani L, et al. Mechanistic Challenges and Advantages of Biosensor Minaturization into the Nanoscale. ACS Sens. 2017; 2(4): 458-467

[36] Holzinger M, et al. Nanomaterials for Biosensing Applications: a review. Front Chem. 2014;2:63

[37] Bertazzo S, Zambuzzi W, Da Silva H, Ferreira C, Bertran C. Bioactivation of Alumina by Surface Modification: a possibility for improving the applicability of alumina in bone and oral repair. Clinical Oral Implants Research. 2009; 20:288-293

[38] London G, Chen K, Carroll G, Feringa B. Towards Dynamic Control of Wettability by Using Functionalized Altitudinal Molecular otors on Solid Surfaces. Chemistry- An European Journal. 2013;19:10690-10697

[39] Sabatier P. Top-Down and Bottom-Up Approaches to Implementation Research: a Critical Analysis and Suggested Synthesis. Journal of Public Policy. 1986; 6(1); 21-48

[40] Reichelt K, Jiang X. The Preparation of thin films by physical vapour deposition methods. Thin Solid Films. 1990; 191(1):91-126

[41] Lyu S, Zhang Y, Lee C. Low-Temperature Growth of ZnO Nanowire Array by a simple physical Vapour-Deposition Method. Chem. Mater. 2003;15(17): 3294-3299

[42] Boone D. Physical Vapour Deposition Processes. Materials Science and Technology. 1986; 2(3): 220-224

[43] Pauleau Y. Generation and evolution of Residual Stresses in Physical Vapour-Deposited Thin Films. Vacuum. 2001;61: 175-181

[44] Humphreys R, Satchell J, Chew N, Edwards J, Goodyear S, Blenkinsop S, Dosser O, Cullis A. Physical Vapour Deposition Techniques for the Growth of YBa2Cu3O7 Thin Films. Superconductor Science and Technology. 1990; 3: 38-52

[45] Nichollsa J, Deakinb M, Rickerbyb D. A Comparison between the Erosion Behaviour of Thermal Spray and Electron Beam Physical Vapour Deposition Thermal Barrier Coatings. Wear. 1999; 233-235: 352-361

[46] Matthews A, Lefkow A. Problems in the Physical Vapour Depositon of Titanium Nitride. Thin Solid Films. 1985; 126: 283-291

[47] Jensen K. Chemical Vapour Deposition. Advances in Chemistry. 1989;221:199-263

[48] Archer N. Chemical Vapour Deposition. Physics in Technology. 1979;10:153-161

[49] Yu Q, Jauregui L, Wu W, Colby R, Tian J, Su Z, Cao H, Liu Z, Pandey D, Wei D, Chung T, Peng P, Guisinger N, Stach E, Bao J, Pei S, Chen Y. Control and Characterization of Individual Grains and Grain Boundaries in Graphene Grown by Chemical Vapour Deposition. Nature Materials. 2011; 10: 443-449

[50] Choy K. Chemical Vapour Deposition of Coatings. Progress in Materials Science. 2003;48: 57-170

[51] Carlsson J, Martin P. Chemical Vapor Deposition. Science, Applications and Technology. 2010;3:314-363

[52] Chen Z, Ren W, Gao L, Liu B, Pei S, Cheng H. Three- dimensional flexible and conductive interconnected graphene networks grown by chemical vapour deposition. Nature Materials. 2011;10: 424-428

[53] Mattevi C, Kim H, Chhowalla M. A Review of Chemical Vapour Deposition of Graphene on Copper. J. Mater. Chem. 2011; 21: 3324-3334

[54] Zhou H, Yu W, Liu L, Cheng R, Chen Y, Huang X, Liu Y, Wang Y, Huang Y, Duan X. Chemical Vapour Deposition Growth of Large Single Crystals of Monolayer and Bilayer Graphene. Nature Communications. 2013;4:1-8

[55] Kawarada H. Large Area Chemical Vapour Deposition of Diamond Particles and Films Using Magneto-Microwave Plasma. J. Appl. Phys. 1987;26: 1032-1034

[56] Lux B, Colombier C, Altena H, Stjernberg K. Preparation of Alumina Coatings by Chemical Vapour Deposition. Thin Solid Films. 1986; 183: 49-64

[57] Reina A, Jia X, Ho J, Nezich D, Son H, Bulovic V, Dresselhaus M, Kong J. Large Area, Few-Layer Graphene Films on Arbitrary Substrates by Chemical Vapor Deposition. Nano Letters. 2009; 9:30-35

[58] Balzani V, Credi A, Venturi M. The Bottom-Up Approach to Molecular-Level Devices and Machines. Chem. Eur. J. 2002;8: 5524-5532

[59] Shimomura M, Sawadaishi T. Bottom-up Strategy of Materials Fabrication: A new trend in Nanotechnology of Soft Materials. Current Opinion in Colloid & Interface Science. 2001; 6(1):11-16

[60] Rosei F. Nanostructured Surfaces: Challenges and Frontiers in Nanotechnology. Journal of Physics: Condensed Matter. 2004;16:1373-1436

[61] Wang J, Gao W. Nano/Microscale Motors: Biomedical Opportunities and Challenges. ACS Nano, 2012; 6(7): 5745-5751

[62] Lau J, Shaw J. Magnetic Nanostructures for Advanced Technologies: Fabrication, Metrology and Challenges. Journal of Physics D: Applied Physics. 2011; 44: 1-43

[63] Zurutuza A, et al. Challenges and opportunities in Graphene Commercialization. Nat Nanotechnology. 2014; 9:730-734

[64] Nair RR, Blake P, Grigorenko AN, Novoselov KS, Booth TJ, Stauber T, Peres NMR, Geim AK. Fine structure constant defines visual transparency of graphene. Science. 2008; 320:1308

[65] Gorbachev RV, Jalil R, Belle BD, Schedin F, et al. Field-effect tunneling transistor based on vertical graphene heterostructures. Science. 2012;335:947–50.

[66] Britnell L, et al. Field- effect Tunneling Transistor Based on Vertical Graphene Heterostructures. Science. 2012; 335:947-950

[67] Ma HM, et al. Graphene-based optical and electrochemical biosensors: a review. Anal Lett. 2013;46(1):1–17

[68] Yin P, et al. Design, synthesis, and characterization of graphene–nanoparticle hybrid materials for bioapplications. Chem Rev. 2015;115:2483–531

[69] Li D, et al. Processable aqueous dispersions of graphene nanosheets. Nat Nanotechnol. 2008a;3:101–5

[70] Chen J, et al. An improved Hummers method for eco-friendly synthesis of graphene oxide. Carbon. 2013;64:225–9

[71] Toh S, et al. Graphene production via electrochemical reduction of graphene oxide: synthesis and characterization. Chem Eng J. 2014; 251:422–34

[72] Zhu Y, et al. Graphene and graphene oxide: synthesis, properties, and applications. Adv Mater. 2010; 22:3906–24

[73] Yin P, et al. Design, synthesis, and characterization of graphene–nanoparticle hybrid materials for bioapplications. Chem Rev. 2015; 115:2483–531

[74] Dreyer D, et al. Harnessing the Chemistry of Graphene Oxide. Chem. Soc. Rev. 2014; 43: 5288-5301

[75] Chen J, et al. An improved Hummers method for eco-friendly synthesis of graphene oxide. Carbon. 2013;64:225–9

[76] Toh S, et al. Graphene production via electrochemical reduction of graphene oxide: synthesis and characterization. Chem Eng J. 2014; 251:422–34

[77] Zhu Y, et al. Graphene and graphene oxide: synthesis, properties, and applications. Adv Mater. 2010; 22:3906–24

[78] Shendure J, et al. Next-generation DNA Sequencing. Nature Biotechnology. 2008; 26: 1135-1145

[79] Sanger F, et al. DNA Sequencing with Chain-Terminating Inhibitors. 1977; 74: 5463-5467

[80] Grompe M. The Rapid Detection of Unknown Mutations in Nucleic Acids. Nature Genetics. 1993; 5: 111-117

[81] Hayashi K. PCR-SSCP: A Method for Detection of Mutations. Genetic Analysis: Biomolecular Engineering. 1992; 9: 73-79

[82] Liu R, et al. Label-Free DNA Assay by Metal Stable Isotope Detection. Anal. Chem. 2017; 89: 13269-13274

[83] Weisshart K, et al. Coordinated Regulation of Replication Protein A Activities by Its Subunites p14 and p32. The Journal of Biological Chemistry. 2004; 279: 35368-35376

[84] Stengel G, et al. High Density Labeling of PCR Products with the Fluorescent Analogues tCO. Anal Chem. 2009; 81: 9079-9085

[85] Duan L, et al. Rapid and Simultaneous Detection of Human Hepatitis B Virus and Hepatitis C Virus Antibodies Based on a Protein Chip Assay Using Nano-Gold Immunological Amplification and Silver Staining Method. BMC Infect Dis. 2005; 5:53

Chapter 2 : Literature Review

The use of nanotechnology is widely used in many applications, particularly in Cancer Detection. This review of different DNA biosensors is presented with the applications explained. With the idea of how these biosensors work, different techniques are presented for DNA detection leading to Cancer applications. From some of the techniques from each biosensor, different nanostructures are used. The concept of implementing nanostructures have been great starting materials used in biosensors. The use of different nanomaterials is discussed to enhance the selectivity and sensitivity in biosensors.

2.1 Nanotechnology in Cancer Applications

According to World Health Organization (WHO), over 8.8 million people worldwide died from cancer in 2015, and it represents one of the major leading causes of death in the United States [1]. Cancer is caused by the uncontrolled growth and spread of abnormal cells. Cancer cells can evade apoptosis as these malignant tumor cells keep dividing and undergo different stages. [2] Firstly, there is proto-oncogenesis that initiate the cell division and mutation of these genes to generate cancer related genes. Secondly, mutated tumor-suppressor genes lead to cancer formation. Thirdly, mutations of genes regulated by apoptosis tend to be carcinogenic. Lastly, mutations of the DNA repairing genes also increase the chances of leading to cancer. These mutations that occur may arise from: deletion, duplication, or insertion of the nucleotides. [3] General cancer treatment techniques are normally associated with delineating the cancer cells at the early stages like chemotherapy, surgery and radiation. However, traditional diagnostic tools, including magnetic resonance imaging (MRI), computed tomography (CT), and X-ray scan, are expensive and normally require a long waiting time to access. Furthermore, traditional diagnostic tools require several million cells for accurate clinical diagnosis. [4] The challenges of early diagnosis and effective treatment of cancer requires a sensitive sensor to detect a small amount of samples with high sensitivity and selectivity. For instance, an ideal molecular imaging is expected to correctly diagnose early-stage tumor of approximately 100–1000 cells. [3,5,6] Table 2.1 shows the target molecules with the recognizing elements to target different Cancer Applications.

Table 0.1: Target Molecules with Recognizing Elements in Cancer Applications

Targeted Molecules	Surface Modification and Recognizing Elements	Disease	Reference
DNA-t	**DNA-C and DNA-r.AuNP**	**Breast Cancer**	**Rasheed P., et al.** ***Sensors and Actuators B. 2014;*** **204: 777-782.** [7]
Nucleolin	Aptamers, eg. AS1411	Any type of Cancer	Feng L., et al. *Biomaterials.* *2011;* 32: 2930-2937. [8]
Anti-CRP Antibody	CRP Antibody	Lung Cancer, Colorectal Cancer, Myleoma Cancer, Prostate Cancer	Zhu C. et al, *2D Mater*. 2015; 2: 032004-10. [9]
PCG	PPi	Melanoma Cancer	Muthuraj B., et al. *Biosens. Bioelectron*. 2017; 89:636-644. [10]
Folate Receptor	Folate Modified Hydrophilic	Epithelial-Derived Tumors	Li T., et al., *J. Mater. Chem.*

	Polymers		*B*. 2016; 4: 2972-2983. [11]
Anti- CRP Antibody	HRP, Antii-CRP Antibody	Lymphoma Cancer	Zhu Y., et al.. *Adv. Mater*. 2012; 22: 3906- 3924. [12]

2.2 DNA Sensors

Biosensors are small devices where a biological reaction detects a specific target analyte. [13] These devices engage the coupling reaction of the biological recognition element with the target analyte using a physical transducer that translates the bio-recognition event into a useful electrical signal. Different types of transducer elements are electrochemical, optical or mass-sensitive devices that generate current, light or frequency signals, respectively. From these types of signals, the signal processor can output the information to readable data from the respective signals. These devices have a selective binding towards the target analyte through a confined ligand partner (e.g. antibody, oligonucleotide). The immobilized enzyme used for recognizing the target substrate is used for many biological applications such as towards the goal of rapid, simple and inexpensive testing of infectious diseases, detection of DNA damage and interactions, etc.

2.2.1 Electrochemical Biosensors

The electrochemical design consists of a three-electrode system: The Working Electrode (W.E.), the Counter Electrode (C.E.), and the Reference Electrode (R.E). [14] The electrolyte plays a vital role in having a chemical substance conjugating onto the specific material. Cyclic Voltammetry (CV) is where the voltage gets tested between the reference electrode and the working electrode Another electrochemical technique involved is Electrochemical Impedance Spectroscopy (EIS) where the applications range from studying the corrosion of metals, adsorption and desorption to electrode surface, electrochemical synthesis of materials, catalytic reaction kinetics, and ions mobility in energy storage devices such as batteries and supercapacitors. [15] EIS technology can distinguish the electrochemical behaviour between the

coating and the metal substrate through the use of built in electrical circuits such as resistors and capacitors. [15-17]

Electrochemical devices have proven to be useful for sequence-specific bio-sensing of DNA. The electrochemical DNA sensing strategy is based on the reduction and oxidation of DNA. The amount of DNA reduced or oxidized would reflect the amount of DNA captured. Electrochemical measurements such as Cyclic Voltammetry and the Electrochemical Impedance Spectroscopy are used to develop methodologies for detecting DNA. [18]

2.2.2 Optical Biosensors

Optical biosensors use the interaction between light and matter to report the presence of analyte. A form of spectroscopy is used to isolate the signal due to the analyte, including Fourier Transform Infrared (FTIR) spectroscopy and Ultraviolet-Visible (UV-Vis) spectroscopy. One of the main techniques is fluorescence. At room temperature most molecules occupy the lowest vibrational level of the ground electronic state, and on absorption of light they are elevated to produce excited states. Excitation can result in the molecule reaching any of the vibrational sub-levels associated with each electronic state. From achieving the excited states, the molecule rapidly loses energy by collision and falls to the lowest vibrational level of the excited state. From the level of excitation, the molecule can return to any of the vibrational levels of the ground state, emitting in the form of fluorescence. The electronic structures that allow for excitation and emission of light are referred to as fluorophores. Species exposed to minimal fluorescence when exposed to a particular wavelength of light is labeled as a fluorophore to enable detection based on the intensity and spectrum of emitted light. The fluorescence signal is isolated using optical filters to eliminate background and excitation light. [19,20]

One of the most common fluorescence bio-sensing is the sandwich assay. This experiment shows the analyte is selectively bound to the surface of the targeting molecule which has been immobilized through some sort of interaction. By having a fluorescent tag, its surface concentration can be measured via highly sensitive fluorescence spectroscopy. With the use of a fluorescent label, the use of the emission signal offers a great promise for direct detection of DNA. [21]

For optical sensors, different types of mechanisms involving energy transfers are involved such as Forster Resonance Energy Transfer, Fluorescence Energy Transfer, Resonance Energy Transfer, or Electronic Energy Transfer. Theodor Forster developed this technique where the mechanism influences energy transfers between two light-sensitive molecules. For example, when a donor chromophore is in its high excitation state, energy is transferred to the acceptor chromophore through dipole-dipole interactions. The criteria for the stated energy mechanisms involve the distance between the donor and acceptor chromophore, and the orientation of the chromophores. The methods used in these energy transfers help in identifying how surface modification will take place. The FRET mechanism is between two fluorophores used as donor (D) and acceptor (A). The energy transfer efficiency (E, *i.e.* the fraction of energy transferred) is reverse proportional to the distance of two fluorophores as shown in Equation 1. [22-25]

$$E = \frac{1}{[1+(\frac{r}{R_0})^6]} \qquad (1)$$

where r is the distance between two fluorophores, R_0 the distance at which 50% E was achieved. R_0 is a characteristic parameter for given partners at given medium.

2.2.3 Mass- Sensitive Devices

The use of quartz crystal microbalance (QCM) devices allow the dynamic monitoring of hybridization events. The DNA is immobilized onto the quartz crystal where the increased mass associated with the hybridization results in a decrease of oscillating frequency.. QCM transducers can also be used for the investigation of other DNA interactions, including protein-DNA binding.

2.2.4 Magnetic Biosensors

A different type of biosensor uses change in the magnetic properties to detect a species of interest. Functionalized superparamagnetic nanoparticles can bind specifically to an analyte upon exposure to a sample or injection into an organism. The particles can be designed in a way to interact with the analyte through polyvalent bonding which can amplify the contrast in magnetic properties. [26-29]

A common type of magnetic biosensor uses materials whose resistivity changes with applied magnetic field. Changes in the current across these devices can be measured as analyte molecules labeled with ferromagnetic nanoparticles specifically adsorb to the sensor surface and introduce magnetic fields. With the help of magnetic nanoparticles bonded to target DNA, the magnetoresistance changes can be applied for DNA detection. [27]

Several drawbacks have been present in this technology and have to be improved upon. Few biological molecules can be exploited in magnetic resonance or magneto-resistive biosensors. Another disadvantage associated is that nonspecific interactions can occur between magnetic nanoparticles and other materials. Also, aggregation in solution onto the sensor surface can lead to false measurements. [28]

2.3 Different Techniques Used in Different Biosensors

With different biosensors widely used for DNA detection, different techniques associated have been implemented. Different nanomaterials have been used for different systems to test out the selectivity and sensitivity. The same techniques and procedures can be sought out with different materials used using these methods. In table 2.1, surface modification techniques of nanomaterials have been used to

2.3.1 Graphene-DNA Electrochemical Sensor for Target DNA Detection

Breast Cancer 1 (BRCA 1) gene is a tumor suppressor gene that is expressed in breast cells and other tissues. Mutations associated with this gene lead to high risk of breast cancer. This technology can detect the concentration level of BRCA 1 levels within the human body. [30] Breast Cancer 2 (BRCA 2) gene is another tumor suppressor gene that is expressed. Mutations associated with BRCA 1 and BRCA 2 resulted in 54% and 23% for ovarian cancer, respectively. [31-36]

The CV took measurements from ranging targeted DNA (DNA-t) concentrations on GCE/graphene/DNA-r|DNA-t|DNA-AuNP electrode and the oxidation peaks could be analyzed with increasing concentrations of DNA-t. In Fig. 2.1, it shows the design on the electrode. With the gold particles hybridizing better, the oxidation of the gold nanoparticles increases and higher

peaks on the CV could be detected. [37] The CV could target 1 fM BRCA1 gene which is the biomarker of breast cancer. The gold nanoparticles have a big impact on the hybridization factor with DNA enhancing the levels of oxidation. [7]

Another design on the three-electrode cell is established where the working/sensing electrodes consist of modified MDEAs, Ag/AgCl as the reference electrode, and BSA/anti- CRP antibodies/MPA/rGO-NP/ITO on the counter electrode. Eight circular electrodes are immersed onto the Indium Titanium Oxide electrode. [8]

Using the chronoamperometry analysis, the redox current had a linear proportion with increasing DNA-t concentration. When 10 fM of DNA-t was deposited, it showed a high current value as opposed to the 3 base mismatch complementary probe DNA-t. This system proved that the sensor is selective towards DNA and can be utilized for detecting mismatches in BRCA 1 gene mutations. [7, 37-40]

The detection capability of the GCE/Gr/DNA-c|DNA-t|DNA-r.AuNP with different DNA-t concentrations were monitored at 1.1 V. With an increase in concentration of DNA-t, the change was detectable up to 100 aM DNA-t. [7]

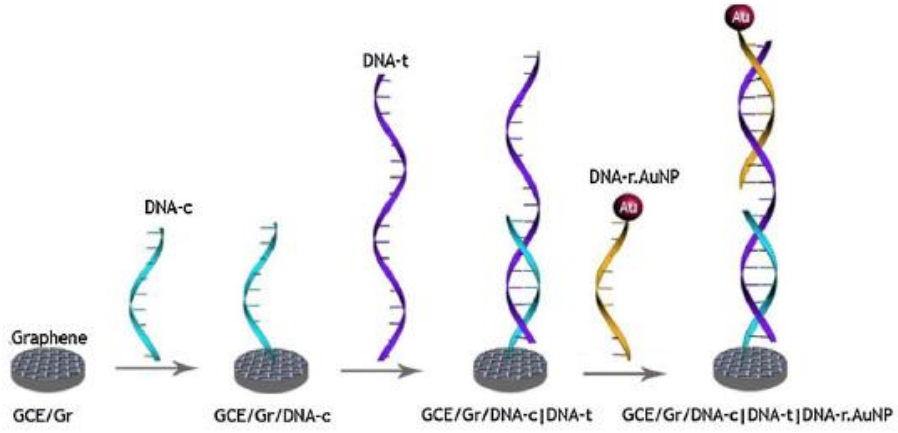

Figure 2.1 : Electrochemical Design for DNA-t Detection [7]

Electrochemical Impedance Spectroscopy (EIS) technique helps in detecting the electrode surface composition by monitoring the electron transfer resistance (R_{et}). From different

compositions involved where Nafion was used to immobilize the nanocomposite layer, a lower R_{et} value was achieved compared to the involvement of using an aptamer. With a higher impedance value, cancer cell detection based on aptamer-graphene-modified electrode is suited the best. The technique implemented provides the high binding affinity of AS 1411 to the nucleolin surface of cancer cells. The EIS assists in indicating the affinity level of the aptamer to the cancer cells compared to normal cells. [8, 41-43]

HeLa cells, K 562 cells, MDA 231 cells, and NIH 3T3 cells were tested in this work. The cells were measured using EIS and found that the breast cancer cell line, MDA-231, had the highest R_{et} value. From this, the conclusion is that the MDA-231 cells monitored the cancer cells much better than other type of cells using the cell culture technique. [8]

The detection capability of the GCE/Gr/DNA-c|DNA-t|DNA-r.AuNP with different DNA-t concentrations were monitored at 1.1V. With an increase in concentration of DNA-t, the change was detectable up to 100aM DNA-t. [7]

2.3.2 FRET and CRET in Optical Sensors

Here, we are focusing on two major optical biosensors, i.e. Fluorescence Resonance Energy Transfer (FRET), and Chemi-luminescence Energy Resonance Transfer (CRET).

The distance-dependent energy resonance transfer between donor and acceptor makes them offer great benefits in accurately detecting biomolecules/cells *in vivo* and *in vitro*.

Fluorescent amino acid (histidine) functionalized perylenediimide (PDI-HIS) is a technique where the “turn-off and turn-on” can detect Cu^{2+} ions. The disaggregation of PDI-HIS-Cu^{2+} of the fluorescence quenching helps detect the PPi levels. [10]

A unique optical approach on detecting the concentration of pyrophosphate (PPi) has a direct correlation with the cancer diagnosis. The fabrication technique of using the fluorescent probe of PDI-HIS, copper ion and graphene oxide (GO) enhances the selectivity and sensitivity for detecting PPi, a cancer biomarker. [10] The results show that the self-assembled

nanocomposites made of PCG (PDI-His+GO+Cu^{+2}) have a low detection limit (LOD), 1 fM, for PPi in comparison to PDI-HIS-Cu^{+2}.

In addition, FRET technique by utilizing quantum dots for the chemotherapy of ovarian cancer has been reported. The FRET technique transfers energy to the drug molecule from the Quantum Dot (QD) as they are attached on graphene. The fluorescence emission was recorded and the quenching indicates the release of Doxorubicin (DOX) from QD. Some reports show that graphene or graphene oxide-based FRET sensor incorporating the design with antibody-DNA-AuNP can be used for detecting DNA. [44]

CRET techniques using luminescence organic chemicals to excite an acceptor in CRET pair. The interaction between anti- C-Reactive Protein (CRP) and the C-Reactive Protein (CRP) can be detected in the graphene-based CRET. Such immune-sensor can accurately detect the C-reactive protein level.

CRP (C- Reactive Protein) have been investigated to primarily look at the diseases closely related to the heart. The amount of CRP with respect to the normal levels is usually less than 3 mg/L. The concentration of CRP significantly increases when there is an infection associated with cardiovascular disease, in this case, the primary issue is focused towards Lymphoma Cancer. Higher CRP concentrations have been reported towards lung, pancreatic, breast, ovary, esophagus, liver, biliary tract, stomach and multiple myeloma. [44,45]

The surface modified DNA-PBMC and the CRP-capturing ability is examined. The new innovation drives as a stepping stone fluorescence imaging towards the detection of CRP has been examined. The new surface modified engineering application is a new innovative idea towards cancer treatment. The DNA-PBMC complex had a recognition towards different concentrations towards CRP and had an impact towards the fluorescence intensity levels. As the concentrations of the CRP increased, the fluorescence intensity increased. [46]

2.3.3 DNA Hybridization with Mass-Sensitive Devices

Here, one of the techniques is the development of a QCM-based DNA biosensor for the detection of the hybridization of CaMV 35S promoter sequence in genetically modified organisms. Using

the quartz crystal, two methods were proposed: (1) Thiol-derivatized Probe Immobilization and (2) Amino- derivatized Probe Immobilization. [47-49]

In the thiol-derivatized probe immobilization, the thiol-derivatized probe was interacting with the gold surface of the quartz crystal which was one of the methods to see how the hybridization of the thiolated probe responded with the CaMV 35S sequence based in the change of frequency.

In the amino-derivatized probe immobilization, the quartz crystals were functionalized with glutaraldehyde and the changes of frequency was recorded upon the hybridization between two DNA sequences. The DNA sequence of the amino probe in relation to the CaMV 35S sequence was recorded based on the change of frequency.

2.3.4 Magnetic Tunnel Junction Sensors on DNA Detection With Magnetic Nanoparticles

In this section, the study of how target DNA was detected based on the use of the magnetic tunnel junction between the iron oxide nanoparticles and DNA. A magnetic tunnel junction (MTJ) sensor bridge was designed to detect the presence of magnetic NPs bonded to target DNA. [50,51]

Using the magnetic field strength of the magnetic particles, the magnetic tunneling bridge was designed to detect the presence of magnetic NPs bonded to the sensor area, in this case, the target DNA. [50]

With the traditional methods, this is one of the innovative approaches of using magnetic field strength to detect the selectivity and sensitivity of the target DNA and is still under improvement. [51]

2.4 The Different Nanostructures Used in Biosensors

Nanomaterials have demonstrated a big impact as the starting materials in the bio-sensing application. Nanomaterials are being used for the bio-recognition element to improve on the selectivity and sensitivity of the bio-catalytic event. [52,53] In the field of biosensors, different materials sought out offer high sensitivity and specificity detected by various mechanisms.

2.4.1 Iron Oxide Nanostructures

Nanoparticles with average particles size in the range from 1-100 nm have been considered as an alternative tool for cancer diagnosis and therapy at an early stage as they have special physiochemical and unique size-dependent properties. [54,55] The magnetic nanostructures are a vital material used in various applications in sensors, cancer treatment, drug delivery, solar cells, high performance batteries, data storage materials, etc. The advantages of using magnetic nanoparticles are: chemically stable under physiological conditions, functionalized with other materials, and have a high magnetization moment. The disadvantages associated with magnetic nanostructures are: aggregation and instability of nanoparticles. [56-59] Since the nanostructures can oxidize, a non-reactive coating layer is coated on the surface of the magnetic core. By fabricating the core-shell structure, the magnetic core could be isolated from a corrosive environment. The shell can include two major types to protect the core: organic materials (polymer) and inorganic materials (silica). Complex materials can be embedded such as: carbon nanotubes, graphene derivatives, and polymers, etc. [60,61] The synthesis process of the magnetic nanostructures is divided into four different types: co-precipitation [60], thermal decomposition [61], and hydrothermal process. [62] Different processes give out different size and shape of the magnetic nanostructures.

In the co-precipitation process, the anion and cation solution mix and the nucleation process takes place. Next, the particles agglomerate and the precipitation occurs. Then, the filtration process takes over and finally the calcination occurs to obtain the pure product. The process illustrated below is the chemical reaction to obtain the magnetite version using this technique. Also, it is noted to scale up the yield of the product by using this technique.

$$Fe^{2+} + 2OH^{-} \rightarrow Fe(OH)^{2}$$

$$3Fe(OH)_2 + 0.5O_2 \rightarrow Fe(OH)_2 + 2FeOOH + H_2O$$

$$Fe(OH)_2 + 2FeOOH \rightarrow Fe_3O_4 + 2H_2O$$

$$Fe^{3+} + 3OH^{-} \rightarrow Fe(OH)_3$$

$$Fe(OH)_3 \rightarrow FeOOH + H_2O$$

$$12FeOOH + N_2H_4 \rightarrow 4Fe_3O_4 + 6H_2O + N_2$$

In the thermal decomposition technique, an endothermic reaction occurs to break the chemical bonds to produce the magnetite. In this process, sodium oleate breaks down to iron oleate at high temperature, roughly around 320 degrees Celsius and later produces magnetite. The temperatures are well above the flash point of the organic vapors generated by the reaction mixture, under anaerobic conditions. Therefore, safety considerations are typically carried out when molecular oxygen has to be used. [61]

$$FeCl_2 + Na\text{-}Oleate \rightarrow Fe\text{-}Oleate + NaCl$$

In the hydrothermal synthesis, it is defined as a method of synthesis of single crystals that depends on the solubility of minerals in hot water under high pressure. A solvent is used with respect to the iron chloride where the high temperature and pressure are being involved to produce the iron oxide nanostructures.

The major drawback of magnetite is that it can easily oxidize in exposure to oxygen. To minimize the interaction of the oxidation, Fig. 2.2 shows the transition from magnetite to maghemite. [62]

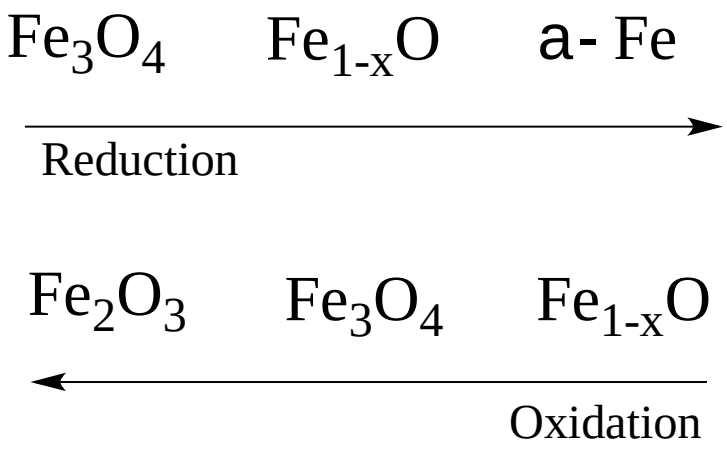

Figure 2.2: Oxidation and Reduction of Iron Oxide Compounds [62]

2.4.2 The Idea Behind Deoxyribonucleic Acid (DNA)

DNA structure, was first worked out by two scientists, Watson and Crick. They determined the structure of DNA was a double-helix polymer, or a spiral of DNA strands, each containing a long chain of monomer nucleotides, wound around each other. [63]

DNA, which is called deoxyribonucleic acid, is the molecule that contains the genetic code of any organism. In other words, it is a nucleic acid that contains the genetic instructions used in the development and functioning of all known living organisms. The organisms include any of the following: animals, plants, protists, archaea, and bacteria. In prokaryotes, DNA is circular in shape; while in eukaryotes, it is linear with histone proteins. [64,65]

The structure of DNA is a long polymer of simple units called nucleotides, where the backbone is made up of sugars and phosphate groups joined by ester bonds. The sugar is attached to a certain base where it could be adenine, cytosine, guanine, or thymine. The sequence of these four bases along the backbone encodes long term information. Fig. 2.3 shows the full structure of DNA.

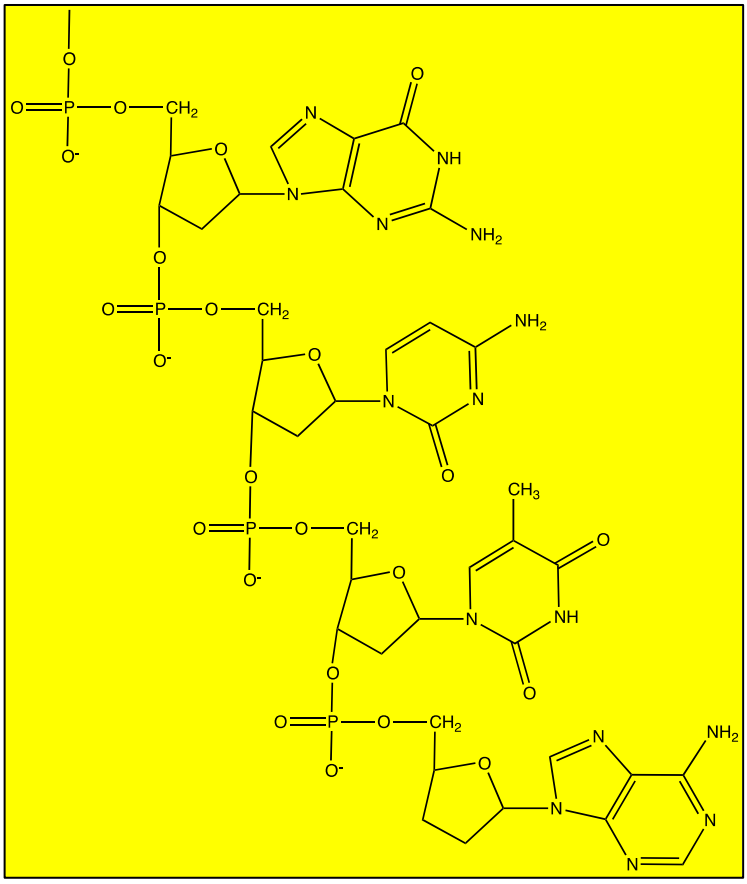

Figure 2.3: Structure of DNA

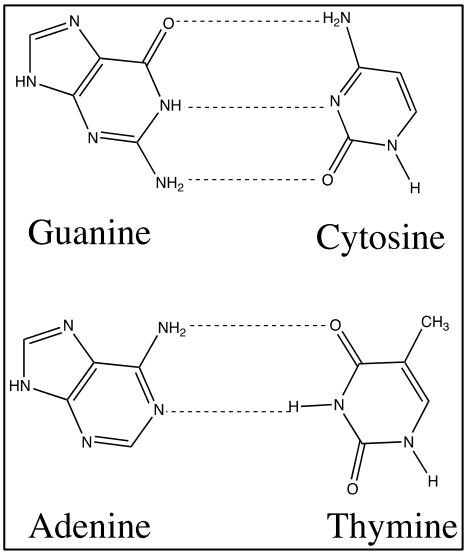

Figure 2.4: The Structure of Bases in a and b

Since DNA is double stranded in nature, the composition of the bases was determined using Chargaff's rule. The amount of A always equals the amount of T; while the amount of C always equals the amount of G. The bases would bind together forming the double helix structure with the use of hydrogen bonds. A and T would bind using 2 hydrogen bonds while C and G would bind using 3 hydrogen bonds. In Fig. 2.4, it shows the complete structure of the different types of bases. In a double-stranded DNA molecule, the 5' end (phosphate-bearing end) of one strand aligns with the 3' end (hydroxyl-bearing end) of its partner, and vice versa. DNA is composed of:

- A phosphate backbone where each phosphate radical has negative charge
- Deoxyribose sugar
- 4 types of bases or nucleotides. These are adenine (A), thymine (T), Cytosine (C), Guanine (G)

DNA contains instructions to construct other components, such as proteins and RNA molecules. DNA undergoes a transcription process to produce RNA. The transcription process is where the double stranded DNA is copied to a single stranded mRNA and RNA polymerase synthesizes it. The RNA produced undergo a translation process to make proteins. In the translation process, ribosomes translate the sequence of bases in the mRNA to proteins which perform functions inside and outside the cell. [65-69]

2.4.3 Graphene Oxide and Graphene

Graphene Oxide has been synthesized from graphite oxide where the functional groups associated with the material are a good candidate for chemical functionalization. Aside from the oxidative mechanisms being explained, the chemical structure of GO is a considerable debate over the years. The structure of GO is a continuous aromatic lattice of graphene interrupted by epoxides, alcohols, ketone carbonyls, and carboxylic acid groups. GO contains sp^3 carbon atoms bound to oxygen, which makes it an insulator. [71-72]

The functionalization of GO can be used on a large scale for preparing large graphitic films, as a binder for carbon products, and as a component of the cathodes of lithium batteries. The hydrophilicity of GO allows them to participate in lithographical processes like deposited on

substrates to produce thin films which is necessary in electronics. GO can be functionalized for optoelectronics, biodevices or as a drug-delivery material. [71-73]

With the hydrophilicity property of GO, it can be easily dispersed in water and other organic solvents due to the presence of the oxygen functionalities. This remains as a high property when mixing the material with ceramic or polymer matrixes when trying to improve their electrical and mechanical properties. [72-73]

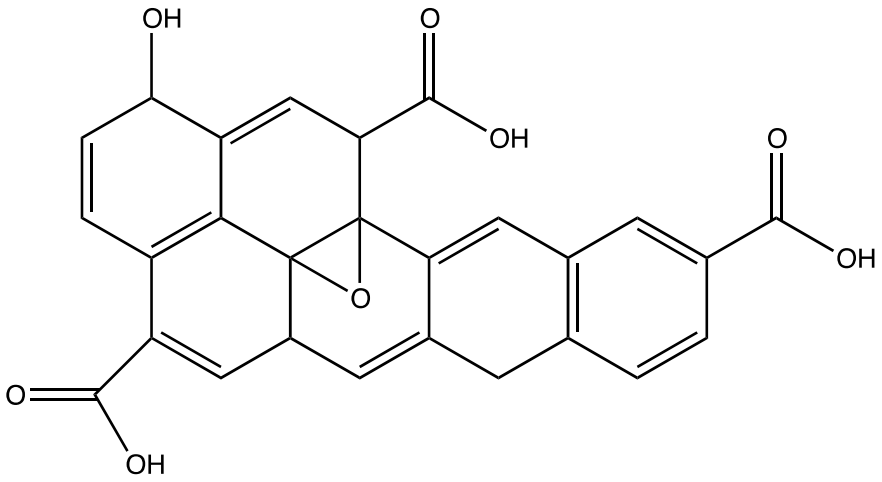

Figure 2.5 : Graphene Oxide Structure

Quite recently, graphene and graphene oxide, the ultra-thin two-dimensional nanomaterials, have attracted extensive attention because of their unique structure and remarkable mechanical, electrical, thermal and optical properties. Fig. 2.5 shows the structure of Graphene Oxide with the respective functional groups. More studies have shown that nanoparticles incorporating with graphene or graphene oxide could show great potential for sensing cancer biomarkers or cells at very low concentration, and realizing targeted treatment. [74-75]

In this review, the recent key findings of the newly developed hybrid graphene-based biosensor for detecting cancer cells are summarized. The surface modification of hybrid graphene/graphene oxide used in electrochemical biosensors and optical biosensors for detecting cancer biomarkers or cancer cells are addressed. [76-80]

2.5 Future Perspectives and Summary

2.5.1 Future Perspectives

Another proposed strategy for future purposes is using Streptavidin and Biotin for the covalent bonding to see how selective the design is towards DNA sensing. The design can show how selective and sensitive it is towards DNA sensing and quantify in a more convenient way how much DNA gets conjugated.

The composition of Streptavidin is composed of 4 essential identical polypeptide chains, also known as a homotetramer. The molecular weight of the protein is 55,000 daltons. It contains no cysteine residues, carbohydrate side chains or associated cofactors. Different preparations of streptavidin show considerable heterogeneity at both the amino- and carboxy-termini of each subunit polypeptide due to proteolysis during biosynthesis and secretion. Streptavidin lacks the glycoprotein portion of the molecule and therefore shows less non-specific binding than avidin. It has a molecular weight of 53.6 kDa and reactive towards Biotin.

The composition of Biotin contains an ureido ring fused with a tetrahydrothiophene ring. A valeric acid substituent is attached to one of the carbon atoms of the tetrahydrothiophene ring and is a water-soluble B-vitamin, also called a vitamin B_7. The valeric acid side chain incorporates various reactive groups that facilitate the addition of a biotin tag to to other molecules. The chemical composition is $C_{10}H_{16}N_2O_3S$. In Fig. 2.6, it shows the structure of Biotin. [81,82]

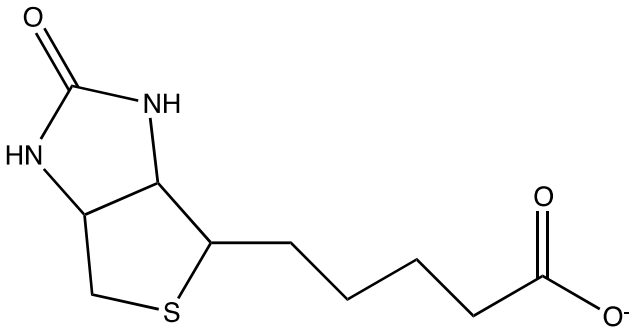

Figure 2.6: The Structure of Biotin [82]

The streptavidin-biotin complex is the strongest known non-covalent interaction between a protein and a ligand. The bond formation between biotin and streptavidin is very rapid, and once formed, is unaffected by pH, temperature, organic solvents, and other denaturing agents. Streptavidin has four sites for Biotin to bind to via non-covalent interaction.

This type of technology is used in applications when constructing a biosensor for DNA detection. Different techniques are being proposed, and this strategy will help to test the selectivity and sensitivity of DNA at an earlier stage. With the covalent binding strategy in place, one can study how this is used in the sensing technology when placed in an electrical, optical, mass-sensitive, or magnetic transducer. [81-83]

2.5.2 Summary

In summary, this section deals with the types of biosensors used in many applications, particularly in DNA sensing. The four main types of biosensors listed are: Electrochemical, Optical, Mass-Sensitive and Magnetic. With different biosensors used, different techniques were involved with the four listed sensors. The use of certain nanostructures with each technique was used for a certain transducer to analyze the biological application. With the types of biosensors, some of the techniques involved and the use of the nanostructures, it sets up the process of identifying the biological application.

2.6 References

[1] Forouzanfar M H H., et al. GBD 2015 Risk Factors Collaborators. Global, regional, and national comparative risk assessment of 79 behavioural, environmental and occupational, and metabolic risks or clusters of risks, 1990-2015: a systematic analysis for the Global Burden of Disease Study 2015. Lancet. 2016 Oct; 388 (10053):1659-1724.

[2] Herr H. Percivall Pott, The Environment and Cancer. BJUI International. 2011;108:479-481.

[3] Ecsedy J, and Hunter D. The origin of cancer in "*Textbook of Cancer Epidemiology"* . (2nd Edition). Ed. Adami, H.-O., Hunter, D., and Trichopoulos, D. Oxford: Oxford University Press. 2008; 3: pp. 61-85.

[4] Hsieh M, et al. The effect of comorbidity on the use of adjuvant chemotherapy and type of regimen for curatively resected stage III colon cancer patients. Cancer medicine 2016;5(5): 871–80.

[5] Peng H, Lin C. Nanomaterials for Cancer Diagnosis and Therapy. Journal of Nanomaterials. 2010; 2010: 1.

[6] Keshavarzi M, et al. Molecular Imaging and Oral Cancer Diagnosis and Therapy. J Cell Biochem. 2017; 118(10): 3055-3060

[7] Rasheed P, et al. Graphene-DNA Electrochemical Sensor for the Sensitive Detection of BRCA 1 gene. Sens Actuators B. 2014; 204: 777-782

[8] Feng L, et al. A Graphene Functionalized Electrochemical Aptasensor for Selective Label Free Detection of Cancer Cells. Biomaterials. 2011; 32: 2930-2937

[9] Zhu C, et al. Graphene and graphene-like 2D materials for optical biosensing and bioimaging: a review. 2D Mater. 2015; 2: 1-17

[10] Muthuraj B, et al. An efficient strategy to assemble water soluble histidine-perylenediimide and graphene oxide for the detection of PPi in physiological conditions and in vitro. Biosens Bioelectron. 2017; 89: 636-644

[11] Li T, et al. One-step reduction and PEIylation of PEGylated nanographene oxide for highly efficient chemo-photothermal therapy. J Mater Chem B. 2016; 4: 2972-2983

[12] Zhu Y, et al. Graphene and Graphene Oxide: Synthesis, Properties, and Applications. Advanced Materials. 2010; 22: 3906-3924

[13] Jung J, et al. A graphene oxide based immune-biosensor for pathogen detection. Angew Chem Int Ed. 2010; 49: 5708-5711

[14] Samet S, et al. Enzymatic Fuel Cells with an Oxygen Resistant Variant of Pyranose-2-Oxidase as Anode Biocatalyst. Biosensors and Bioelectronics. 2018;107:17

[15] Piro B, et al. Study of the DNA hybridization transduction behavior of a quinone-containing electroactive polymer by Cyclic Voltammetry and Electrochemical Impedance Spectroscopy. Journal of Electroanalytical Chemistry. 2005; 577 (1): 155-165

[16] Chang B, et al. Electrochemical Impedance Spectroscopy. Annu Rev anal Chem. 2010;3: 207-229

[17] Gan X, et al. A review: nanomaterials applied graphene-based electrochemical biosensors. Sens mater. 2015; 27: 191-215

[18] Orazem M, et al. Electrochemical Impedance Spectroscopy. New York: Wiley; 2011: 48-60

[19] Borisov S, et al. Optical Biosensors. Chem. Rev. 2008; 108:423-461

[20] Cooper M, et al. Optical Biosensors in Drug Discovery.

[21] Ramsden J. Optical Biosensors. Journal of Molecular Recognition. 1997; 10: 109-120

[22] Sekar RB, et al. A Fluorescence Resonance Energy Transfer (FRET) microscopy imaging of live cell protein localizations. The Journal of Cell Biology. 2003; 160: 629-633

[23] Jares-Erijman EA, et al. FRET Imaging. Nature Biotechnology. 2003; 21: 1387:1395

[24] Rizzo MA, et al. An Improved cyan fluorescent protein variant useful for FRET. Nature Biotechnology. 2004; 22: 445-449

[25] Alam R, et al. Near Infrared Bioluminescence Resonance Energy Transfer from Firefly Luciferase—quantum dot bionanoconjugates. Nanotechnology. 2014;25: 495606

[26] Mass Sensitive

[27] Hahm J. Functional Polymers in Protein Detection Platforms: Optical, Electrochemical, Electrical, Mass-Sensitive, and Magnetic Biosensors. Sensors. 2011; 11(3): 3327-3355

[28] Haun J, et al. Magnetic Nanoparticle Biosensors. John Wiley & Sons. 2010; 2: 291-304

[29] Mohri K, et al. Recent Advances of Micro Magnetic Sensors and Sensing Application. Sensors and Actuators A: Physical. 1997; 59: 1-8

[30] Miki Y, et al. A Strong Candidate for the Breast and Ovarian Cancer Susceptibility Gene BRCA 1. Science. 1994; 266: 1-7

[31] King M, et al. Breast and ovarian cancer risks due to Inherited Mutations in BRCA 1 and BRCA 2. Science. 2003; 302: 643-646

[32] Futreal P, et al. BRCA 1 mutations in primary breast and ovarian carcinomas. Science. 1994; 266: 5182

[33] Easton D, et al. Breast and Ovarian Cancer Incidence in BRCA 1 Mutation Carriers. Breast Cancer Linkage Consortium. Am J Hum Genet. 1995; 56 (1): 265-271

[34] Ford D, et al. Risks of Cancer in BRCA 1- mutation carriers. The Lancet. 1994; 343: 692-695

[35] Lerman C, et al. BRCA 1 Testing in Families With Hereditary Breast- Ovarian Cancer. JAMA. 1996; 275 (24): 1885-1892

[36] Farmer H, et al. Targeting the DNA Repair Defect in BRCA mutant cells as a therapeutic strategy. Nature. 2005; 434: 917-921

[37] Zhang S, et al. Electrochemical Biosensor for Detection of Adenosine Based on Structure-Switching Aptamer and Amplification with Reporter Probe DNA Modified Au Nanoparticles. Anal. Chem. 2008; 80(22): 8382-8388

[38] Diculescu V, et al. Applications of a DNA-electrochemical biosensor. TrAC Trends in Analytical Chemistry. 2016; 79: 23-26

[39] Liu A, et al. Development of Electrochemical DNA Biosensors. TrAC Trends in Analytical Chemistry. 2012; 37: 101-111

[40] Mascini M, et al. DNA Electrochemical Biosensors. Journal of Analytical Chemistry. 2001;369(1): 15-22

[41] Odenthal K, et al. An Introduction to Electrochemical DNA Biosensors. Analyst. 2007; 132: 603-610

[42] Palecek E, et al. Electrochemical Biosensors for DNA Hybridization and DNA Damage. Biosens Bioelectron. 1998; 13(6): 621-628

[43] Hajkova A, et al. Electrochemical DNA Biosensor for Detection of DNA Damage Induced by Hydroxyl Radicals. Bioelectrochemistry. 2017; 116: 1-9

[44] Savla R, et al. Tumor Targeted Quantum Dot-Mucin 1 Aptamer-Doxorubicin Conjugate for Imaging and Treatment of Cancer. J Conrol Release. 2011;153: 16-22

[45] Heikkila K, et al. A Systematic Review of the Association Between Circulating Concentrations of C- Reactive Protein and Cancer. J Epidemiol Community Health. 2007;61:824-832

[46] Hwang J, et al. Aptamer-Conjugated Live Human Immune Cell Based Biosensors for the Accurate Detection of C-Reactive Protein. Sci Rep. 2016;6:1-9

[47] Bao P, et al. High-Sensitivity Detection of DNA Hybridization on Microarrays Using Resonance Light Scattering. Anal. Chem. 2002; 74: 1792-1797

[48] Martinez G, et al. Development of Mass Sensitive Quartz Crystal Microbalance (QCM)-Based DNA Biosensor Using a 50 MHz Electronic Oscillator Circuit. Sensors. 2011; 11(8): 7656-7664

[49] Rahman M, et al. Electrochemical DNA Hybridization Sensors Based on Conducting Polymers. Sensors. 2015; 15 (2): 3801-3829

[50] Zhu J, et al. Magnetic Tunnel Junctions. Materials Today. 2006; 9; 36-45

[51] Shen W, et al. Quantitative Detection of DNA Labeled with Magnetic Nanoparticles Using Arrays of MgO-based Magnetic Tunnel Junction Sensors. Applied Physics Letters. 2008; 93: 1-3

[52] SalmanOgli A, Nanobio applications of quantum dots in cancer: imaging, sensing, and targeting, Cancer Nanotechnology (2011) 2:1–19

[53] Chinen A B, Guan C M, Ferrer J R, Barnaby S N, Merkel T J, and Mirkin C A. Nanoparticle Probes for the Detection of Cancer Biomarkers, Cells,and Tissues by Fluorescence, Chem. Rev. 2015, 115, 10530−10574

[54] Ito A, et al. 2005. Medical Application of Functionalized Magnetic Nanoparticles. Journal of Bioscience and Bioengineering. 2005; 100(1): 1-11

[55] Arruebo M, et al. 2007. Magnetic Nanoparticles for Drug Delivery. Nanotoday. 2007; 2(3): 22-32

[56] Dr An, et al. Magnetic Nanoparticles: Synthesis, Protection, Functionalization, and Application. 2007; 46: 1222-1244

[57] Gao J, et al. Multifunctional Magnetic Nanoparticles: Design, Synthesis, and Biomedical Applications. Acc. Chem. Research. 2009; 42(8): 1097-1107

[58] Predoi D. A Study On Iron Oxide Nanoparticles Coated With Dextrin Obtained By Coprecipitation. Digest Journal of Nanomaterials and Biostructures. 2007; 2(1): 169-173

[59] Kim D, et al. Synthesis and Characterization of Surfactant- Coated Superparamagnetic Monodispersed Iron Oxide Nanoparticles. Journal of Magnetism and magnetic Materials. 2001; 225:30-36

[60] Wu S, et al. Fe_3O_4 Magnetic Nanoparticles Synthesis From Tailings by Ultrasonic Chemical Co-Precipitation. Materials letters. 2011;65 (12): 1882-1884

[61] Park J, et al. Ultra-large-scale Syntheses of Monodisperse Nanocrystals. Nature Materials. 2004; 3: 891-895

[62] Wetterskog E, et al. Precise Control Over Shape and Size of Iron Oxide nanocrystals Suitable for Assembly Into Ordered Particle Arrays. Sc. Technology. Adv. Materials. 2014;15: 1-9

[63] Park J, et al. Ultra-large –scale Syntheses of Monodisperse Nanocrystals. Nature Materials. 2004; 3:891-895

[64] Wolstenholme D, et al. Animal Mitochondrial DNA: Structure and Evolution. International Review of Cytology. 1992; 141: 173-216

[65] Lindahl T. Instability and decay of the primary structure of DNA. Nature. 1993; 362: 709-715

[66] Travers A, Muskhelishvili G. DNA structure and function. FEBS Journal. 2015; 282: 2279-2295

[67] Prof E, et al. Mimicking the Structure and Function of DNA: Insights into DNA Stability and Replication. Angew. Chem. Int. Ed. 2000, 39, 990-1009

[68] Watson J, et al. The Structure of DNA. Cold Spring Harb Symp Quant Biol. 1953; 18: 123-131

[69] Watson J, et al. The Complementary Structure of Deoxyribonucleic acid. Royal Society. 1954; 223: 1-18

[70] Isom L, et al. DNA Structure: Cations in Charge. Current Opinion in Structural Biology. 1999; 9(3): 298-304

[71] Stankovich S, et al. Synthesis of Graphene-based nanosheets Via Chemical Reduction of Exfoliated Graphite Oxide. Carbon. 2007; 45(7): 1558-1565

[72] Marcano D, et al. Improved Synthesis of Graphene Oxide. ACS Nano. 2010; 4(8): 4806-4814

[73] Dikin DA, et al. Preparation and Characterization of Graphene Oxide Paper. Nature. 2007; 448:457-460

[74] Dreyer D, et al. Harnessing the Chemistry of Graphene Oxide. Chem. Soc. Rev. 2014; 43: 5288-5301

[75] Chen D, et al. Graphene Oxide: Preparation, Functionalization, and Electrochemical Applications. Chem. Rev. 2012; 112 (11): 6027-6053

[76] Hu X, et al. Effects of Particle Size and pH value on the hydrophilicity of Graphene Oxide. Applied Surface Science. 2013; 273: 118-121

[77] Li D, et al. Processable Aqueous Dispersions of Graphene Nanosheets. Nature Nanotechnology. 2008; 3: 101-105

[78] Sun X, et al. Nano- graphene oxide for Cellular Imaging and Drug Delivery. Nano Res. 2008; 1: 203-212

[79] Feng LY, et al. New Horizons for Diagnostic and Therapeutic Applications of Graphene and Graphene Oxide. Adv Mater. 2013; 25(2): 168-186

[80] Ma HM, et al. Graphene-based Optical and Electrochemical Biosensors: a review. Anal Lett. 2013; 46(1): 1-17

[81] Loh K, et al. Graphene Oxide as a Chemically Tunable Platform for Optical Applications. Nature Chemistry. 2010;2: 1015-1024

[82] Chilkoti A, Stayton P. Molecular Origins of the Slow Streptavidin-Kinetics. J. Am. CHem. Soc. 1995; 117: 10622-10628

[83] Wacker R, et al. Performance of Antibody Microarrays Fabricated by either DNA-directed Immobilization, direct spotting, or streptavidin-biotin attachment: a comparative study. Analytical Biochemistry. 2004; 330: 281-287

[84] Dolatabadi J, et al. Optical and Electrochemical DNA Nanobiosensors. TrAC Trends in Analytical Chemistry. 2011; 30: 459-47

Chapter 3 : Experimental Methods

In this chapter, the experiments performed in this project are described in detail: (1) Synthesis of the core structure, (2) Synthesis of the core-shell structure, (3) Synthesis of graphene oxide derivatives, (4) DNA-t Loading on MFNP, (5) DNA-c Loading on GO, (6) DNA-c and DNA-t Hybridization, (7) Amino Based Functionalization on Iron Oxide-Silica, (8) Characterization Methods

3.1 Synthesis of Magnetite

The synthesis of Fe_3O_4 Nanocrystals was based on reference (1). The process is broken down into two parts: (1) Synthesize the Iron-Oleate Complex, (2) Synthesize the Iron Oxide Nanocrystals.

The metal- oleate complex was prepared by reacting metal chlorides and sodium oleate. In this process, 10.8 g of iron chloride ($FeCl_3 \cdot 6H_2O$, 40 mmol, Aldrich, 98%) and 36.5 g of sodium oleate (120 mmol, TCI, 95%) were dissolved in 80 mL ethanol, 60 mL distilled water and 140 ml of hexane. The solution was heated to 70 °C and kept for four hours. When the reaction was completed, the upper organic layer which contained the iron-oleate complex was washed three times with 30 mL distilled water in a separatory funnel. After washing, hexane was evaporated off, resulting in a red waxy solid form of iron-oleate.

The sodium oleate complex forms the monodisperse iron oxide nanocrystals using thermal decomposition. In this process, 12g (40 mmol) of iron oleate complex from [1] and 1.9 g of oleic acid were dissolved in 67 g of 1-octadecene at room temperature. The mixed solution was increased to 320 °C with a kinetic rate of about 3 °C min^{-1}. At the desired temperature, the solution was kept for 30 minutes. A severe reaction occurred where the transparent solution became brownish black. The resulting solution containing the nanocrystals was then cooled to room temperature, and 167 mL of ethanol was added to precipitate the nanocrystals. The nanocrystals were separated by centrifugation as a final step.

3.2 Synthesis of Core-Shell Structure

The average 15 nm sized Fe_3O_4 nanocrystals were synthesized by this reference [2]. The Fe_3O_4 nanocrystals were stabilized with oleic acid and dispersed in chloroform at a concentration of 6.7 mg Fe/mL. From the ratio given, the amount of Fe_3O_4 could be theoretically calculated using stoichiometry.

On the side, 10 mg of rhodamine B isothiocyanate (RITC) was reacted with 44 uL of 3-aminopropyltriethoxysilane (APTES) (molar ratio of RITC: APTES=1:10) in 0.75 mL of ethanol under dark conditions for 2 days. The stock solution prepared has to be kept in the fridge at -4°C. [2]

From the exact concentration ratio, 0.5 mL of Fe_3O_4 nanocrystals in chloroform was poured into 5 mL of 0.055 M aqueous cethyltrimethylammonium bromide (CTAB) solution and the resulting solution was stirred vigorously for 30 minutes. After a vigorous shaking, the formation of an oil-in-water micro-emulsion resulted in a turbid brown solution. The mixture was heated up to 60 ^oC and stabilized at this temperature for 10 minutes to evaporate the chloroform, resulting in a transparent black Fe_3O_4/CTAB solution. Next, 45 mL of water and 0.3 mL of 2M NaOH was added where the mixture was heated up to 70 ^oC under stirring. Then, 0.5 mL of tetraethylorthosilicate (TEOS), 50 μL of RITC-APTES solution, and 3 mL of ethylacetate was added to the reaction solution in sequence. After 10 minutes, 50 μL of APTES was added and the solution was stirred for 3 hours. The synthesized Fe_3O_4@SiO_2 NP's were washed several times with ethanol to remove the unreacted species and dispersed in 20 mL of ethanol. Finally, to extract CTAB from the NPs, 40 μL of HCl was added to the dispersion and stirred for 3 hours at 60 ^oC. The resulting product was re-dispersed in ethanol and a magnetic bar could be used to see if the magnetism is still in effect. [2] Fig. 3.1 shows the chemical structure of Iron Oxide Silica Structure.

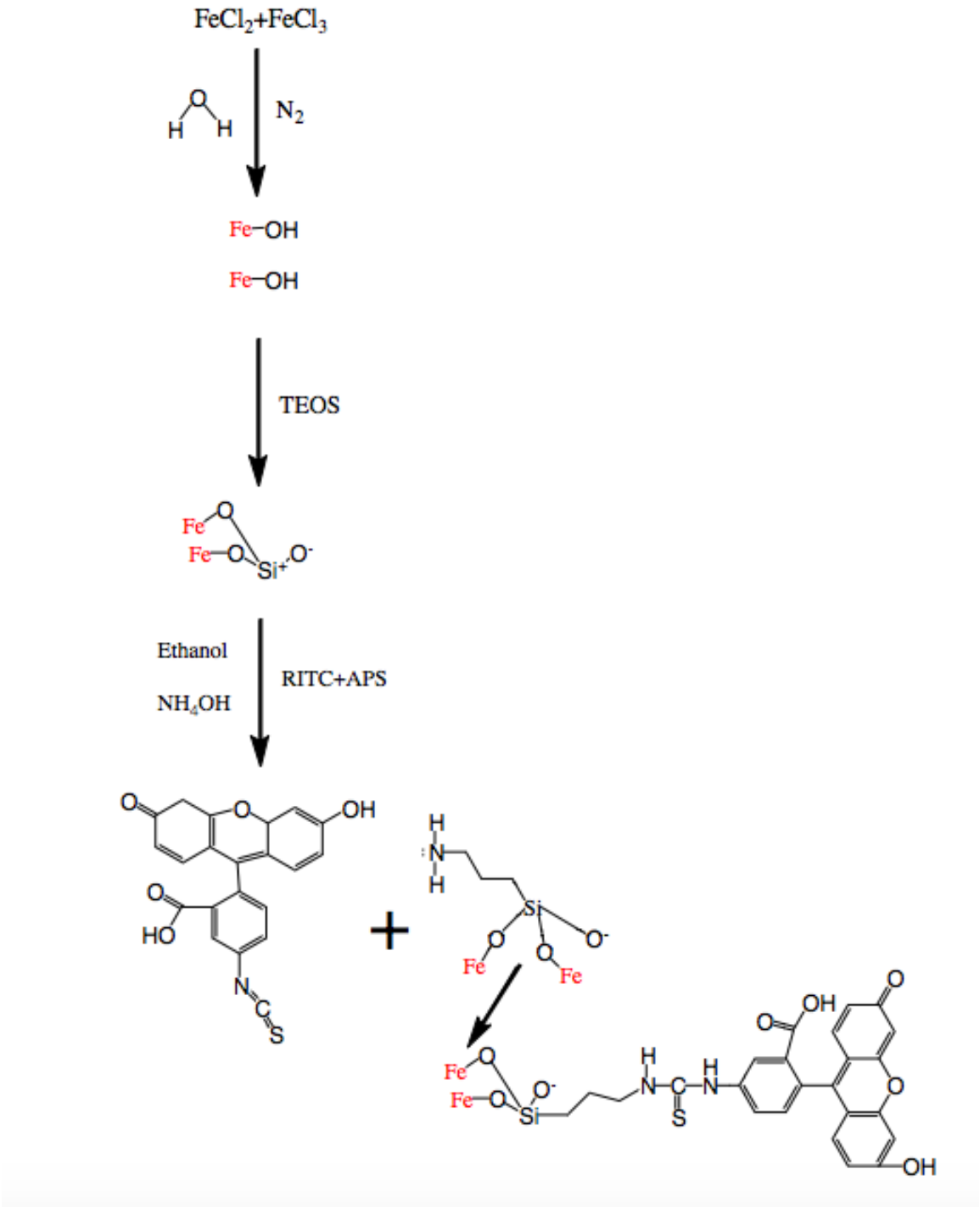

Figure 3.1: Iron Oxide Silica Structure

3.3 Synthesis of Graphene Oxide

The process of making graphene oxide derivatives followed that of Hummer based on this reference [3]. 1 g of graphite flakes was added to 50mL concentrated sulfuric acid while stirring in an ice bath. 3 g of potassium permanganate was slowly added by maintaining the temperature under 10 ^{o} C to obtain graphite oxide. The suspension was stirred at room temperature for 25 minutes followed by 5-minute sonication in an ultrasonic bath where this process was done 12 times. The reaction was quenched by the addition of 200 mL distilled water and an extra 2-hour ultrasonic treatment was carried out producing graphene oxide. After the pH was adjusted to around 6 by the addition of 1 M NaOH, the suspension was further sonicated for 1 hour. Also the same process was worked out where the pH was adjusted to around 8 to ionize the COOH groups for the interaction with the phosphate group on DNA-c using a monovalent ion. [3,4] In Fig 3.2, it shows the process of synthesizing Graphene derivatives. In Fig 3.3, it shows the structure of Graphene oxide with the respective functional groups.

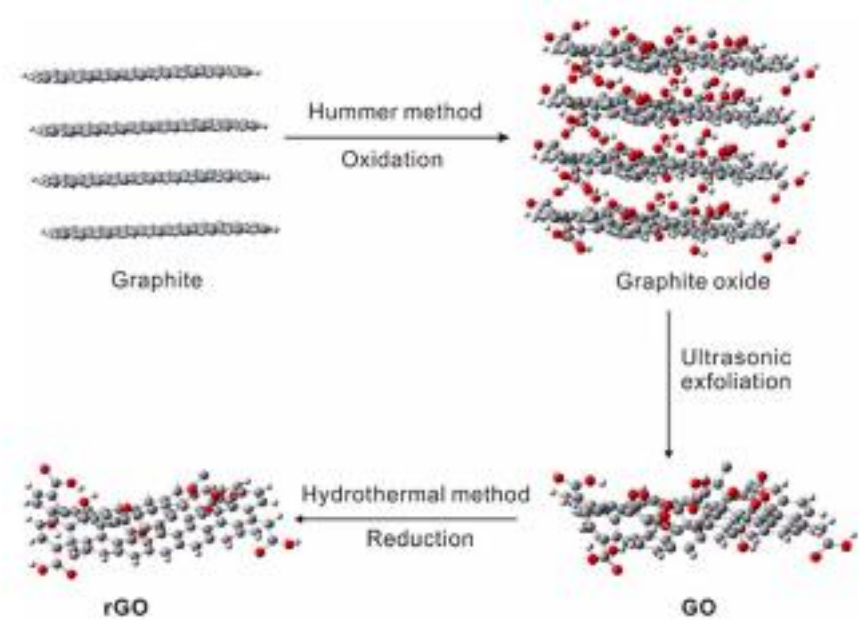

Figure 3.2: The Structure of the Hummer's Approach [5]

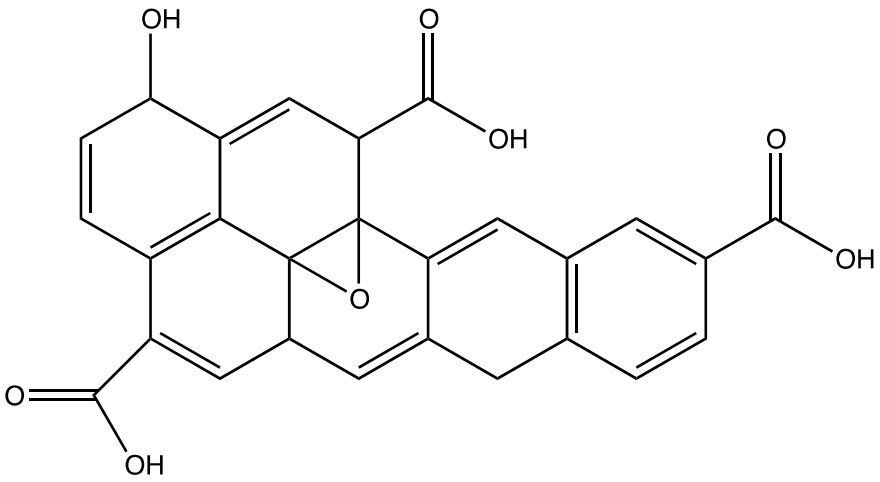

Figure 3.3: The Functional Groups Associated with Graphene Oxide

3.4 Target-Probe DNA Loading on Iron-Core Shell Particles

The target probe DNA (DNA-t) was 5’ CTT TTG TTC 3’ in a stock solution prepared by dissolving it in 1.9 mL of Tris-HCl buffer (pH 7.4) .

The fluorescence measurements were performed by keeping the concentration of Fe_3O_4@SiO_2-RITC MNPs constant while varying the DNA concentration. There was a cationic bridge where the negative charge from the phosphate group binds to the positive charge from the Na^+ from the sodium chloride in the hydrate form added and the negative charge from the silica group binds to the positive charge as well creating a bridge. [6,7,8]

3.5 Capture-Probe DNA Loading on Graphene Oxide

The DNA-c strand was 5’ GAA CAA AAG 3’ dissolved in 1.9 mL of Tris-HCl buffer (pH 7.4).

Different concentration amounts of GO were used ranging from 0.01 M to 0.05 M. In each different concentration labelled, 100 µL of 25 mM NaCl solution was added. The reaction was mixed and later, 100 µL of 10 µM DNA was added to the solution. The solutions were incubated for 10 minutes at room temperature. [9]

The carboxylic acid groups get deprotonated when the pH ~8. [10,11] The negative charge on the silica and GO create a bridge with the Na^+.

3.6 Hybridization of DNA-t and DNA-c

All fluorescence measurements were performed using a fluorometer using a quartz cuvette of 1 cm path length by keeping the concentration of the core-shell constant while keeping the DNA concentration constant at 5 µM at 313K. Samples were excited at 570 nm and the emission spectra were recorded in the range from 530-700nm.

The concentration of DNA-c that was mixed with GO was fixed at 1 mg/ mL. The concentration of the DNA-t and the core-shells were incubated at 313 K for 16 hours for the hybridization process with DNA-c bound GO. [12]

In addition, the competitive interaction between the core-shell particles with DNA-t was studied. Different amounts of DNA added produced different emission intensities.

3.7 5’ Modification of Target Probe DNA

The goal is to modify the 5’ phosphate group on DNA by directly forming a phosphoramidate bond.

First, dissolve ethylene-diamine to a final concentration of 0.25 M in 10 µL of 0.1 M imidazole. Then, weigh 1.25 mg (6.52 µmol) of EDC into a microcentrifuge tube. Next, add 7.5 µL of the prepared oligonucleotide to the tube containing EDC and immediately add 5 µL of the ethylene-diamine/imidazole solution. Then, vortex the tube until contents are completely dissolved, and briefly centrifuge the tube to gather contents. The next step involves adding 20 µL of 0.1 M imidazole, pH 6. Finally, incubate the reaction to 37 °C for 24 hours. In Fig 3.4, it shows the chemical structure of the 5’ Mod process.

3.8 Amino Modification of Silica Particles

The core-shell particles were functionalized by adding 15 µL of APTS to 15 mg of non functionalized core-shell particles suspended in 1 mL of ethanol (95%), using a glass vial and a magnetic stirrer. Just before the addition of APTS, the suspension of the core-shell particles was sonicated for 15 minutes to remove the possible clumps and, thus, to maximize the surface available for functionalization. After sonication and addition of APTS, the mixture was stirred overnight. These core-shell particles were also dried at room temperature. [12,13]

3.9 Glutaraldehyde- Amino Modified Iron Oxide Silica Particles

The dried amino modified core-shell particles were transferred to a glass vial and dispersed in 3 mL distilled water to obtain a final concentration of 2.5 mg mL^{-1}. Following dispersion, the amino modified iron oxide- silica particles were mixed and reacted with 50 µL of 25 % commercial grade glutaraldehyde (Glu) solution overnight in the dark to form Glu- FMNPs. The mixture was purified by centrifugation to remove the supernatant, and further re-suspended in 10mL of water. [14,15]

3.10 DNA-t-Glutaraldehyde-Amino Modified Iron Oxide Silica Particles

The 5' Modified DNA were transferred to a glass vial and dispersed in 3 mL of HEPES Buffer (20 mM HEPES, 150mM NaCl, pH 7.4) to obtain a final concentration of 0.1 µM. Following dispersion, the 5' DNA was mixed and reacted with 50 µL of 25% commercial grade glutaraldehyde-amino modified iron oxide silica particles overnight and incubated at 40 degrees Celsius. [14] The final product was labelled as Fe_3O_4@SiO_2@NH_2@Glu@5'Mod DNA-t.

3.11 5' Mod DNA-c Loading on Graphene Oxide

The DNA-c strand was modified using the same technique done for DNA-t. The strand was kept in the Tris-HCl buffer at pH ~6.

Different concentration amounts of GO were used ranging from 0.01 M to 0.05 M. The reaction was mixed where 100 µL of 10 µM DNA was added to the solution. The solutions were incubated for 10 minutes at room temperature. [9]

The GO was prepared at around pH~6 and so the carboxylic acid groups were not deprotonated and bonded to DNA-c through peptide bonding. [10].

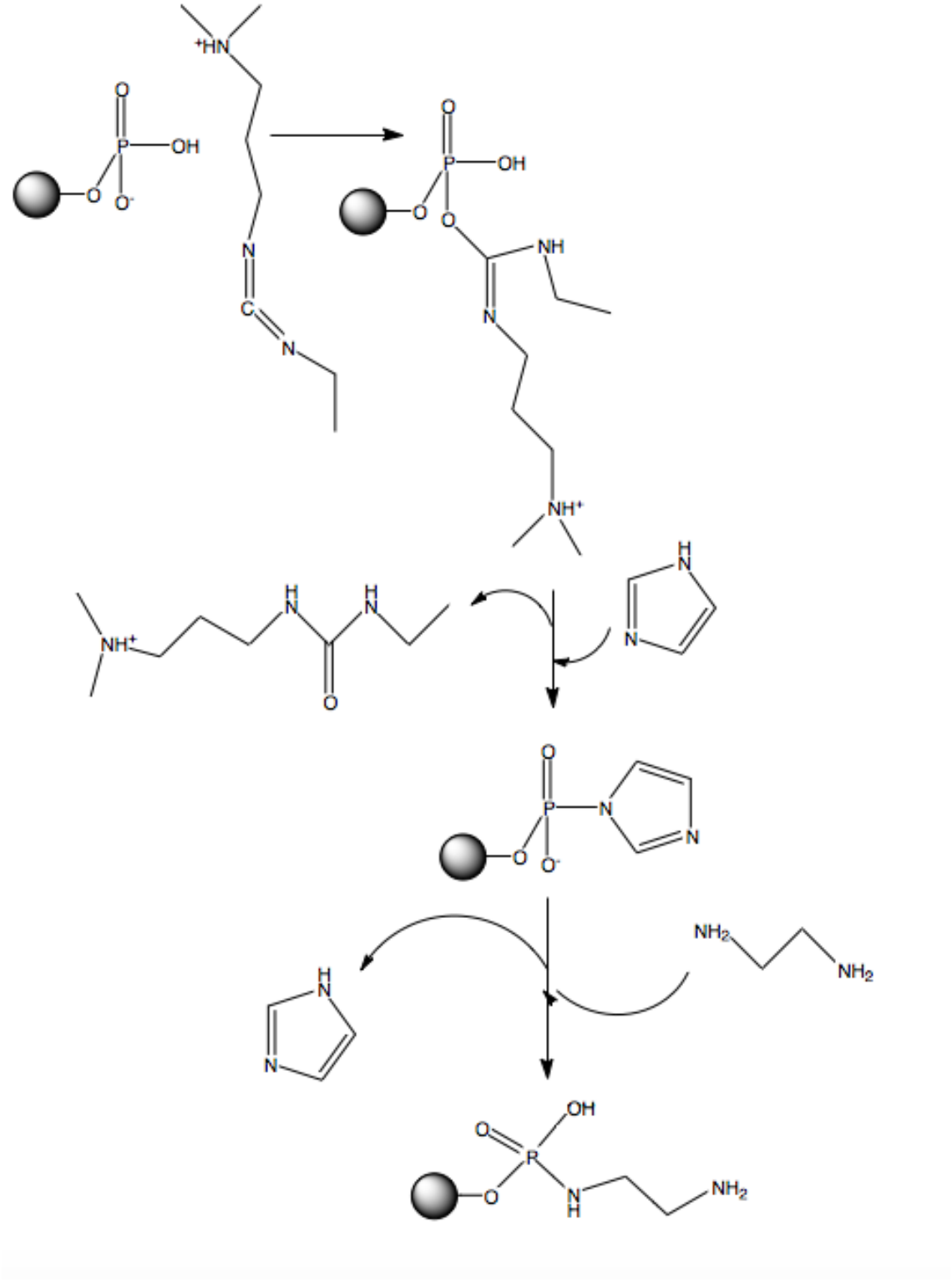

Figure 3.4: 5' Mod DNA Structure

3.12 Characterization Methods

3.13 Transmission Electron Microscopy

This technology supported by the Biotron Facility at The University of Western Ontario is a microscopy technique which uses a beam of electrons transmitted through a thin specimen where it interacts as it passes through. A two-dimensional image is formed by the interaction from the beam and the specimen where it can be displayed onto an imaging device or detected by the camera. The TEM micrographs of Fe_3O_4 nanocrystals of 15 nm in diameter, and surface modified Fe_3O_4@SiO_2 were collected by a Phillips CM 10 TEM. The substrates of the samples were put onto the carbon coated copper grids (200 meshes) through the drop casting method. The TEM samples were prepared by placing a drop of the sample solution onto the copper grid where light would evaporate the sample before put into use.

3.14 Fourier Transform Infrared Spectroscopy

This technology known as Fourier Transform Infrared Spectroscopy (FTIR) is a technique to characterize the functional groups of a material. This technique generates an infrared spectrum absorption or emission of the liquid, gas, and solid specimen. It absorbs energy from a monochromatic beam where it can target the molecule to output the correct functional groups of the certain material. In this study, FT-IR technique was used to characterize the core structure, the core-shell structure, surface modified core-shell with DNA-t, graphene oxide, and DNA conjugation on graphene oxide. In this study, the FT-IR spectra of samples were characterized with a Bruker Vector 22 FT-IR spectrometer. The scan range for the FT-IR was 600-4000 cm^{-1} and the resolution was set at 1 cm^{-1}. Before the experiment was run, the background was tested as air was the medium to characterize the sample.

3.15 Ultraviolet-visible Spectroscopy

Ultraviolet-visible spectrophotometry (UV-Vis) refers to the absorption and reflectance spectroscopy in the ultraviolet and visible spectral region. The range of light differs in the visible, near-UV and near-infrared regions. This technique differentiates the surface plasmon

resonance (SPR) of nanomaterials. The absorbance or reflectance in the visible region directly affects the perceived color of the chemicals. In this study, Agilent Cary 60 UV-Vis Spectrophotometer was used to characterize the absorption spectrum of the graphene oxide and DNA-c bridged to Graphene Oxide.

3.16 Vibrating Sample Magnetometer

The vibrating sample magnetometer (VSM) is one of the most successful implementations of a magnetometer. The sample is introduced in a constant uniform external magnetic field which shows the magnetization in the sample. As the magnetized sample is vibrated, it introduces perturbations in the external magnetic field. A set of coils can be arranged around the sample to measure the perturbations. The test process is that specimen is placed in a uniform magnetic field to magnetize the sample. The sample is put in a quartz holder which is connected to a vibration motor. The information would be collected by the detector and the hysteresis curves can be analyzed. The system has various applications on superconducting materials, magnetic films, anisotropic materials, monocrystal magnetic materials, etc. The magnetic properties were measured by LakeShore 7407 vibrating sample magnetometer.

3.17 Fluorescence Spectroscopy

This technology shows the fluorescence properties of the nanomaterials can be studied upon. A beam of light is applied to the instrument to excite the electrons and the emission is studied upon by the other end of the equipment. This data is collected by the detector. In this study, the fluorescence is measured at different emissions on the DNA-t on the modified core shell structures. Also, when DNA-c was conjugated on graphene oxide, it would be hybridized with DNA-t and the fluorescence studies would be measured.

3.18 References

[1] Park J, An K, Hwang Y, et al. Ultra-large-scale syntheses of Monodisperse Nanocrystals. Nature Materials. 2004; 3: 891-895

[2] Kim J, Kim H, et al. Multifunctional Uniform Nanoparticles Composed of Magnetite Nanocrystal Core and Mesoporous Silica Shell for Simultaneous Magnetic Resonance and Fluorescence Imaging, and Drug Delivery. 2008; 3: 1-11

[3] Abdolhosseinzadeh S, Asgharzadeh H, Kim H. Fast and fully-scalable synthesis of reduced graphene oxide. Scientific Reports. 2015;5: 1-7

[4] He K, Chen G, et al. Stability, Transport and Ecosystem Effects of Graphene in Water and Soil Environments. Nanoscale. 2017; 9: 5370-5388

[5] Wang H, et al. Demulsification of Heavy Oil-In-Water Emulsions by Reduced Graphene Oxide Nanosheets. RSC Adv. 2016; 6: 106297-106307

[6] Dreyer D, et al. Harnessing the Chemistry of Graphene Oxide. Chem. Soc. Rev. 2014; 43: 5288-5301

[7] Ahmadi M, Fattahi A. On the binding of Mg+2, Ca+2, Zn+2 and Cu+2 metal cations to 2' – deoxyguanosine: Changes on sugar puckering and strength of the N-glycosidic bond. Scientia Iranica. 2011;18: 1343-1352

[8] Albers L, Baumgartner J, Marschner C, Muller T. Cationic Si-H-Si Bridges in Polysilanes: Their Detection and Targeted Formation in Stable Ion Studies. 2016; 22: 7970-7977

[9] Giuliodori A, et al. Development of a graphene oxide-based assay for the sequence-specific detection of double- stranded DNA molecules. PLos ONE. 2017; 12(8): 1-17

[10] Konkena B, Vasudevan S. Understanding Aqueous Dispersibility of Graphene Oxide and Reduced Graphene oxide through pKa Measurements. J. Phys. Chem. Lett. 2012; 3: 867-872

[11] Wu M, Kempaiah R, et al. Adsorption and Desorption of DNA on Graphene Oxide Studied by Fluorescently Labeled Oligonucleotides. Langmuir. 2011; 27: 2731-2738

[12] Dong C, Zhang P, Bi R, Ren J. Characterization of solution-phase DNA hybridization by fluorescence correlation spectroscopy: Rapid genotyping of C677T from methylenetetrahydrofolate reductase gene. Talanta. 2007; 71: 1192-1197

[13] Toral A, et al. Synthesis of amino- functionalized silica nanoparticles for preparation of new laboratory standards. Spectrochimica Acta Part B. 2017; 138: 1-7

[14] Shahabadi N, Akbari A, Jamshidbeigi M, Falsafi M. Functionalization of Fe3O4@SiO2 Magnetic Nanoparticles with Nicotinamide and in vitro DNA Interaction. Journal of Molecular Liquids. 2016; 224: 227-233

[15] Chen L, Razavi F, Mumin A, Guo X, Sham T, Zhang J. Multifunctional Nanoparticles for Rapid Bacterial Capture, Detection, and Contamination. RSC Adv. 2013;3:2390-2397

Chapter 4 : Development of Multifunctional Nanoparticles for DNA Sensing Using the Charging Effect

Fe_3O_4 nanocrystals were synthesized using the thermal decomposition method to which later silica was hydrolyzed around the core structure. The surface morphologies of the core and the core-shell structure were studied using the TEM. Since the material contains magnetic properties, the VSM was instigated to look at the properties of the material. The FTIR Analysis was used to confirm the chemical structure of the compounds from the characterization of the peaks.

The production of graphene oxide (GO) using Hummer's approach was obtained and the conjugation with DNA-c was established. UV spectroscopy was used to confirm the DNA-c conjugated onto graphene oxide (GO) by the use of a monovalent ion. FTIR tests were also instigated to see the difference when DNA-c was conjugated onto GO.

Once the two systems above were established, the hybridization between the DNA-t and the DNA-c took place. Fluorescence studies showed the system at different target probe DNA concentrations to study the selectivity and sensitivity of the interaction with the core-shell particle

4.1 Introduction

Magnetic nanostructures are a novel idea for scientists and engineers to work on for different applications. Different methods were developed for various magnetic nanostructures. The nanostructures vary from nanoparticles, nanocrystals, nanoplates, nano-rods, etc. Different synthetic methods were developed to precisely control the size of the magnetic nanostructures and fabricate monodisperse magnetic structures. The magnetic nanostructures have been applied in different fields. These applications include: MRI Imaging [1], drug delivery [2], and in Biosensing [3]. The advantages associated with these core structures are: Chemical stable under physiological conditions [4], functionalization with other materials such as silica [5], and a high magnetic moment [6]. The disadvantages of these core structures: Aggregation of the Particles [7], and the Stability of the Structures. [7] The conventional methods to produce the iron oxide nanostructures are from the sol-gel technique, co-polymerization, thermal decomposition, etc. [8,9] The challenges are that different processes will control the shape and size, achieve mono-

dispersity better than others, reproduce and scalability of process and provide a better attachment for complex nanostructures.

In biotechnology fields, the core particle, which is composed of magnetite, would be further functionalized with inorganic materials to improve on the stability as well as the aggregation. The modification between the core and the shell structure for the immobilization is studied. Having the core-shell structure from the surface modification strategies improves the aggregation as well as the stability of the nanostructure. The observations and the particle distribution can confirm the diameter for the optimal size of the core and the core shell for further process in the certain application. With the core and core-shell structure, the magnetic properties are studied. Also, the type of magnetism is viewed from the extrapolation of the data to fully convey from the hysteresis curve.

In relation to the core-shell structure observed, further functionalization of DNA is incorporated through the charging effect. DNA is composed of three main components: Phosphate backbone, sugar and base. The 5' end of DNA is composed of the phosphate backbone and the 3' end is the hydroxyl group. [10-13] With different functional groups, the particular group is studied for the interaction with the core-shell particles. The researchers have developed various synthesis methods to overcome the challenges of controlling the composition and size of the core-shell structure, as well as the aggregation.

Synthesizing graphene oxide (GO) from Hummer's approach can help us to functionalize it further with other materials. [14-16] Graphene Oxide has functional groups such as the hydroxyl, epoxide, and carboxylic acid groups. [17] These groups can lose the negative charge at certain buffer conditions where it can interact with other materials such as DNA, in this case.

4.2 Results

The core (Fe_3O_4) and the core-shell ($Fe_3O_4@SiO_2$) were used by the TEM. The TEM looks at the bulk of the material where the core of the material could be sought out. Using the SEM would be not as efficient as it scans the surface of the sample and the core would not be fully distinguished.

4.3 Characterization of Fe_3O_4 Nanoparticles

The iron oxide nanocrystals were prepared and characterized by TEM. Fig. 4.1 shows a TEM micrograph of the iron oxide nanocrystals where the scale bar was set at 100 nm. The result indicates the iron oxide nanocrystals are monodispersed spherical structures. The particle size and size distribution were calculated. Table 4.1 shows that the average particle size is 14.36 nm with a narrow size distribution. Fig. 4.2 and 4.3 shows the TEM micrographs of the iron oxide-silica nanostructures where the scale bar was set at 100 nm and 500 nm, respectively. The particle size and size distribution were calculated. Table 4.2 shows that the average particle size is 37.85 nm.

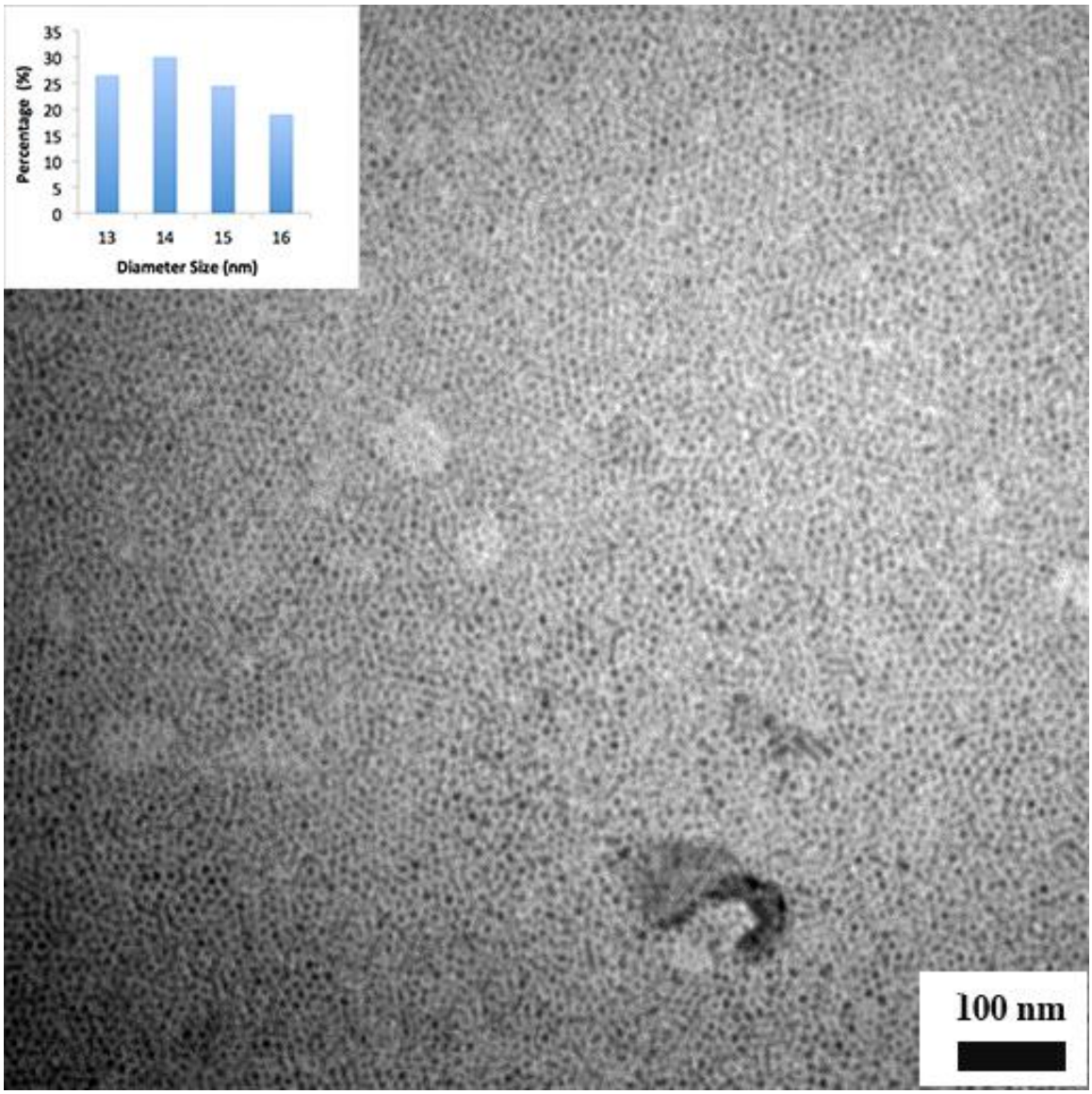

Figure 4.1: TEM Micrograph Image of the Iron Oxide Nanocrystals

Table 4.1: Statistical Analysis of the Iron Oxide Nanocrystals

Measure of Central Tendency	Number
Mean	14.4
Mode	14.2
Median	14.8
Max	16.1
Min	13.3
Standard Deviation	1.1

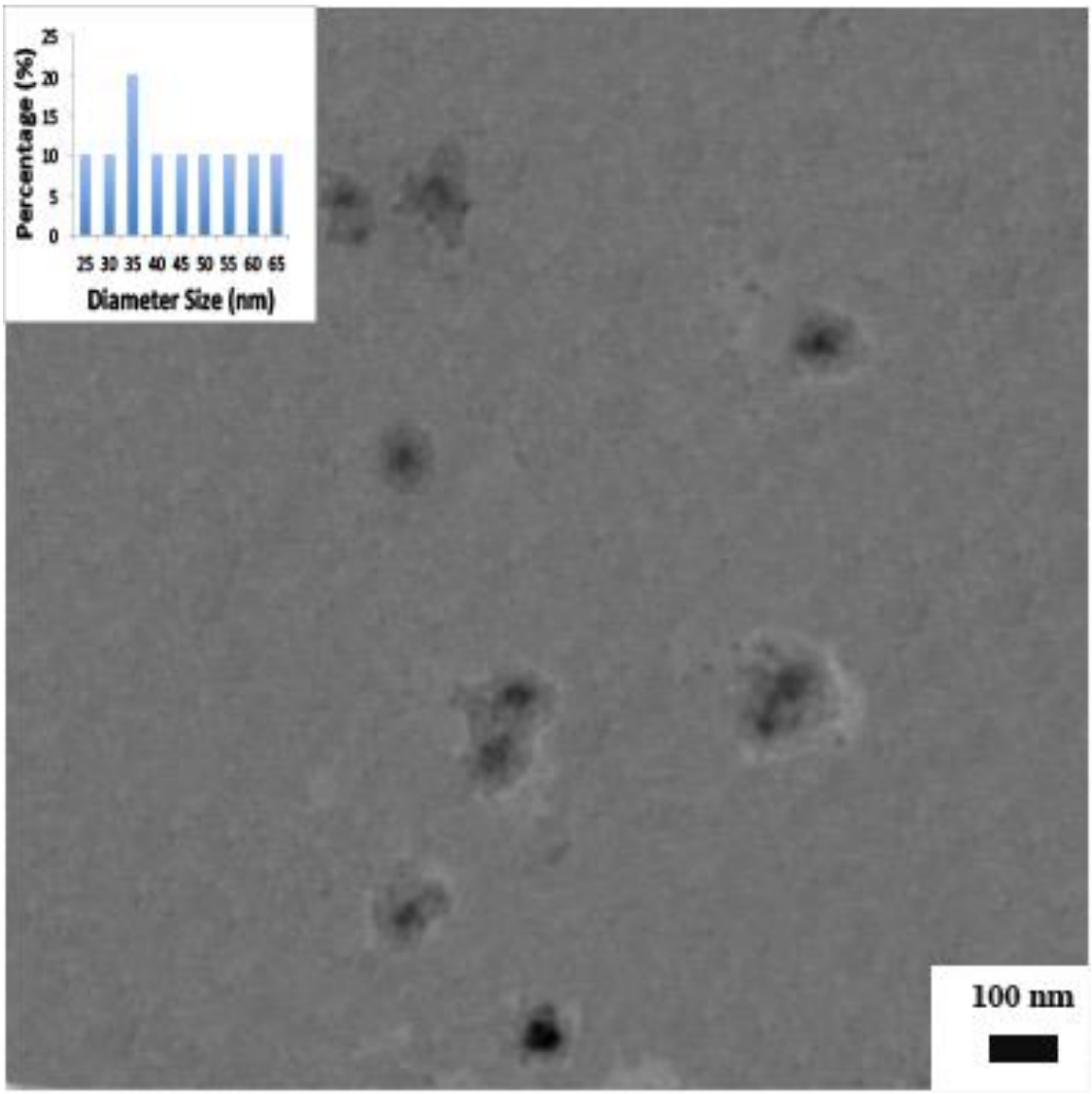

Figure 4.2: TEM Image of the Core-Shell Structures

The picture above illustrates the TEM image of where the silica is layered over the core particles. The scale bar was set to 100 nm and from that measurement; the diameter from the software could be measured.

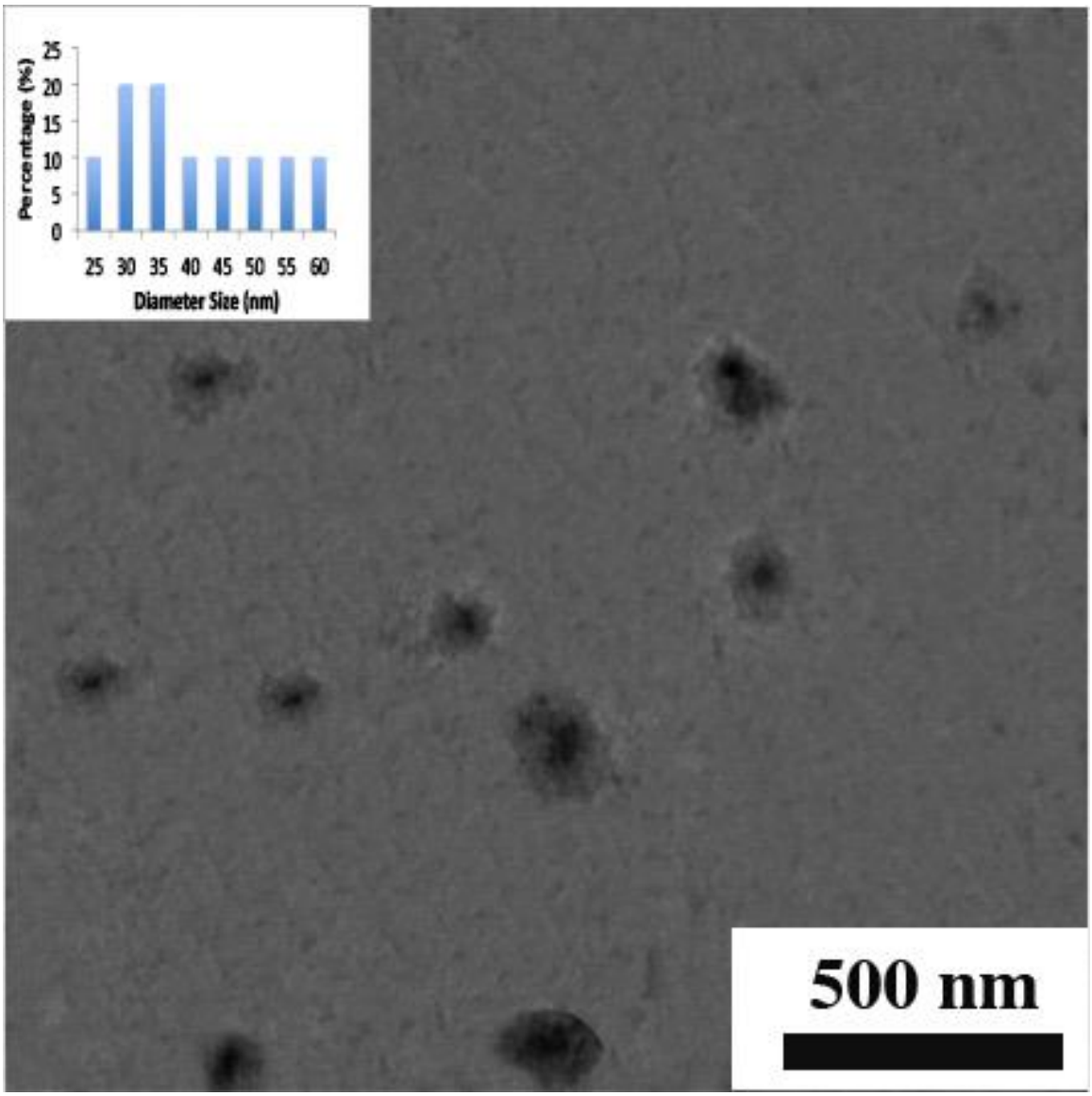

Figure 4.3: TEM Image of the Core-Shell Structures

Table 4.2: Statistical Analysis of Core-Shell Structures

Measure of Central Tendency	Number
Mean	37.9
Mode	35.0
Median	35.0
Max	60.0
Min	25.0
Standard Deviation	11.9

4.5 Fourier Transform (FTIR) Analysis

The Fe_3O_4 nanocrystals, silica-coated Fe_3O_4 nanocrystals and silica-coated Fe_3O_4 nanocrystals with DNA conjugation were identified using a FT-IR spectrometer. In the FT-IR spectra presented in Fig. 4.4, the peaks at around 700 cm^{-1} and 800 cm^{-1} is indicative of the vibration of Fe-O bond.

The FT-IR spectrum of Fe_3O_4@SiO_2 MFNP in Fig. 4.5 shows absorption bands arising from symmetric vibration of Si-O-Si (800 cm^{-1}), asymmetric vibration of Si-OH (1000 cm^{-1}), and asymmetric stretch of Si-O-Si (1100 cm^{-1}). The results prove that the formation of a silica coating on the surface of the Fe_3O_4 MFNC.

The FT-IR spectrum of DNA conjugated on Fe_3O_4@SiO_2 MFNP Fig. 4.6 shows the absorption bands arising from around 700 cm^{-1} are the vibration of the Fe-O bond. The shift in the spectrum of the asymmetric vibration of Si-OH (~1000 cm^{-1}) and asymmetric stretch of Si-O-Si (~1100 cm^{-1}) are shown. The peaks between 1000 cm^{-1} and 2000 cm^{-1} represent the stretches from the bases which is indicative of the DNA and nanoparticles. The stretch around 3700 cm^{-1} represent the –OH peak from the 3’ end of DNA. This represents that DNA has been conjugated onto the MFNP.

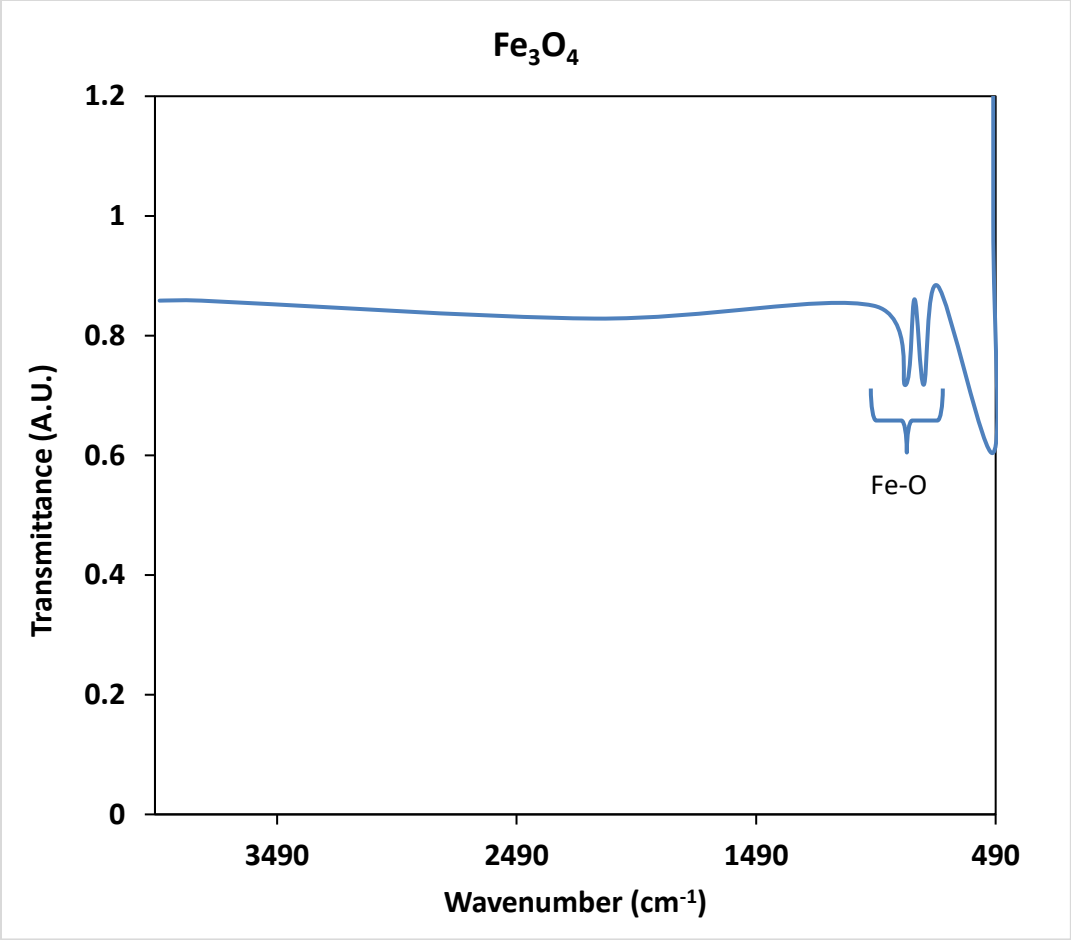

Figure 4.4: FTIR Spectrum of Fe_3O_4 Nanocrystals

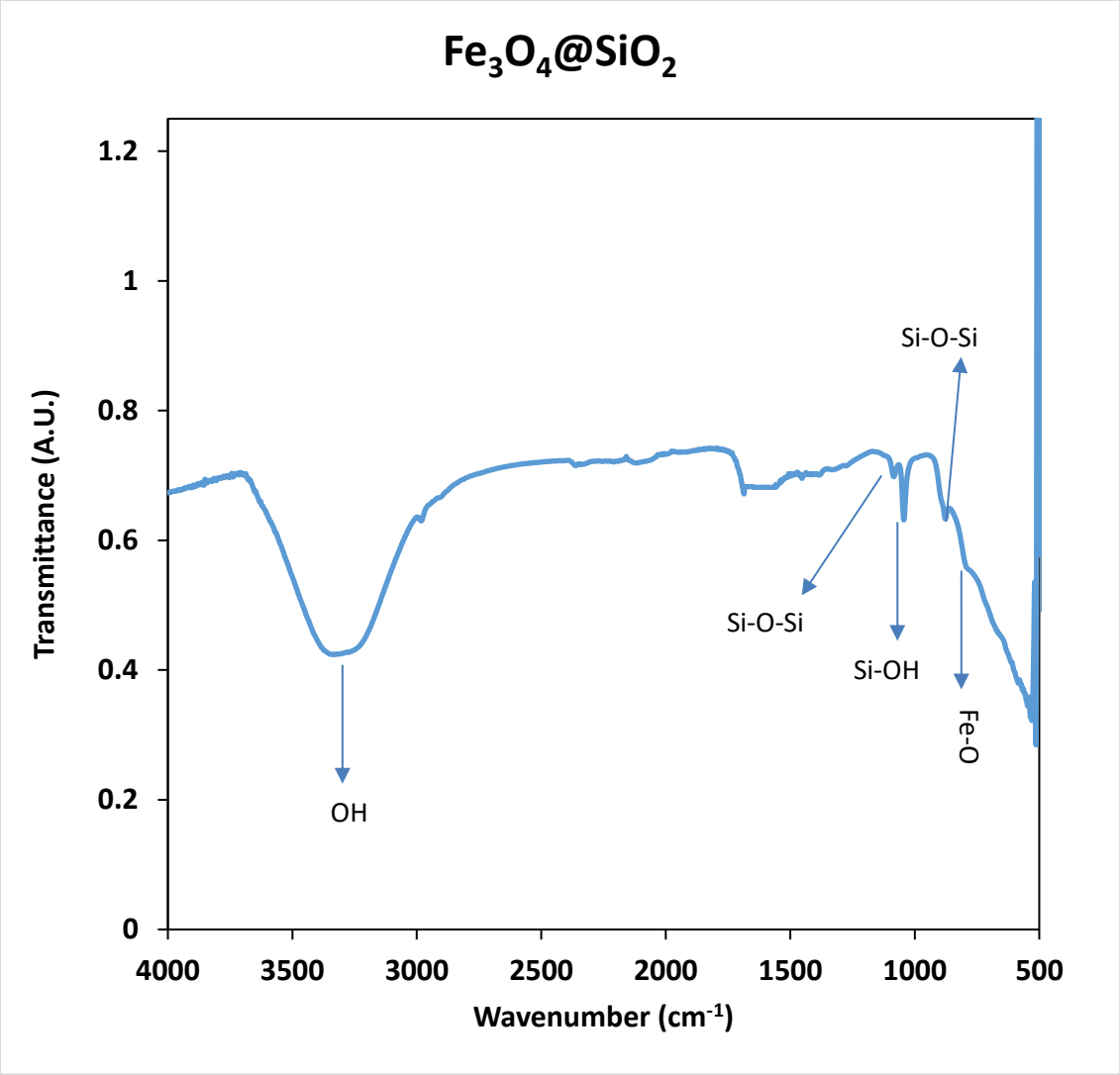

Figure 4.5: FTIR Spectrum of $Fe_3O_4@SiO_2$ Multifunctional Nanostructures

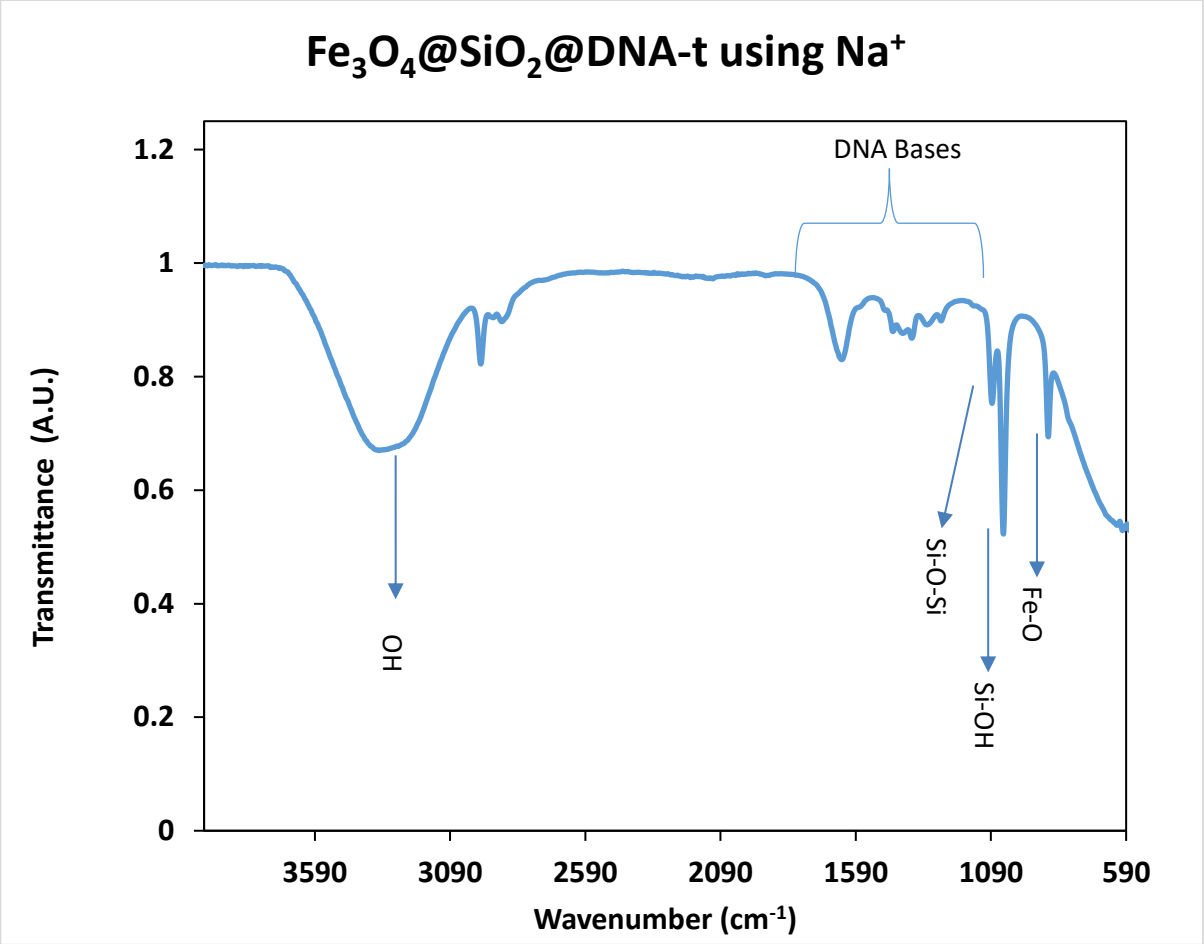

Figure 4.6: FTIR Spectrum of Fe_3O_4@SiO_2@DNA-t

4.6 Vibrating Sample Magnetometer Analysis

The magnetic properties of the Fe_3O_4 nanocrystals were measured by the vibrating sample magnetometer (VSM). The y-axis was represented as the moment (emu/g) and the x axis as Field (G). The hysteresis curve was shown when the data was extrapolated from -1000 G to 1000 G. The saturation magnetization (M_s) of the Fe_3O_4 nanocrystals is dependent on the amount of Fe in the nanocrystals. The saturation magnetization (M_s) of the Fe_3O_4 nanocrystals reached a maximum of 60 emu/g when the magnetic field was approximately at 1000 G. Since there is a hysteresis curve visible, the sample is ferromagnetic. The ferromagnetic sample of Fe_3O_4 has a remanence magnetization (M_r) of around 10 emu/g. The M_r value indicates the magnetization left in the sample when the external magnet is removed. The ferromagnetic sample in Fig. 4.7 has a

coercivity (H_c) of around 50 G. The coercivity indicates how much magnetization is needed to bring back the field to 0 G.

The magnetic properties of the synthesized Fe_3O_4@SiO_2 were measured by the vibrating sample magnetometer (VSM) shown in Fig. 4.8. The y-axis was represented as the moment (emu/g) and the x-axis as Field (G). With the data extrapolation to represent the field from -1000 G to 1000 G, the hysteresis curve was represented. The saturation magnetization (M_s) of the silica bound Fe_3O_4 nanocrystals was 15 emu/g when the field was around 750 G. The remanence magnetization (M_r) value indicates it is around 2.5 emu/g and the coercivity is around 50 G. With the silica shell surrounding the core, it shows the magnetization dropped due to various reasons. One reason could be due to the oxidation of Fe_3O_4 and the encapsulation of the shell makes the core lose some of its magnetization.

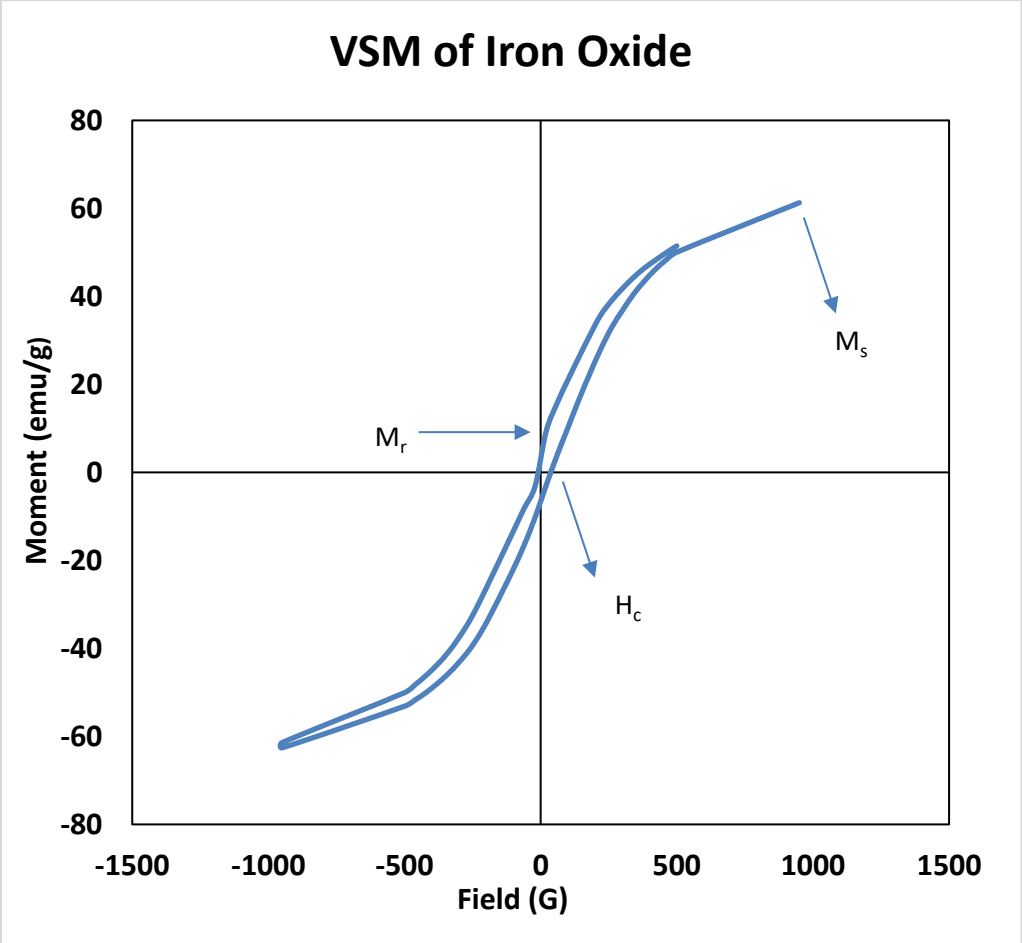

Figure 4.7: VSM of Iron Oxide Nanocrystals

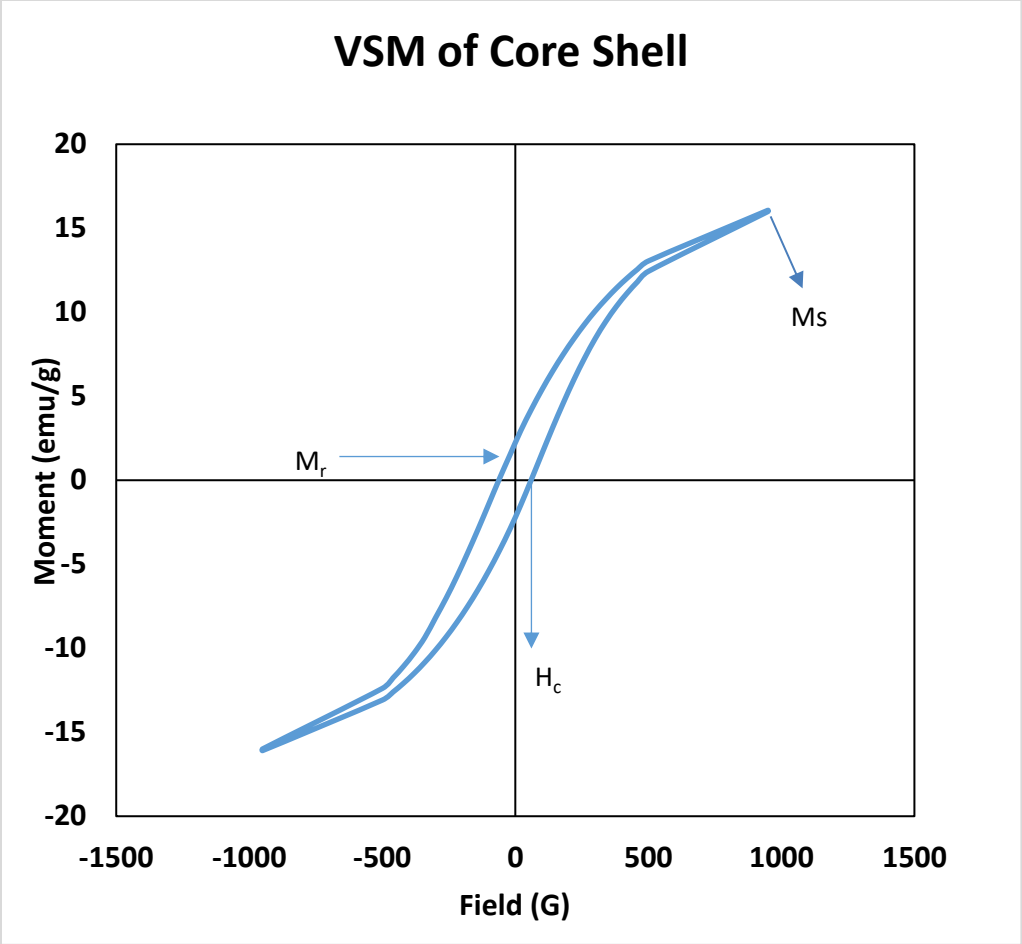

Figure 4.8: VSM of Core Shell Structures

4.7 UV Absorption Tests for DNA-c Conjugated on Graphene Oxide

Before hybridizing DNA-c with DNA-t, the UV tests were done to analyze to see if DNA-c was conjugated onto graphene oxide. The graphene oxide solution in ethanol has an absorbance peak at around 220 nm. After DNA-c was conjugated, the absorbance peak was around 260 nm to represent the peak for DNA and the 220 nm of graphene oxide was still shown. This concept shows that the capture probe DNA was successfully conjugated using the bridging effect at 10 µM. In Fig. 4.9, it shows the UV tests for DNA-c, and DNA-c on GO.

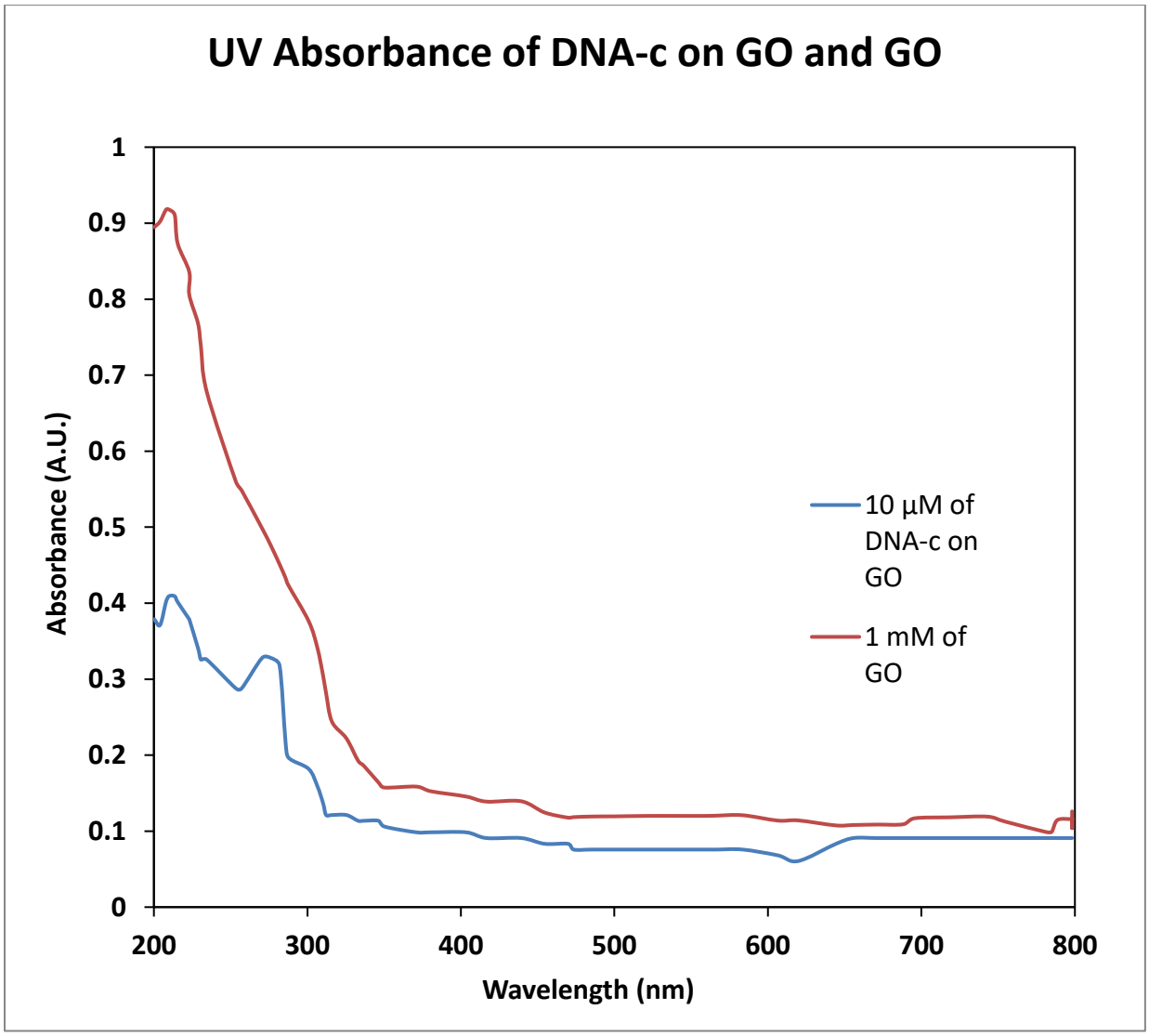

Figure 4.9: UV Absorption of DNA-c on GO and GO

4.8 Fluorescent Studies and Analysis

The DNA-t was done at different concentrations to bind to the iron oxide-silica (core-shell) structures without hybridization. The fluorescence intensity of the MFNPs was observed to decrease with increasing the concentration of DNA-t.

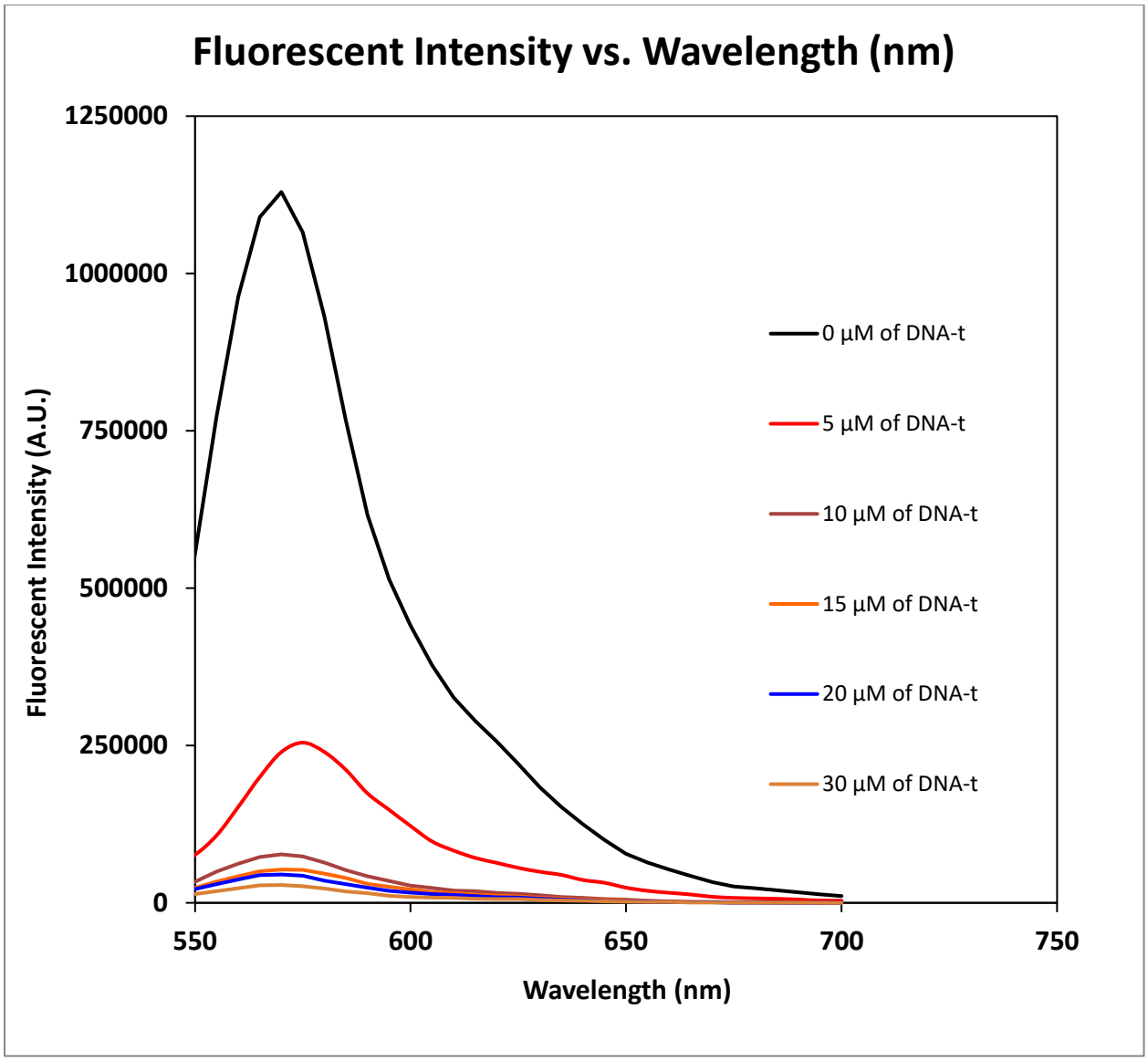

Figure 4.10: The Fluorescent Intensity of DNA-t on Iron Oxide Silica (Core-Shell) Nanostructures

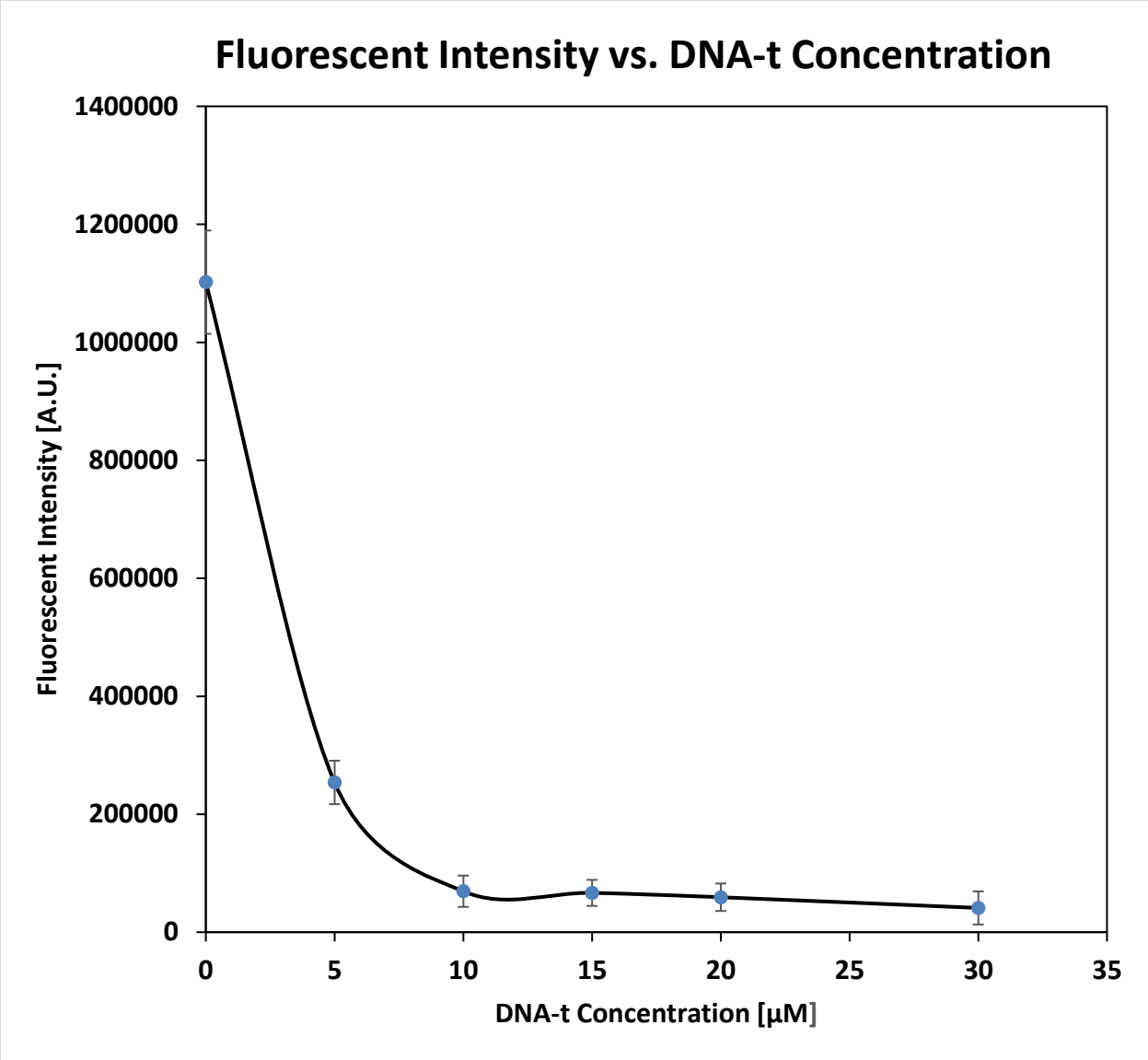

Figure 4.11: Fluorescent Intensity vs. DNA-t Concentration

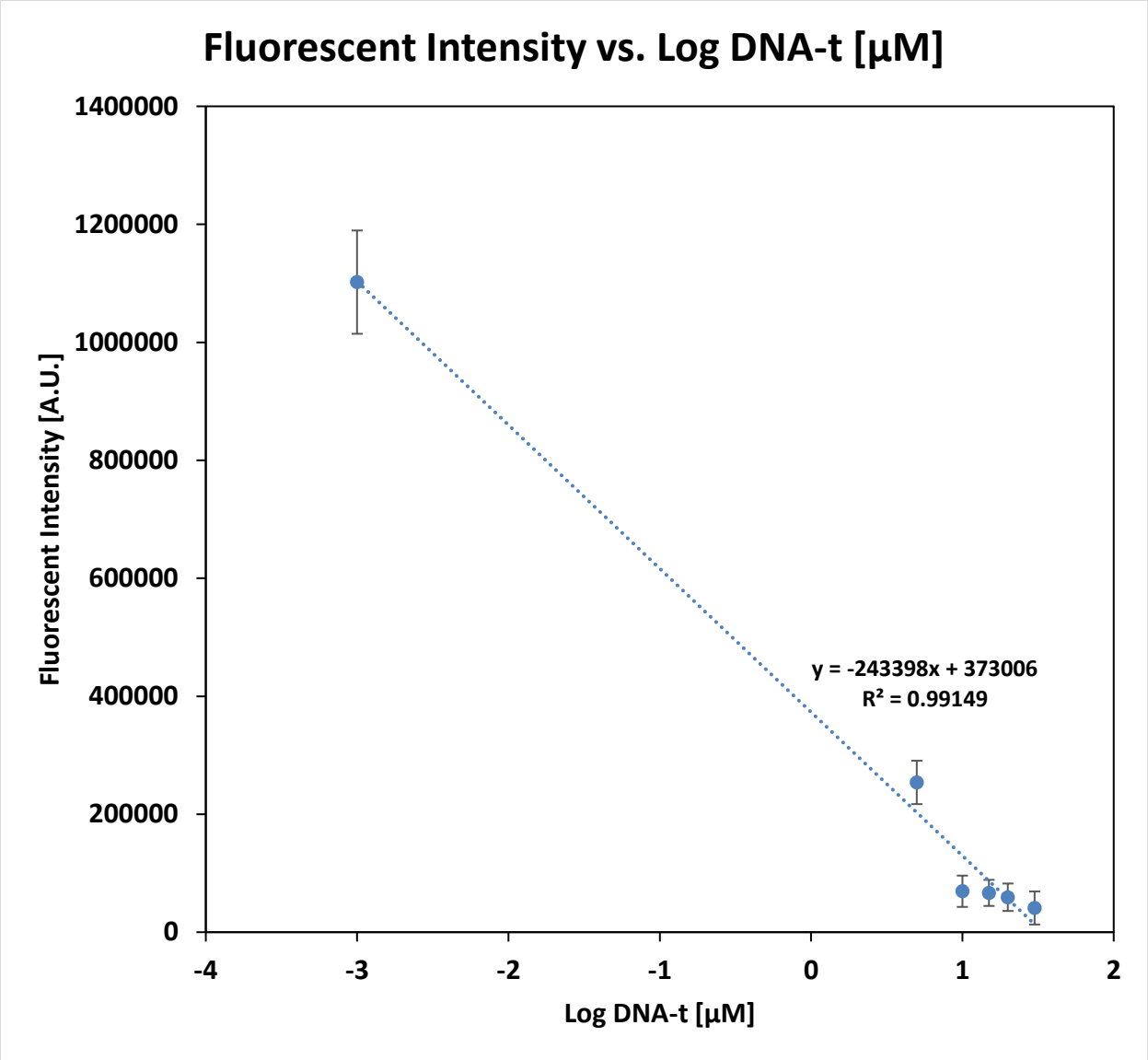

Figure 4.12: Fluorescent Intensity vs. LOG (DNA-t)

The DNA-t binding to Fe_3O_4@SiO_2 through the cation bridge of Na^+ was conducted at different concentrations to see how sensitive it could be. These tests were conducted without hybridization. Without the hybridization, Fig. 4.10 showed the fluorescence intensity (FL) at 580 nm and was sensitive to the target DNA and decreased with increasing concentration of target DNA. The dependence of fluorescence intensity on target DNA concentration is plotted in Fig. 4.11. The fluorescence intensity was proportional to the logarithmic concentration of target DNA shown in Fig. 4.12. The regression equation is expressed as y= -243398x+373006 with a correlation coefficient R^2 of 0.99149, where y is the fluorescence intensity and x is the

concentration of target DNA. The detection limit, based on 3 σ/slope (where σ was the standard deviation of the background signal) was 0.25 µM.

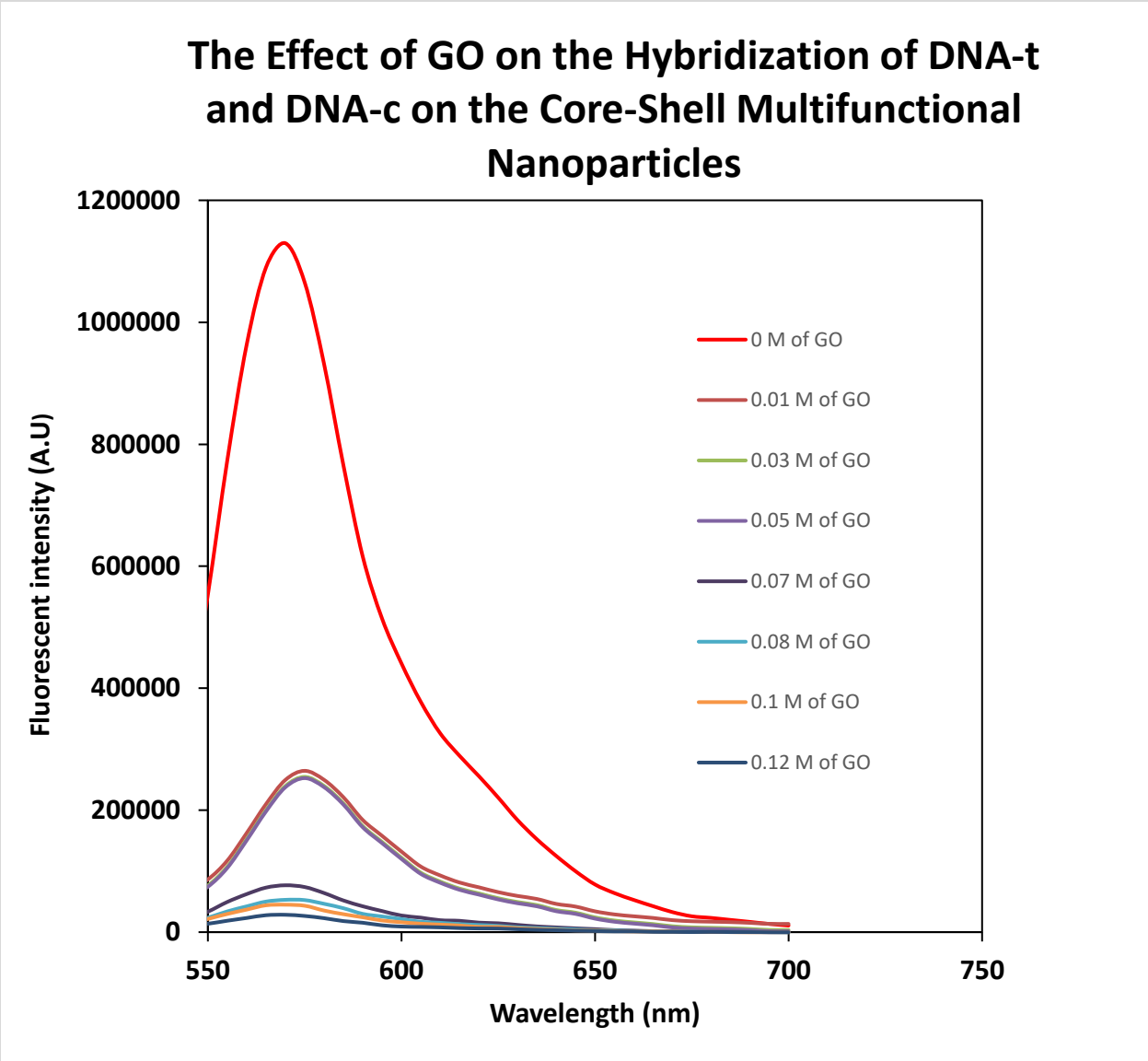

Figure 4.13: The Fluorescent Intensity on The Effect of GO

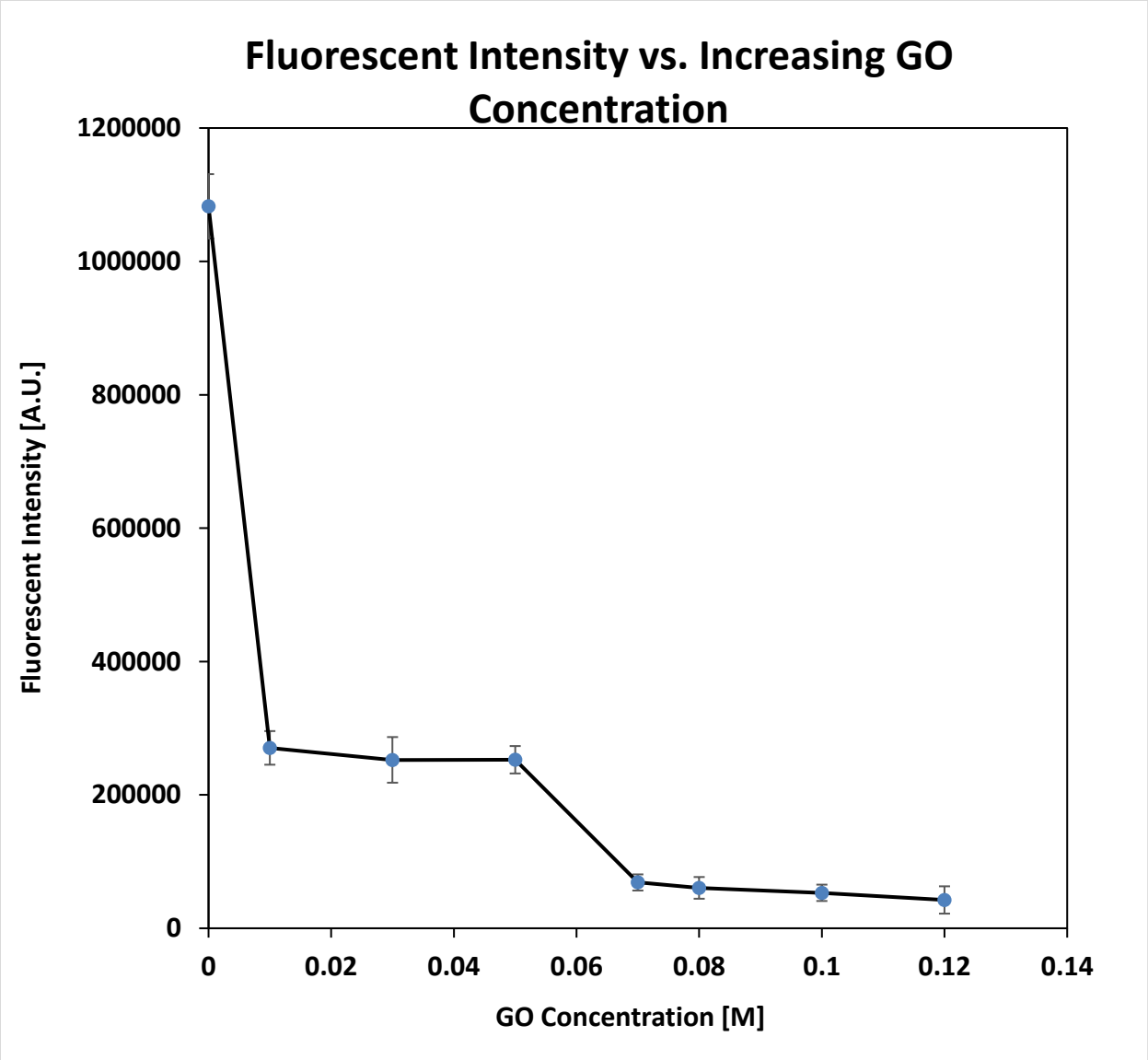

Figure 4.14: Fluorescent Intensity vs. GO Concentration

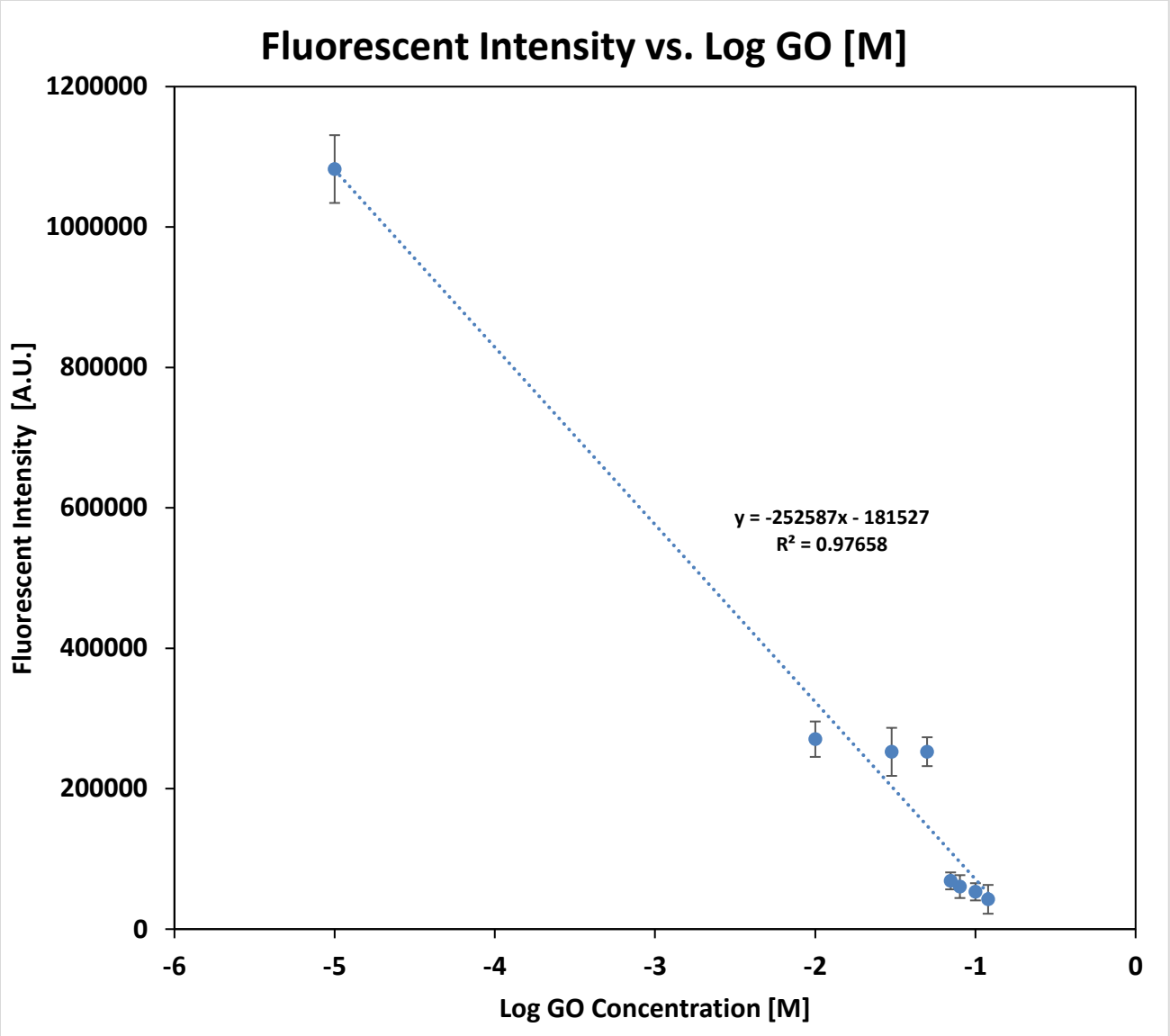

Figure 4.15: Fluorescent Intensity vs. LOG GO [M}

The DNA-t conjugated onto $Fe_3O_4@SiO_2$ through the cation bridge of Na^+ was hybridized with DNA-c onto graphene oxide through the Na^+ were found to emit luminescence at around 580 nm. The fluorescence intensity of the MFNPs was observed to decrease with increasing the concentration of DNA-t. The emission intensity implied that the $Fe_3O_4@SiO_2$ could interact with DNA-t.

Keeping the concentration of the DNA-c constant, DNA-t constant, the concentration of the MFNP constant gave the correspondence of the fluorescence at different concentrations where

the GO was detected and analyzed. The fluorescence spectra of the system upon the addition of GO was shown in Fig. 4.13. In the absence of the GO, the solution emitted strong fluorescence. From Fig. 4.13, it showed that the fluorescence intensity (FL) at 580 nm was highly sensitive to the target DNA and decreased with increasing concentration of GO. The dependence of fluorescence intensity on GO concentration is plotted in Fig. 4.14. The fluorescence intensity was proportional to the logarithmic concentration of GO is shown in Fig. 4.15. The regression equation is expressed as y=-252587x-181527 with a correlation coefficient R^2 of 0.97658, where y is the fluorescence intensity and x is the concentration of GO. The detection limit, based on 3 σ/slope (where σ was the standard deviation of the background signal) was 0.0059 M.

4.9 Summary

In summary, the multifunctional nanoparticle was synthesized to study the sensitivity of the target DNA through the charging effect from 0-30 μM of DNA-t. It was found that the limit of detection was as low as 0.25 μM based on the range of 0-30 μM of DNA-t. Once the target DNA was hybridized with the complementary DNA, the effect of graphene oxide was studied to see if it had any effect on the fluorescent multifunctional nanoparticle. The range of graphene oxide was studied from 0-0.12 M and the limit of detection was as low as 5.9 μM from the quenching effect.

4.10 References

[1] Huang Y, He S, Cao W, Cai K, Liang X. Biomedical nanomaterials for Imaging-guided cancer therapy. Nanoscale. 2012;4: 6135-6149

[2] Hubbell J, Chilkoti A. Nanomaterials for Drug Delivery. Science. 2012; 337:303-305

[3] Holzinger M, Goff A, Cosnier S. Nanomaterials for Biosensing Review. Front. Chem. 2014; 27: 1-10

[4] Teja A, Koh P. Synthesis, properties, and applications of magnetic iron oxide nanoparticles. Progress in Crystal Growth and Characterization of Materials. 2009;55:22-45

[5] Wu W, He Q, Jiang C. Magnetic Iron Oxide Nanoparticles: Synthesis and Surface Functionalization Strategies. Nanoscale Res Lett. 2008; 3:397-415

[6] Laurent S, Forge D, Port M, Roch A, Robic C, Elst L, Muller R. Magnetic Iron oxide Nanoparticles: Synthesis, Stabilization, Vectorization, Physicochemical Characterizations, and Biological Applications. Chem. Rev. 2008; 108: 2064-2110

[7] Colombo M, Romero S, Casula M, Gutierrez L, Morales M, Heverhagen J, Prosperi D, Parak W. Biological Applications of Magnetic Nanoparticles. Chem. Soc. Rev. 2012; 41: 4306-4334

[8] Indira T, Lakshmi P. Magnetic Nanoparticles- A review. International Journal of Pharmaceutical Sciences and Nanotechnology. 2010;3: 1035-1042

[9] Frey N, Peng S, Cheng K, Sun S. Magnetic Nanoparticles: synthesis, functionalization, and applications in bio-imaging and magnetic energy storage. Chem. Soc. Rev. 2009; 38: 2532-2542

[10] Travers A, Muskhelishvili G. DNA structure and function. FEBS Journal. 2015; 282: 2279-2295

[11] Lindahl T. Instability and decay of the primary structure of DNA.

[12] Hunter C. Sequence-dependent DNA Structure: The Role of Base Stacking Interactions. Journal of Molecular Biology. 1993;230: 1025-1054

[13] Sancar A. Structure and Function of DNA Photolyase. Biochemistry. 1994;33: 2-9

[14] Shahriary L, Athawale A. Graphene Oxide Synthesized by using Modified Hummers Approach. International Journal of Renewable Energy and Environmental Engineering. 2014; 2: 58-63

[15] Marcano D, Kosynkin D, Berlin J, Sinitskii A, Sun Z, Slesarev A, Alemany L, Tour J. Improved Synthesis of Graphene Oxide. Nano. 2010; 4: 4806-4814

[16] Chen J, Yao B, Li C, Shi G. An Improved Hummers method for eco-friendly synthesis of graphene oxide. Carbon. 2013; 64: 225-229

[17] Zhu Y, Murali S, Cai W, Li X, Suk J, Potts J, Ruoff R. Graphene and Graphene Oxide: Synthesis, Properties, and Applications. Adv. Materials. 2010;22:3906-3924

Chapter 5 : Development of Multifunctional Nanoparticles for DNA Sensing Using Covalent Bonding

The design approach constructs using the covalent bonding technique between DNA-t and the silica particles with the use of glutaraldehyde.

The production of graphene oxide (GO) using Hummer's approach was obtained and the conjugation with DNA-c was established. UV spectroscopy was used to confirm the DNA-c conjugated onto graphene oxide (GO). FTIR tests were also instigated to see the difference when DNA-c was conjugated onto GO through the use of covalent bonding as well with the use of glutaraldehyde.

Once the two systems above were established, the hybridization between the DNA-t and the DNA-c took place. Fluorescence studies also took place to see the quenching technique between the system at different target probe DNA concentrations to study the selectivity and sensitivity of the interaction through the use of covalent bonding.

5.1 Introduction

The magnetic nanostructures can have different bonding techniques for the same application to see how it varies from other validation strategies. Different designs will show which is more effective. Researchers are constantly finding ways for a best suitable approach for the optimal interaction between the DNA and the nanomaterial. Different functionalization strategies are in place for the interactions to take place. Some strategies propose a better bonding interaction whereas others are not as compatible. [1,2]

The strategy in producing the core and the core-shell structure is the same way as Chapter 4. In this chapter, modification and functionalization strategies are proposed in order for the covalent bonding strategies to take place. 5' Mod on the DNA structure which adds an amino group will be taking place and functionalization strategies on the silica particles with another amino group on the outer surface will be in place where the interaction with glutaraldehyde can be used for the covalent bonding technique.

However, while they have obtained some achievements in the area of magnetic-DNA bonding with the hybridization of other DNA molecules, there are still potential drawbacks in practical applications: (1) the interaction has the potential to leach out from the interaction from the DNA to silica particles or to the graphene oxide during its application, and (2) it is a challenge to precisely control the loading amount of glutaraldehyde and DNA amount to the silica particles as well as the loading of DNA-c on graphene oxide and then tailor to the properties for its desired application.

5.2 The Design Approach with the Binding Strategy

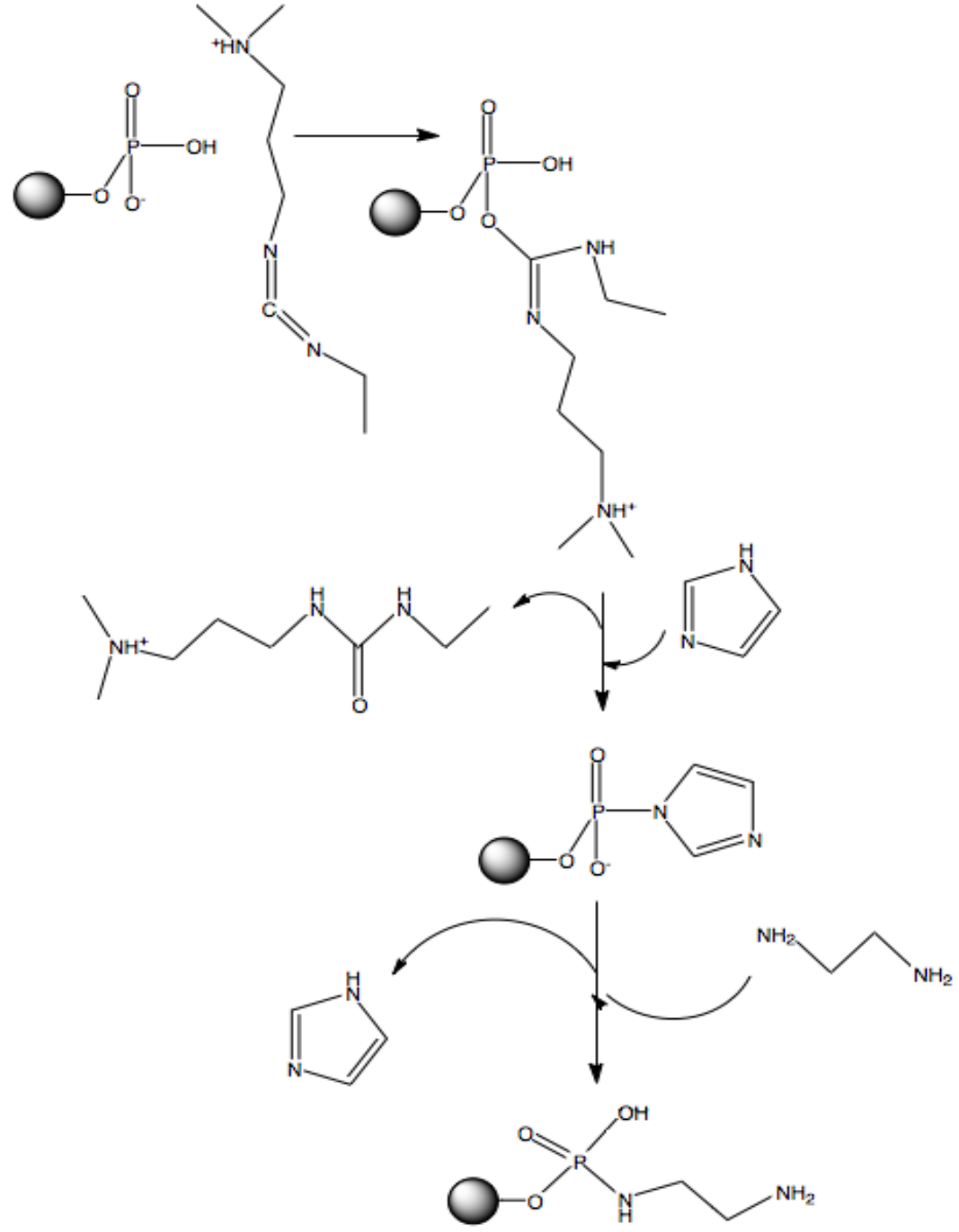

Figure 5.1: 5' Modification of DNA

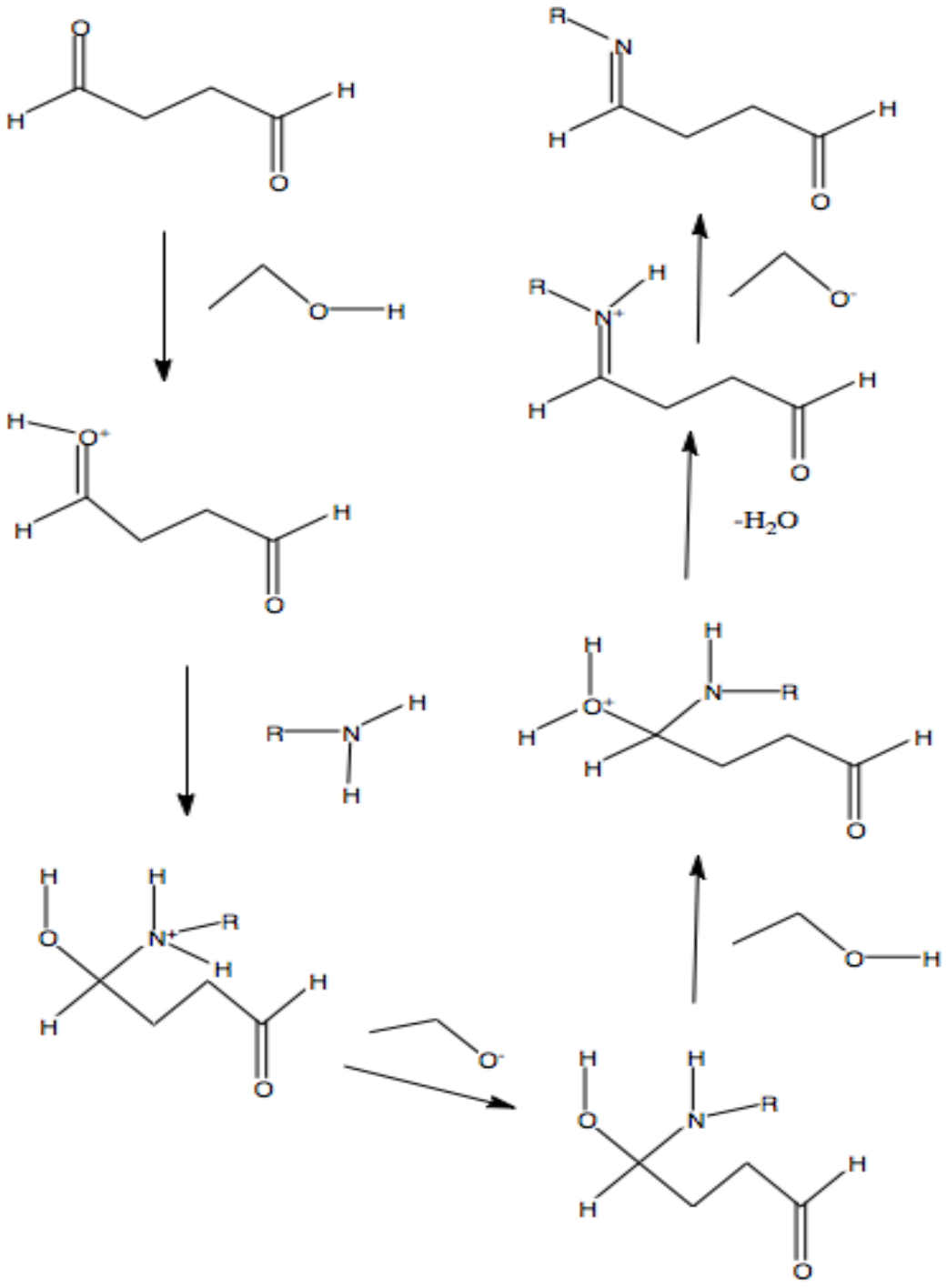

Figure 5.2: Imine Reaction of Amine to Glutaraldehyde

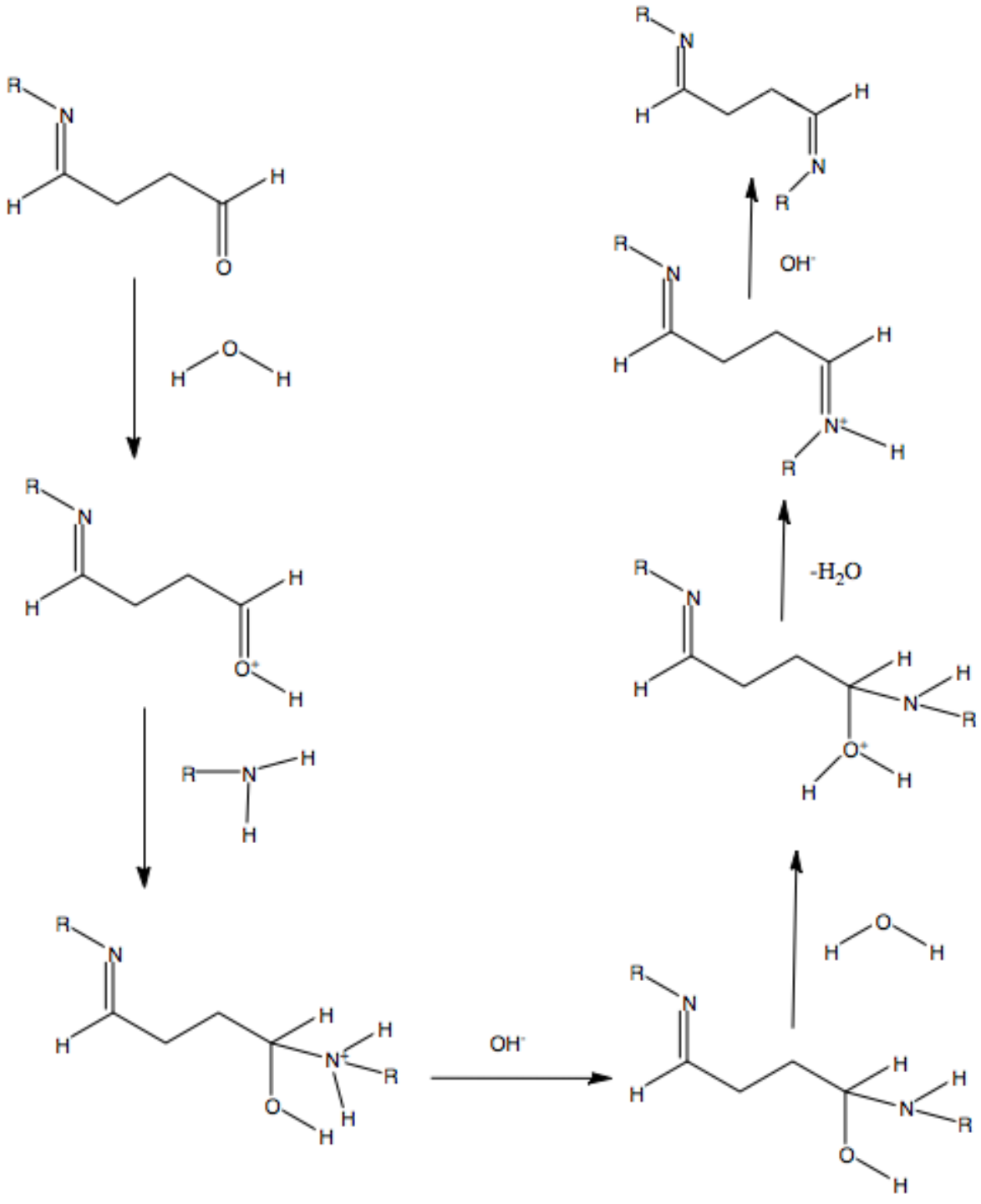

Figure 5.3: Imine Reaction of the 5' Mod DNA to Glutaraldehyde

In Fig. 5.1, it shows the 5' Mod of DNA on the phosphate backbone. In Fig. 5.2, it shows the amino group onto the silica group attaching to the glutaraldehyde through the imine reaction. In Fig. 5.3, it shows the 5' Mod DNA attaching to the other side of the glutaraldehyde.

5.3 Fourier Transform Infrared Spectroscopy Analysis

The silica-coated Fe_3O_4 nanocrystals, $Fe_3O_4@SiO_2@NH_2$, glutaraldehyde, $Fe_3O_4@SiO_2@NH_2@Glu$, DNA-t on glutaraldehyde, DNA t-glutaraldehyde-silica particles will be shown to characterize its peaks by Fourier Transform Infrared Spectroscopy.

The FT-IR spectrum of $Fe_3O_4@SiO_2$ MFNP in Fig. 5.4 shows absorption bands arising from symmetric vibration of Si-O-Si (800 cm^{-1}), asymmetric vibration of Si-OH (1000 cm^{-1}), and asymmetric stretch of Si-O-Si (1100 cm^{-1}). The results prove the formation of silica coating on the surface of the Fe_3O_4 MFNC. The dip around 3250 cm^{-1} is due to iron oxide- silica in the water.

The FT-IR spectrum of $Fe_3O_4@SiO_2@NH_2$ in Fig. 5.5 shows the two peaks at around 3250 cm^{-1} which indicates the amino peaks have been coated onto the surface of the iron oxide-silica particles.

The FT-IR spectrum of glutaraldehyde in Fig. 5.6 shows the C=O bond stretch at around 1600 cm^{-1}. The dip at around 3400 cm^{-1} shows that glutaraldehyde is suspended in water.

The FT-IR spectrum of $Fe_3O_4@SiO_2@NH_2$- Glutaraldehyde in Fig. 5.7 shows absorption bands arising from the asymmetric stretch of Si-O-Si (1000 cm^{-1}), C=N stretch (1600 cm^{-1}), and C=O stretch (1800 cm^{-1}). The peak around 3400 cm^{-1} arises due to the compound suspended in water which corresponds to the –OH group.

The FT-IR spectrum of $Fe_3O_4@SiO_2@NH_2@$Glutaraldehyde@DNA 5' Mod in Fig. 5.8 shows the absorption bands where the Fe-O stretch is visible around 700 cm^{-1}, asymmetric stretch of Si-O-Si (1000 cm^{-1}), the small signal peaks associated past 1000cm^{-1} to 1400 cm^{-1} is associated with the bases from the DNA, C=N stretch is associated with the 1600 cm^{-1} which has been shifted, the 3' end of DNA is around 3400 cm^{-1} collaborates to –OH peak.

The FT-IR spectrum of graphene oxide in Figure 5.9 shows the absorption bands where the C=O is around 2000 cm^{-1} and the –OH peak is around 3500 cm^{-1}.

The FT-IR spectrum of DNA-c in Figure 5.10 shows the absorption bands where the phosphate backbone is showing a band around 870 cm^{-1}, bands showing from 1260 to 1360 cm^{-1} are from the bases of the DNA and the –OH group corresponding to 3400 cm^{-1}.

The FT-IR spectrum of 5’ Mod DNA-c on GO in Figure 5.11 shows the absorption bands where the phosphate backbone is visible around 800 cm^{-1}, DNA bases (930-1218 cm^{-1}), C=O is associated around 1361 cm^{-1}, C=N is associated around 1562 cm^{-1}, OH peak around 3038 cm^{-1}, and the secondary imine peak around 3267 cm^{-1}.

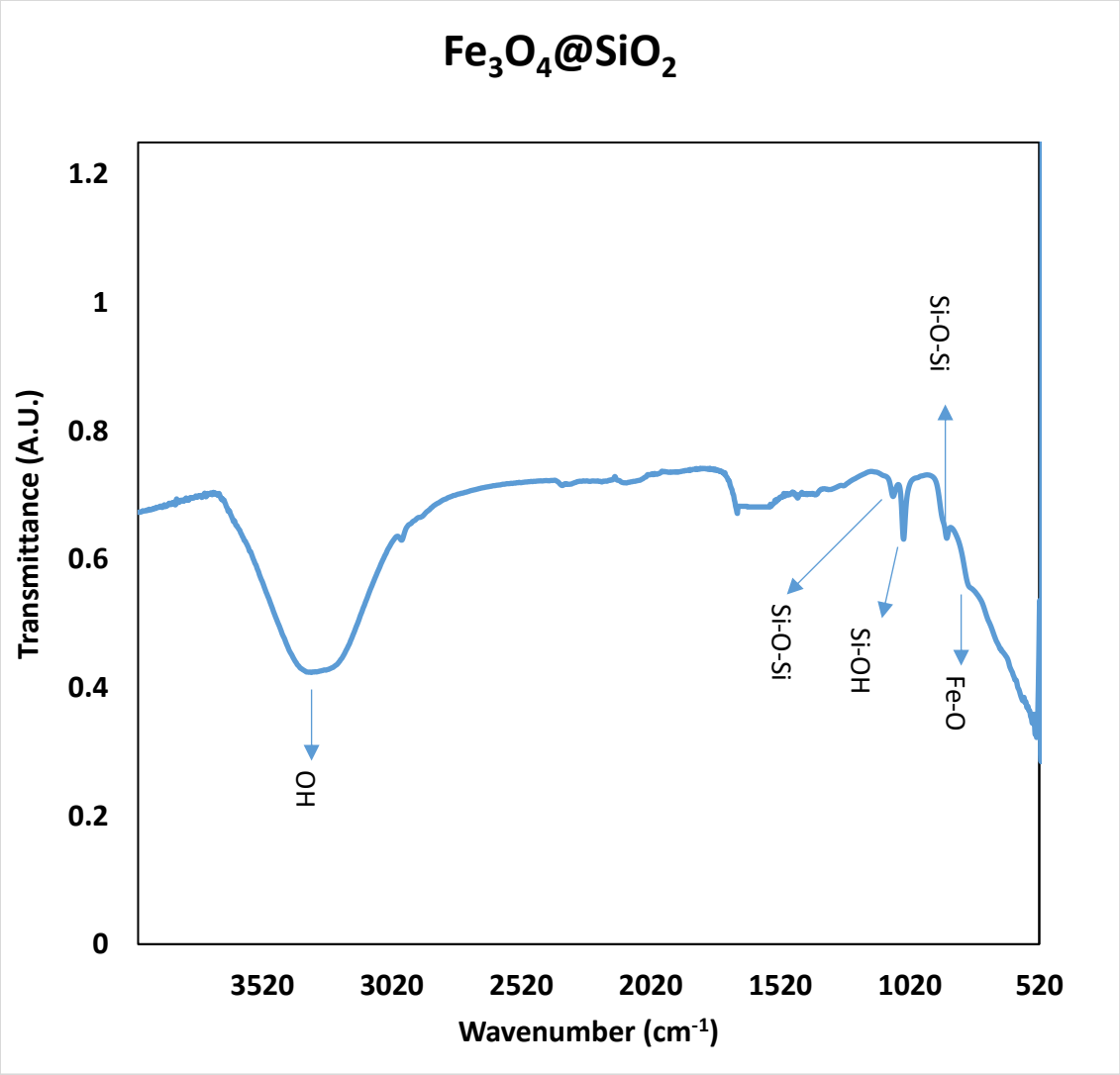

Figure 5.4: FTIR Spectrum of Fe_3O_4@SiO_2

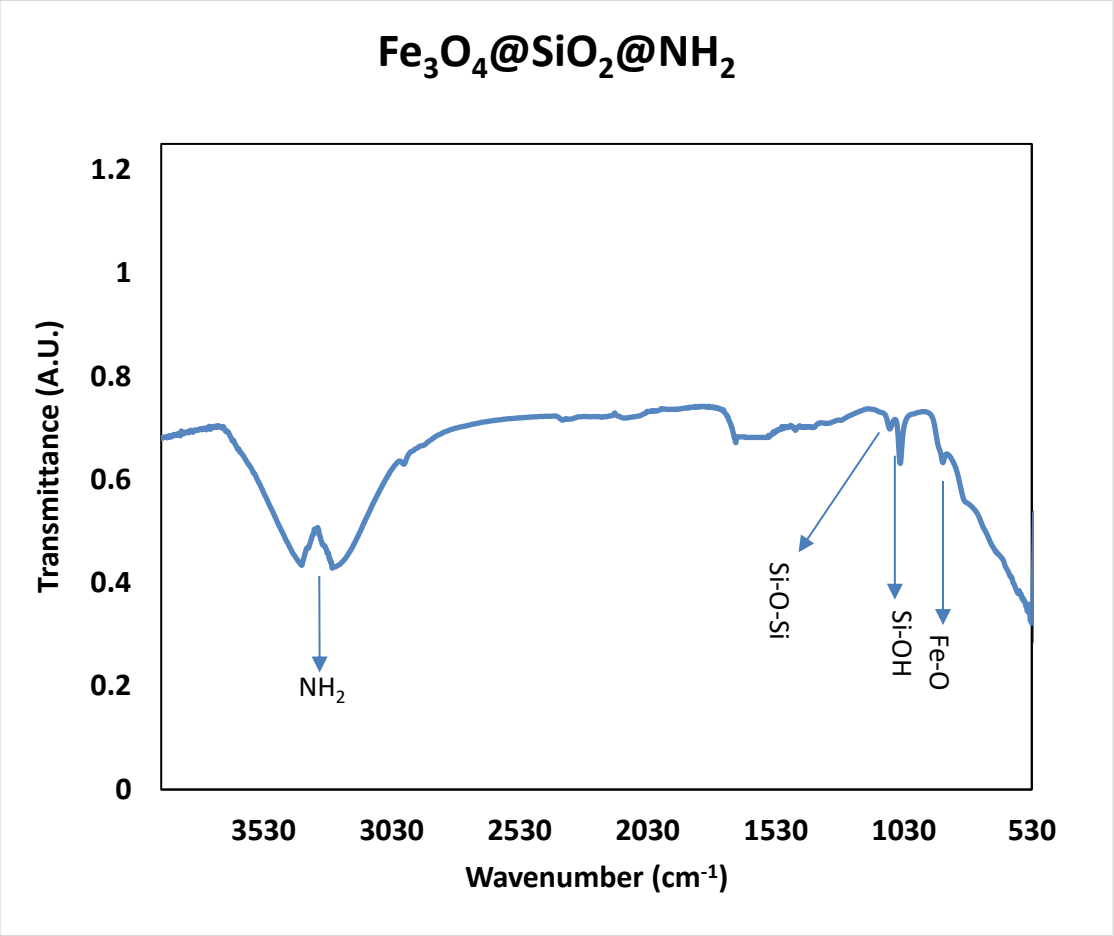

Figure 5.5: FTIR Spectrum of $Fe_3O_4@SiO_2@NH_2$

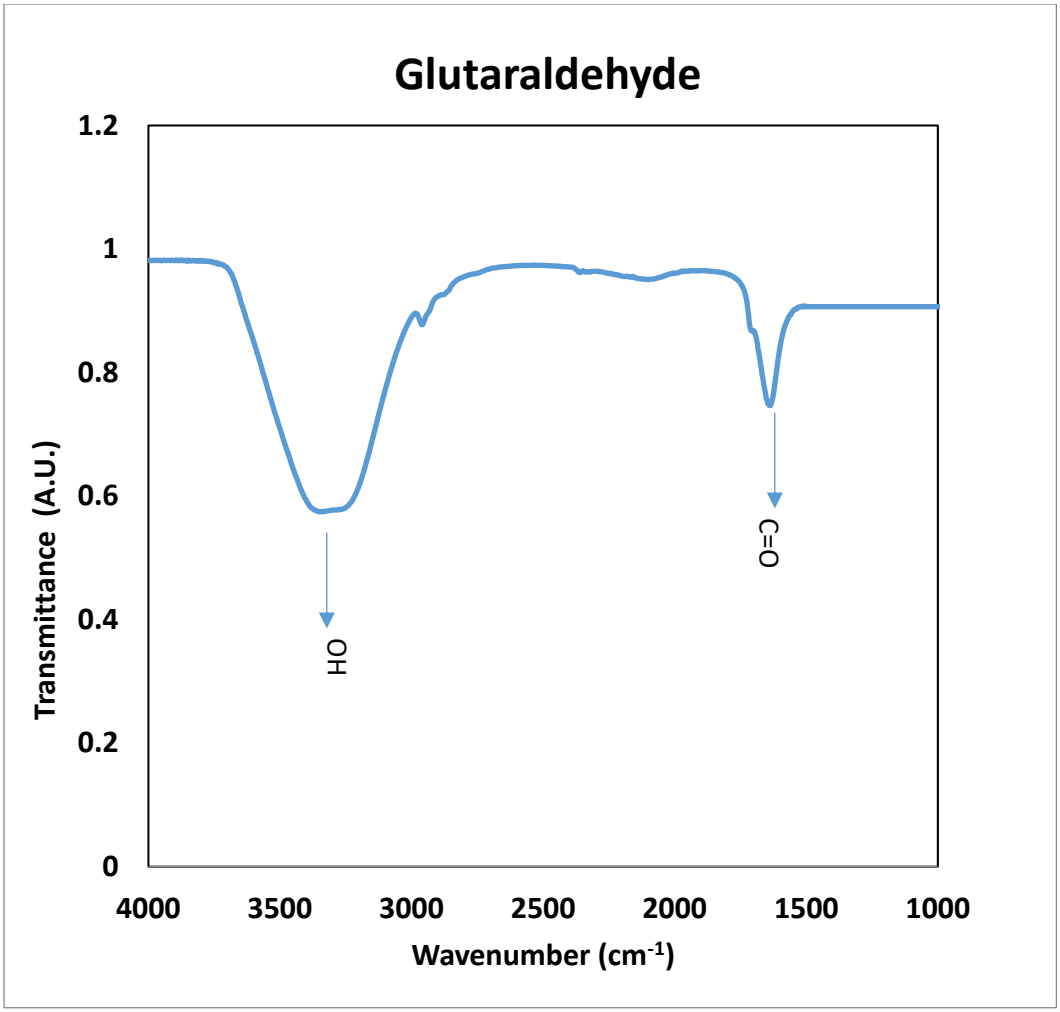

Figure 5.6: FTIR Spectrum of Glutaraldehyde

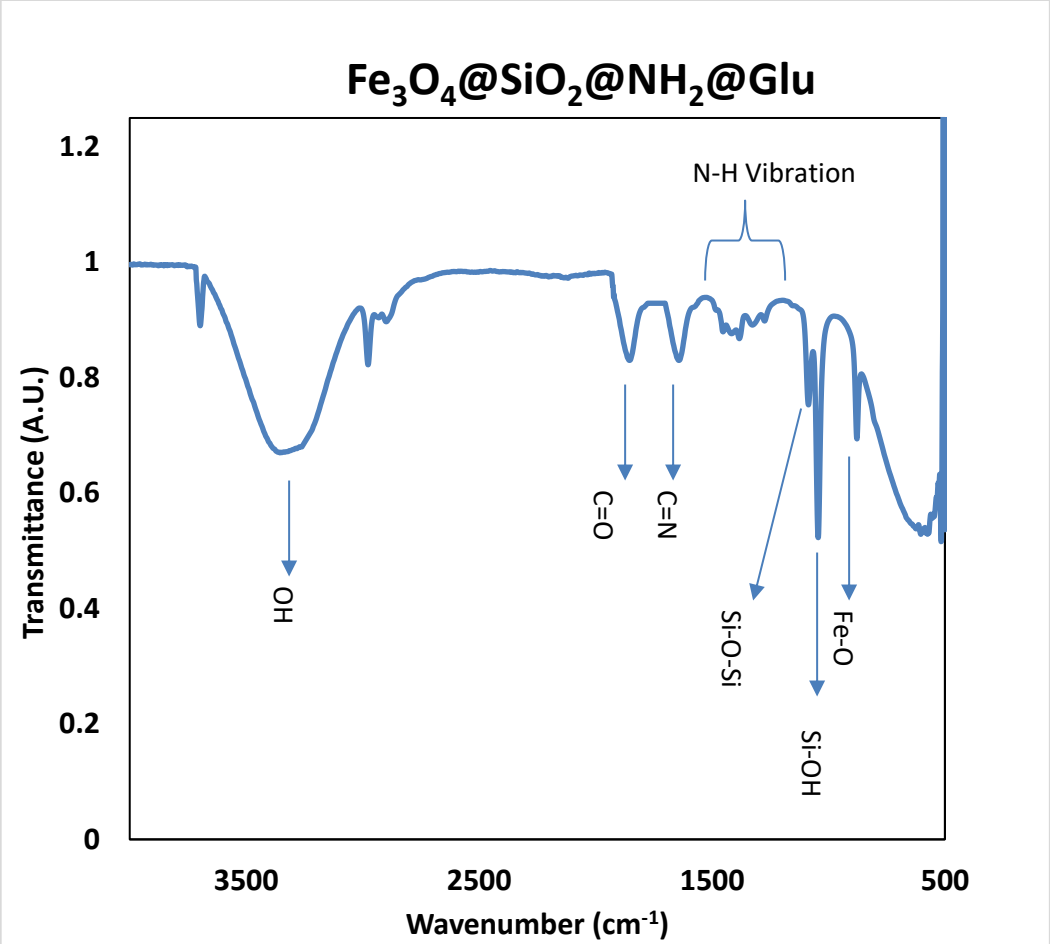

Figure 5.7: FTIR Spectrum of $Fe_3O_4@SiO_2@NH_2@Glu$

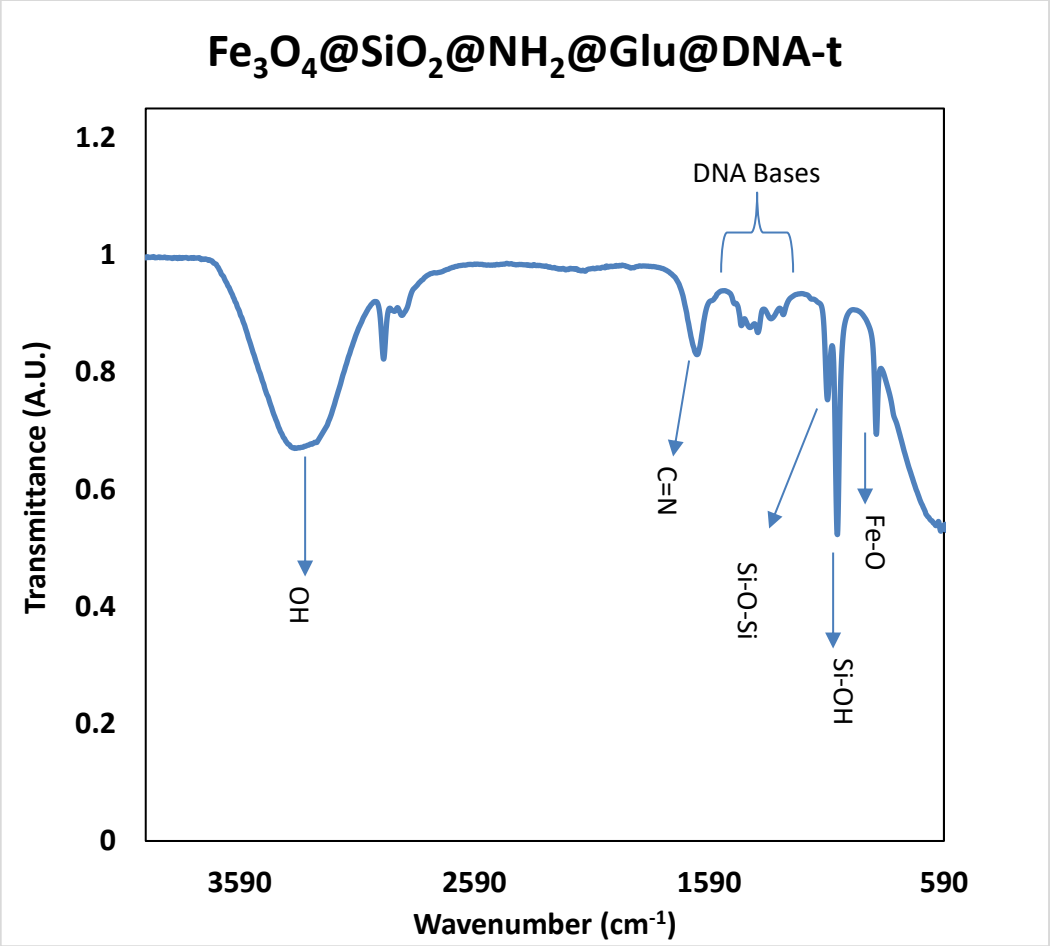

Figure 5.8: FTIR Spectrum of Fe_3O_4@SiO_2@NH_2@Glu@DNA-t

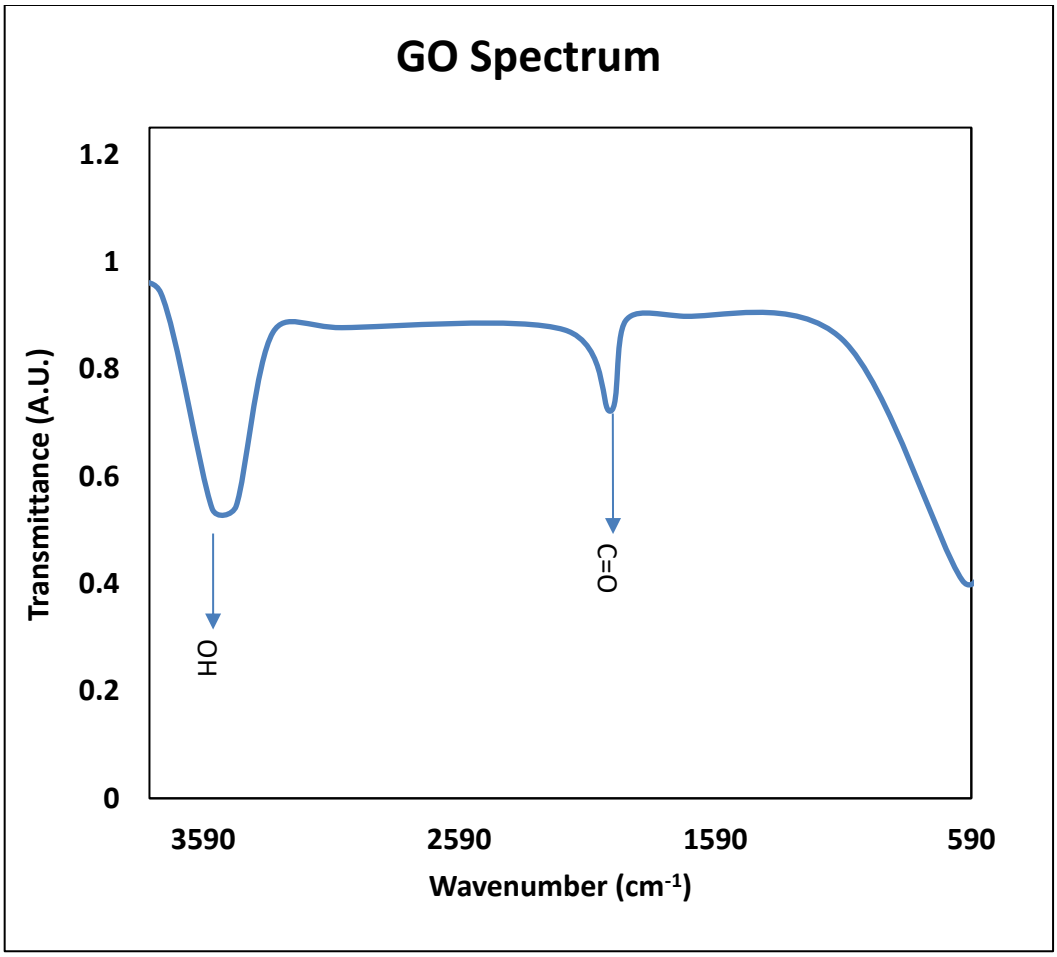

Figure 5.9: FTIR Spectrum of GO

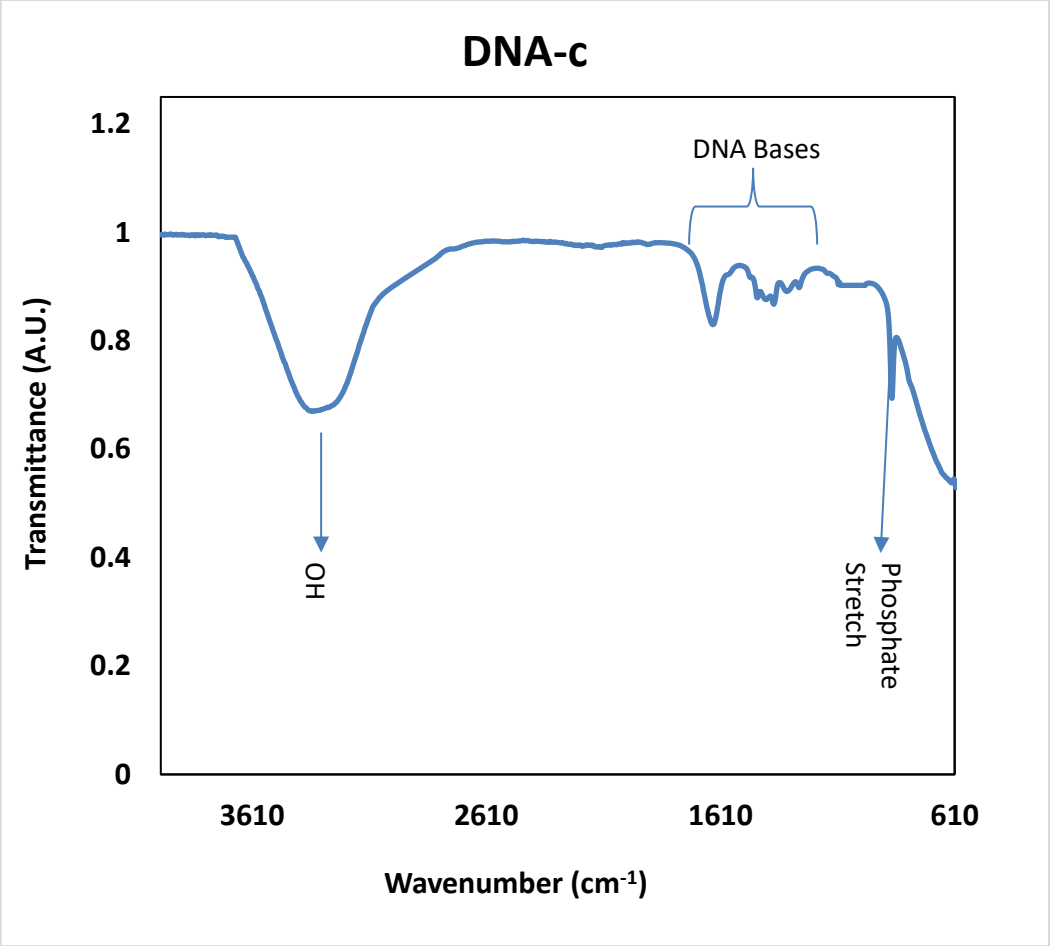

Figure 5.10: FTIR Spectrum of DNA-c

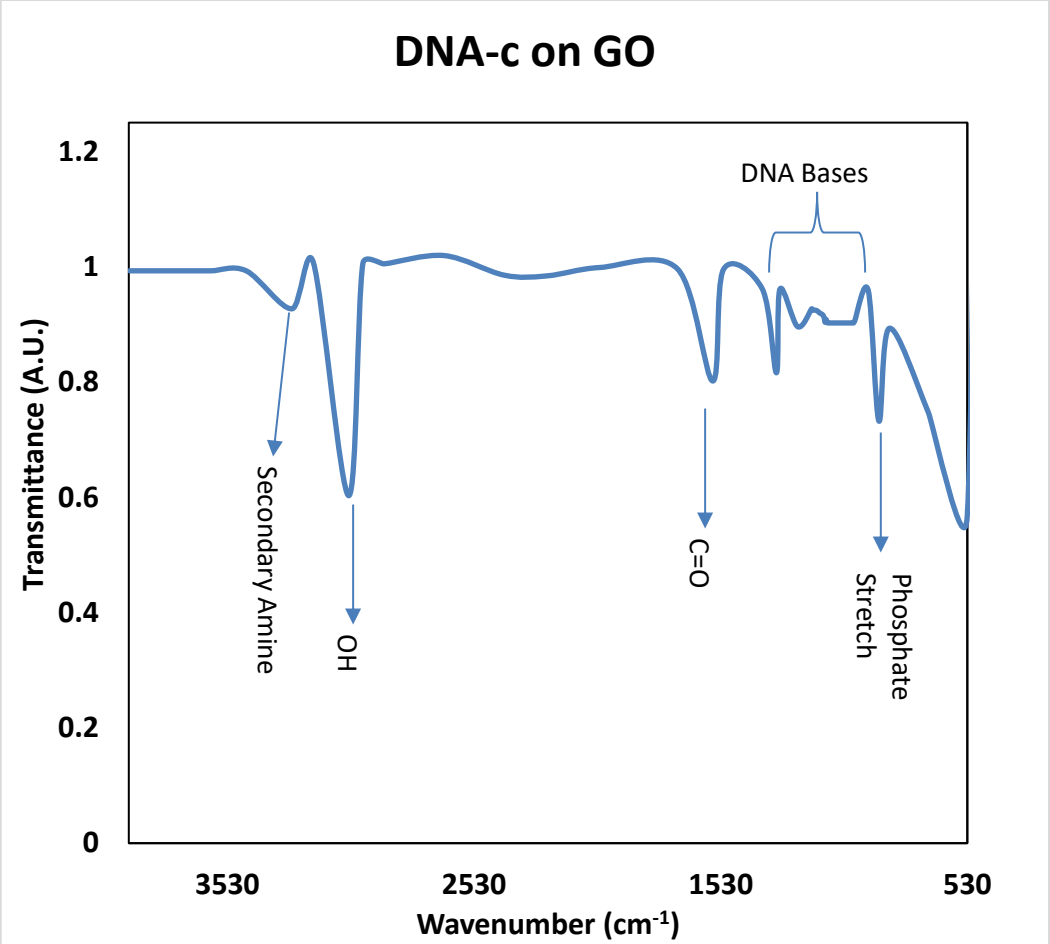

Figure 5.11: FTIR Spectrum of DNA-c on GO

5.4 Fluorescent Studies

The studies here show the different 5’ Mod DNA-t concentrations ranging from 0 µM to 4 µM, keeping the glutaraldehyde volume constant, and the $Fe_3O_4@SiO_2@NH_2$ at 1 mg/mL.

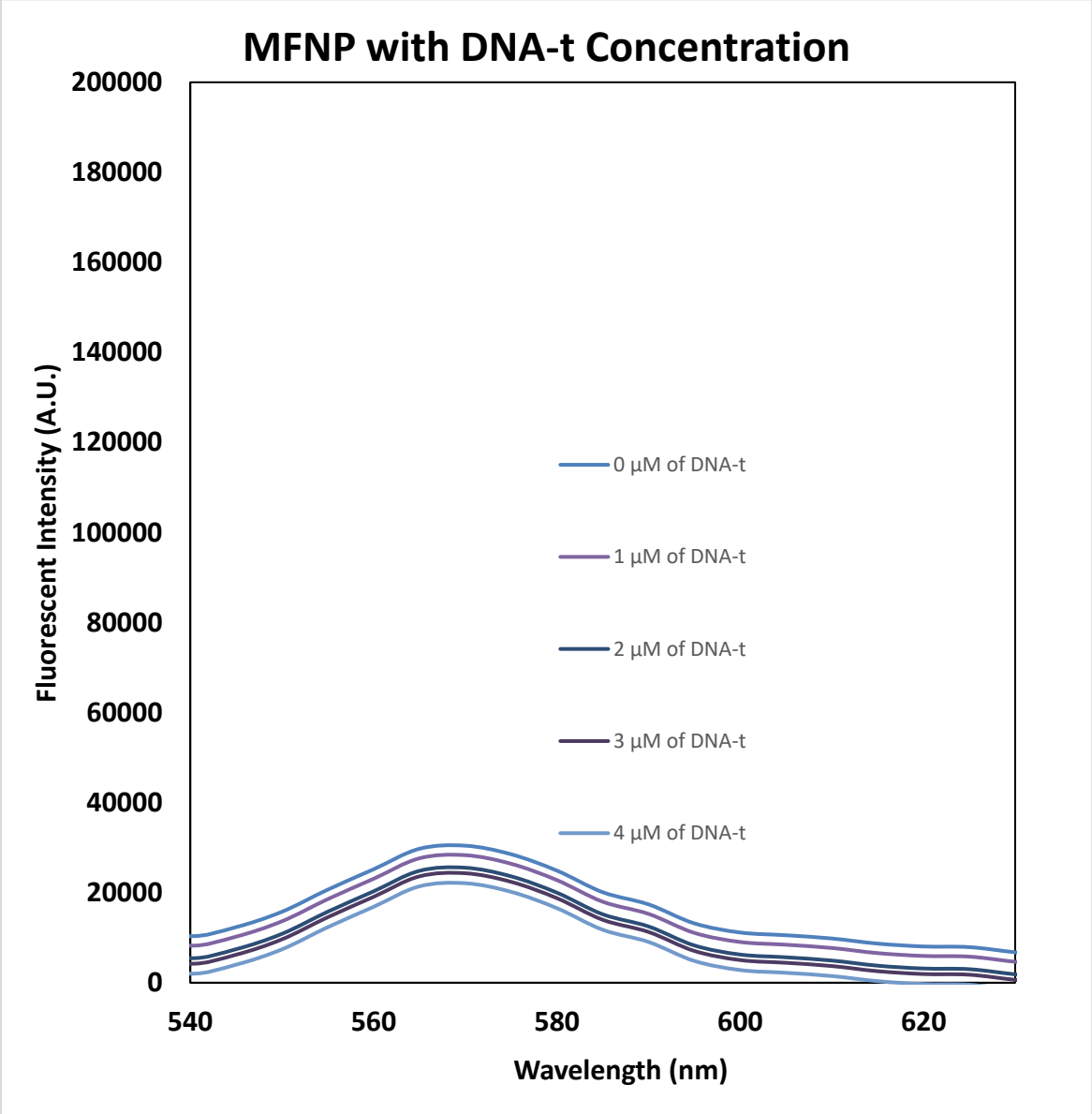

Figure 5.12: Fluorescent Intensity of Different 5’ Mod DNA-t Concentrations

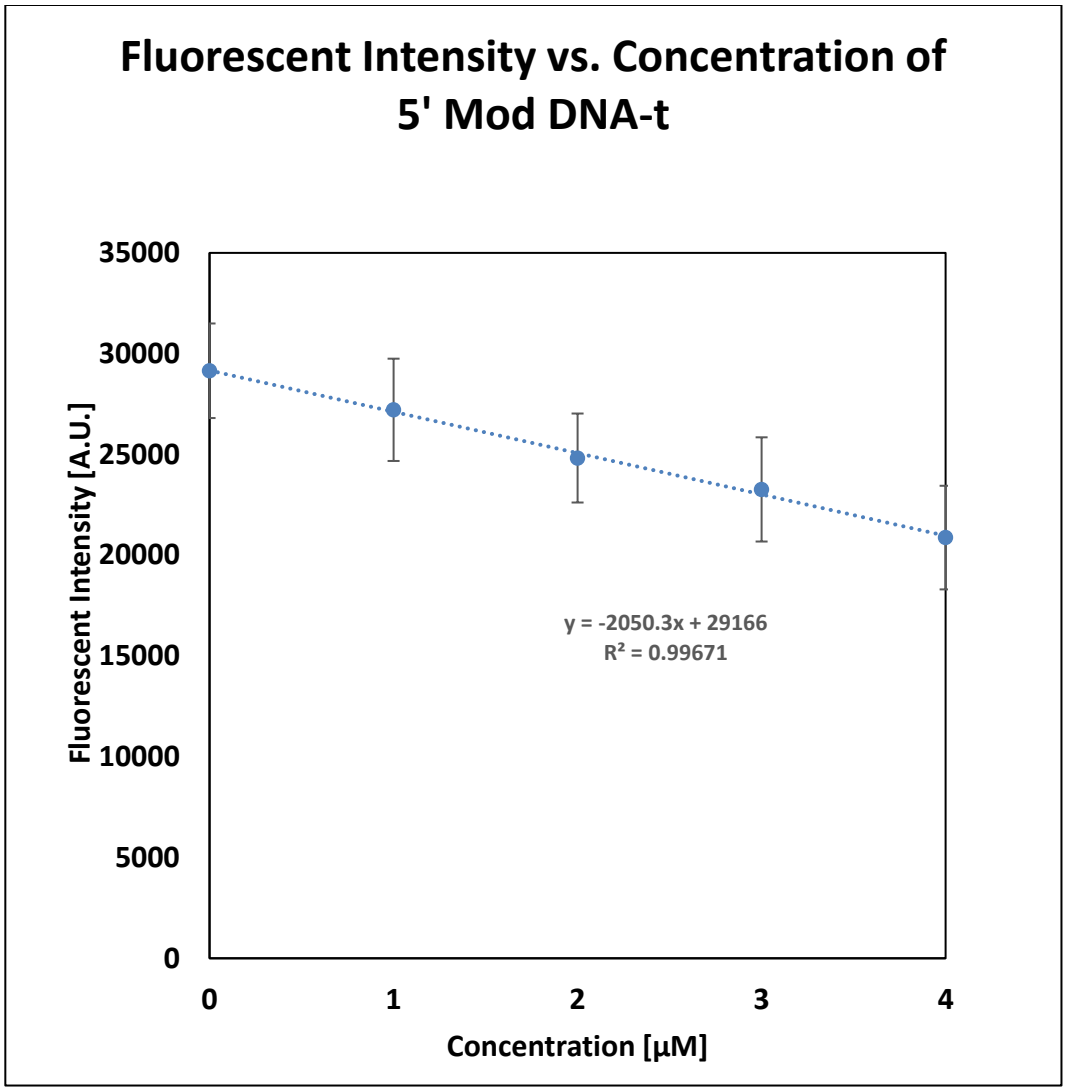

Figure 5.13: Fluorescent Intensity with Different 5' Mod DNA Concentrations

The sensitivity of the method was shown by changing the concentration of the 5' Mod target DNA. Keeping the concentration of the Glutaraldehyde constant, having the concentration of the $Fe_3O_4@SiO_2@NH_2$ of 1 mg/mL constant and only varying the concentration of DNA-t gave the correspondence of the fluorescence at different concentrations where the target DNA was detected and analyzed. The fluorescence spectra of the system upon the addition of the 5' Mod target DNA are shown in Fig. 5.12. The dependence of fluorescence intensity on target DNA concentration is plotted in Fig. 5.13. The regression equation is expressed as y=-2050.3x+29166 with a correlation coefficient R^2 of 0.99671, where y is the fluorescence intensity and x is the

concentration of target DNA. The detection limit, based on 3 σ/slope (where σ was the standard deviation of the background signal) was 0.41 μM.

5.5 Fluorescent Intensity Levels with Different Concentrations of GO

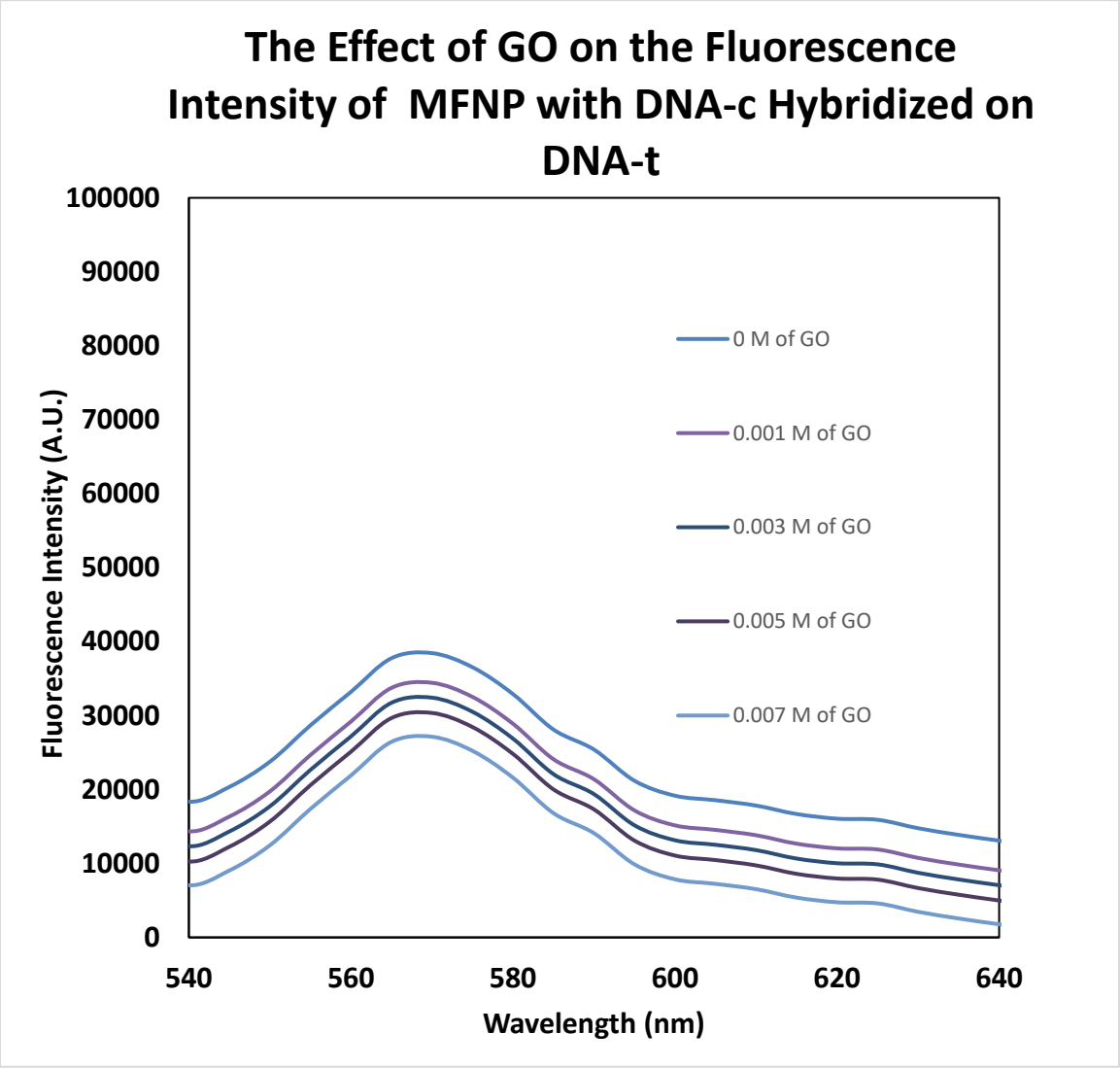

Figure 5.14: The Effect of GO on the Fluorescent Intensity of Fe_3O_4@SiO_2@NH_2 with DNA-c Hybridized on DNA-t

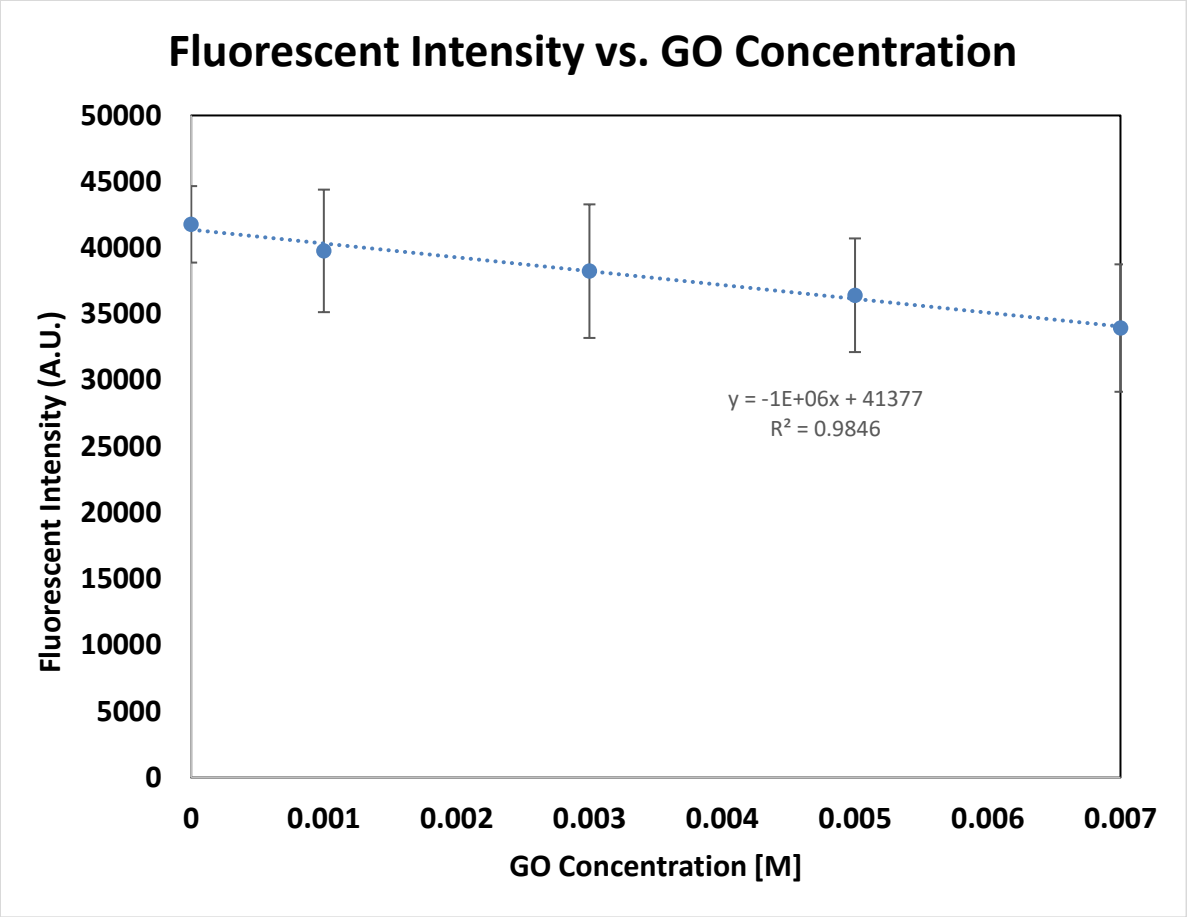

Figure 5.15: Fluorescent Intensity vs. GO Concentration

The 5' Mod DNA-t was conjugated onto Fe_3O_4@SiO_2@NH_2 through the use of the cross-linker Glutaraldehyde and was hybridized with DNA-c in solution onto graphene oxide through peptide bonding to emit luminescence in the Tris-HCl buffer, with the maximum luminescence observed at around 580 nm. The fluorescence intensity of the MFNPs was observed to decrease with increasing the concentration of GO at low concentrations.

Changing the concentration of Graphene Oxide showed the sensitivity. Keeping the concentration of the DNA-c constant, DNA-t constant, the concentration of the MFNP constant gave the correspondence of the fluorescence at different concentrations where the GO was detected and analyzed. The fluorescence spectra of the system upon the addition of GO was shown in Fig. 5.14. In the absence of the GO, the solution emitted strong fluorescence. From Fig. 5.15, it showed that the fluorescence intensity (FL) at 580 nm was highly sensitive with

increasing concentration of GO. The dependence of fluorescence intensity on GO concentration is plotted in Fig. 5.15. The regression equation is expressed as y= -1E+06x + 41377 with a correlation coefficient R^2 of 0.98463, where y is the fluorescence intensity and x is the concentration of GO. The detection limit, based on 3 σ/slope (where σ was the standard deviation of the background signal) was 0.0003 M.

5.5 Summary

In summary, the multifunctional nanoparticle was synthesized to study the sensitivity of the target DNA through the covalent interaction from 0-4 µM of DNA-t. It was found that the limit of detection was as low as 0.41 µM based on the range of 0-4 µM of DNA-t. Once the target DNA was hybridized with the complementary DNA, the effect of graphene oxide was studied to see if it had any effect on the fluorescent multifunctional nanoparticle. The range of graphene oxide was studied from 0-0.007 M and the limit of detection was as low as 3 µM from the quenching effect.

5.6 References

[1] Wu W, He Q, Jiang C. Magnetic Iron Oxide Nanoparticles: Synthesis and Surface Functionalization Strategies. Nanoscale Res Lett. 2008; 3:397-415

[2] Shahabadi N, Akbari A, Jamshidbeigi M, Falsafi M. Functionalization of Fe_3O_4@SiO_2 Magnetic Nanoparticles with Nicotinamide and in vitro DNA Interaction. Journal of Molecular Liquids. 2016; 224: 227-233

[3] Hu Y, Li F, Han D, Wu T, Zhang Q, Niu L, Bao Y. Simple and label-free electrochemical assay for signal-on DNA hybridization directly at undecorated graphene oxide. Analytica Chimica Acta. 2012; 753: 82-89

[4] Goenka S, Sant V, Sant S. Graphene-based Nanomaterials for Drug Delivery and Tissue Engineering. Journal of Controlled Release. 2014; 173: 75-88

[5] Ferguson L, Denny W. Genotoxicity of non-covalent interactions: DNA intercalators. Mutation Research/ Fundamental and Molecular Mechanisms of Mutagenesis. 2007; 623: 14-23

Chapter 6: Summary and Future plan

6.1 Summary

Iron Oxide and Graphene Oxide are two of the most common biomaterials used in the field of biomedical applications. Due to many limitations from their physical and chemical properties, this research goal was to improve on the surface modification where the selectivity and sensitivity towards DNA could be sought out from two different design systems. In this research, our goal was to engineer two different systems: (1) Cationic Bridge System and (2) Covalent Interaction System using these surface modified nanomaterials to establish the selectivity and sensitivity towards DNA sensing. From the two different systems, the fluorescent biosensor can see the sensitivity towards the target DNA. By establishing the groundwork with the DNA sensing capabilities, the effect of GO is also investigated from the two different systems.

In the Cationic bridge system, the iron oxide was surrounded by an inorganic core of silica where the negative charge bridges to Na^+ and the other negative charge from the DNA is attached to the monovalent ion. From the conjugation, the effect of DNA sensing was studied and the limit of detection was calculated to be as low as 0.25 μM from the range of 0 to 30 μM of the target DNA using this design mechanism from the fluorescent biosensor. The target DNA is in the process of hybridizing with the complementary DNA where the DNA-c is bridged with graphene oxide. The effect of GO was investigated keeping DNA-t, DNA-c, and the multifunctional particles constant. The hybridization is underway for more confirmable tests to see if the DNA bonding has a big impact on the fluorescence tests from the effect of Graphene Oxide.

In the Covalent Interaction system, the iron oxide was surface modified with the inorganic core of silica. Later, amino groups were attached to the silica surface which could bond to glutaraldehyde as a cross-linker with the amino groups of DNA-t from the 5’ Modification. From the conjugation, the effect of DNA sensing was studied and the limit of detection was calculated to be as low as 0.41 μM from the range of 0 to 4 μM of the target DNA using the design mechanism from the fluorescent biosensor. Later, the target DNA was in the process of potential hybridization with the complementary DNA which peptide bonded with Graphene Oxide. The effect of GO was studied, but the hybridization is still in the verification process.

A biosensor is composed of a biological agent that attaches to an analyte which uses a form of a transducer that has a signal processor that outputs the data in some form. Here, the fluorescent biosensor was initiated where the multifunctional particles were interacted with the DNA agent and light interacts with the sample to output the data. A novel fluorescent biosensor was used to study the biomedical application and hopefully could be used as a promising tool for Cancer Diagnosis in the future.

6.2 Future Plan

Different transducers are in place ranging from electrochemical, electromechanical, and fluorescent based biosensors. Some of these biosensors are a great application in the biomedical field in the prospects of disease diagnosis, particularly in the Cancer area. The demand and need for using a biosensor for rapid analysis with cost effectiveness is still being worked upon by scientists and engineers. In that situation, both 2D and 3D detection are required with sophisticated transducers for targeting and quantifying small analytes. The level of development in the area of biosensors should take a notch in discovering more robust regenerative biosensors for long term use. If the technology can improve to this level, new diagnostic biosensors can be developed for many biomedical applications and help clinicians and patients understand the integrative understanding of diseases and therapy. In relation to this, the fluorescent biosensor is excellent for assessing the efficacy of the tumor cell concentration and see how early Cancer could be detected. Currently, the use of aptamers, peptides, antibodies, and other materials are examples for the prospective approach in delving into this research. In this thesis, the engineered design of the nanomaterials to see the sensitivity of the target DNA by two different approaches were studied. This approach could be the materials used to view the Cancer Diagnosis as an in-vitro analysis in the future. Different biological agents can be used in the detection, ranging from other various nanomaterials, polymers that can provide hybrid devices for better usage in the earlier detection. Looking out in the horizon, potential application and characteristics like analyte detection ability, analysis time, portability, cost and customization have to be taken into account and be improved upon in this field.

In this thesis, we constructed the fluorescence system using nanomaterials as biological agents. Different mechanisms can also be put into place to enhance the selectivity and sensitivity

towards DNA sensing. Different cations could be used from different monovalent to divalent ions to see the difference in the sensitivity in DNA sensing. The difference could be studied further upon with various cation bridges to compare the difference. In the other system, the idea of using the streptavidin and biotin could be used to enhance the different covalent interaction systems and look at the selectivity it adheres to the DNA sensing.

With the starting materials used for both the cationic and covalent interaction, the amount of target DNA after introducing graphene oxide can be worked upon. The quantification process of the amount of target DNA bound to the multifunctional nanoparticles in both processes can be looked to further investigate in these two designs. The next steps would be to magnetically separate the multifunctional nanoparticle from the target DNA to check the quantification process.

In conclusion, looking at different biological agents, different mechanisms, and transducers, it can improve the analyte detection, analysis time, portability, cost, etc.

Appendices

Figure 2.1: Electrochemical Design for DNA-t Detection [7]. Copyright Permission is obtained.

Figure 2.2: Oxidation and Reduction of Iron Oxide Compounds [62]. Copyright Permission is obtained.

Figure 3.2: The Structure of the Hummer's Approach. Copyright Permission is obtained.

Curriculum Vitae

Name: Aditya Balaji

Post-secondary Education and Degrees:

The University of Western Ontario
London, Ontario, Canada
2012-2016 B.Sc.

The University of Western Ontario
London, Ontario, Canada
2016-2018 MESc

Honours and Awards:

NSERC USRA Scholarship
2016

Western Graduate Scholarship
2016-2018

Related Work Experience

Teaching Assistant
The University of Western Ontario
2016-2018

CBE 9241 Nanotechnology	2016-2017
MME Introduction to MEMS	2016-2017
BME Fundamentals of Biomedical Engineering	2016-2017
BME Communications	2016-2017

Publications:

Balaji A, Zhang J. Electrochemical and Optical Biosensors for Early-Stage Cancer Diagnosis by using Graphene and Graphene Oxide. Cancer Nanotechnology. 2017; 8: 1-12.

Balaji A, Zhang J. The Engineering Development of Multifunctional Nanomaterials for DNA Sensing. Preparing.